

# Recommendations for Multimodality Cardiovascular Imaging of Patients with Hypertrophic Cardiomyopathy: An Update from the American Society of Echocardiography, in Collaboration with the American Society of Nuclear Cardiology, the Society for Cardiovascular Magnetic Resonance, and the Society of Cardiovascular Computed Tomography

Sherif F. Nagueh, MD, FASE (Chair), Dermot Phelan, MD, PhD, FASE (Co-Chair),  
Theodore Abraham, MD, FASE, Alicia Armour, RDCS, FASE, Milind Y. Desai, MD, MBA,  
Andreea Dragulescu, MD, FASE, Yvonne Gilliland, MD, FASE, Steven J. Lester, MD, FASE,  
Yasdet Maldonado, MD, FASE, Saidi Mohiddin, MD, Koen Nieman, MD, Brett W. Sperry, MD,  
and Anna Woo, MD, FASE, *Houston, Texas; Charlotte, North Carolina; San Francisco, California; Durham, North  
Carolina; Cleveland, Ohio; Toronto, Canada; New Orleans, Louisiana; Scottsdale, Arizona; London, United  
Kingdom; Stanford, California; Kansas City, Missouri*

Hypertrophic cardiomyopathy (HCM) is defined by the presence of left ventricular hypertrophy in the absence of other potentially causative cardiac, systemic, syndromic, or metabolic diseases. Symptoms can be related to a range of pathophysiologic mechanisms including left ventricular outflow tract obstruction with or without significant mitral regurgitation, diastolic dysfunction with heart failure with preserved and heart failure with reduced ejection fraction, autonomic dysfunction, ischemia, and arrhythmias. Appropriate understanding and utilization of multimodality imaging is fundamental to accurate diagnosis as well as longitudinal care of patients with HCM. Resting and stress imaging provide comprehensive and complementary information to help clarify mechanism(s) responsible for symptoms such that appropriate and timely treatment strategies may be implemented. Advanced imaging is relied upon to guide certain treatment options including septal reduction therapy and mitral valve repair. Using both clinical and imaging parameters, enhanced algorithms for sudden cardiac death risk stratification facilitate selection of HCM patients most likely to benefit from implantable cardioverter-defibrillators. (J Am Soc Echocardiogr 2022;35:533-69.)

**Keywords:** Hypertrophic cardiomyopathy, Ischemia, Sudden death, Noninvasive imaging

From the Houston Methodist Hospital, Houston, TX (S.F.N.); Sanger Heart & Vascular Institute, Charlotte, NC (D.P.); University of California, San Francisco, CA (T.A.); Duke University Health System, Durham, NC (A.A.); Cleveland Clinic, Cleveland, OH (M.Y.D., Y.M.); Hospital for Sick Children, Toronto, Canada (A.D.); Ochsner Medical Center, New Orleans, LA (Y.G.); Mayo Clinic, Scottsdale, AZ (S.J.L.); Inherited/Acquired Myocardial Diseases, Barts Health NHS Trust, St Bartholomew's Hospital, London, UK (S.M.); Cardiovascular Medicine and Radiology (CV Imaging), Stanford University Medical Center, CA (K.N.); Saint Luke's Mid America Heart Institute, Kansas City, MO (B.W.S.); Toronto General Hospital, Toronto, Canada (A.W.).

The following authors reported no actual or potential conflicts of interest in relation to this document: Sherif F Nagueh, MD, FASE, Theodore Abraham, MD, FASE, Alicia Armour, RDCS, FASE, Andreea Dragulescu, MD, FASE, Yvonne Gilliland, MD, FASE, Steven J Lester, MD, FASE, Yasdet Maldonado, MD, FASE, Saidi Mohiddin, MD, Anna Woo, MD, FASE

The following authors reported relationships with one or more commercial interests: Milind Y Desai, MD, MBA, has been a Principal Investigator of VALOR-HCM trial, sponsored by Myokardia, Inc. Koen Nieman, MD, has received unrestricted, institutional research support from Siemens Healthineers (Germany), Bayer (Germany), HeartFlow Inc (USA), consultancy for Siemens Medical USA, and is a stockholder for Lumen Therapeutics (USA). Brett W. Sperry, MD, has

participated in the Speakers Bureau for Pfizer and has been a consultant for Alnylam Pharmaceuticals, Inc. Dermot Phelan, MD, PhD, FASE, served on MyoKardia (BMS) Regional HCM Advisory Board, Local PI for BMS for Randomized Study IMB-1018972.

Reprint requests: American Society of Echocardiography, Meridian Corporate Center, 2530 Meridian Parkway, Suite 450, Durham, NC 27713 (E-mail: [ase@asecho.org](mailto:ase@asecho.org)).

#### Attention ASE Members:

Login at [www.ASELearningHub.org](http://www.ASELearningHub.org) to earn continuing medical education credit through an online activity related to this article. Certificates are available for immediate access upon successful completion of the activity and post-work. This activity is free for ASE Members, and \$25 for nonmembers.

0894-7317/\$36.00

Copyright 2022 Published by Elsevier Inc. on behalf of the American Society of Echocardiography.

<https://doi.org/10.1016/j.echo.2022.03.012>

This document is endorsed by the following ASE International Alliance Partners: Argentine Federation of Cardiology; Argentine Society of Cardiology; ASEAN Society of Echocardiography; Australasian Society for Ultrasound in Medicine; Canadian Society of Echocardiography; Cardiovascular Imaging Department of the Brazilian Society of Cardiology; Chinese Society of Echocardiography; Indian Academy of Echocardiography; Indonesian Society of Echocardiography; Iranian Society of Echocardiography; Israel Working Group on Echocardiography; Italian Association of Cardiothoracic Anaesthesiologists; Japanese Society of Echocardiography; Korean Society of Echocardiography; Mexican Society of Echocardiography and Cardiovascular Imaging; Society of Cardiovascular Images of the Inter-American Society of Cardiology; Thai Society of Echocardiography; The Pan-African Society of Cardiology; and Vietnam Society of Echocardiography.

## Abbreviations

**A2/3/4/5C** = Apical 2/3/4/5 Chamber  
**CAD** = Coronary Artery Disease  
**CCTA** = Cardiac Computed Tomographic Angiography  
**CMR** = Cardiac Magnetic Resonance  
**CWD** = Continuous-Wave Doppler  
**FFR** = Fractional Flow Reserve  
**HCM** = Hypertrophic Cardiomyopathy  
**ICD** = Implantable Cardioverter Defibrillator  
**LA** = Left Atrium  
**LV** = Left Ventricle  
**LVH** = Left Ventricular Hypertrophy  
**LVOTO** = Left Ventricular Outflow Tract Obstruction  
**MR** = Mitral Regurgitation  
**MVO** = Mid-Ventricular Obstruction  
**PWD** = Pulsed-Wave Doppler  
**RV** = Right Ventricle  
**SAM** = Systolic Anterior Motion  
**SCD** = Sudden Cardiac Death  
**SRT** = Septal Reduction Therapy  
**TEE** = Transesophageal Echocardiography  
**TTE** = Transthoracic Echocardiography  
**UEA** = Ultrasound Enhancing Agents

## TABLE OF CONTENTS

Abstract 533  
 Abbreviations: 534  
 Preamble 534  
 Introduction 534  
 Section 1: Multimodality Imaging for the Evaluation of Suspected or Confirmed HCM 535  
 A. Assessment of Left Ventricular Hypertrophy 535  
 B. Differentiating HCM from Phenocopies 535  
 C. Assessment of Left Ventricular Systolic Function 539  
 D. Assessment of Left Ventricular Diastolic Function 540  
 E. Assessment of Dynamic Obstruction and Mitral Valve Anatomy 543  
 F. Tissue Characterization 552  
 Section 2: Multimodality Imaging for risk stratification and prognostication 552  
 A. Left Ventricular Wall Thickness 552  
 B. Left Atrial Diameter 552  
 C. Left Ventricular Outflow Tract Obstruction 552  
 D. Apical Aneurysm 553  
 E. Late Gadolinium Enhancement by CMR 554  
 F. Left Ventricular Systolic Dysfunction 554  
 G. Ischemia 555  
 Section 3: Multimodality Imaging in Common Clinical Scenarios 555  
 A. Assessment of Ischemia 555  
 B. Assessment of Coronary Artery Disease 557  
 C. Screening 558  
 D. Role of Imaging in Treatment Selection and Monitoring 559  
 Summary 562

## PREAMBLE

Since the publication of the recommendations for multimodality cardiovascular imaging of patients with hypertrophic cardiomyopathy (HCM) in 2011, an impressive growth and evolution of imaging techniques has occurred, enhancing both the recognition and management of the disease.<sup>1</sup> This update from the American Society of Echocardiography (ASE), American Society of Nuclear Cardiology (ASNC), Society of Cardiovascular Magnetic Resonance (SCMR), and Society of Cardiovascular Computed Tomography (SCCT) provides a contemporary practical framework for the utilization of multimodality imaging in the care of HCM patients. Metabolic disorders that mimic HCM are only included in the differential diagnosis, where appropriate, and are not the focus of this document.

## INTRODUCTION

HCM is defined by the presence of left ventricular hypertrophy (LVH) in the absence of other potentially causative cardiac, systemic, syndromic, or metabolic diseases.<sup>2</sup> It is the most common genetic abnormality of the myocardium, with an estimated prevalence ranging from 1:500 to as high as 1:200.<sup>3-5</sup> Predominantly recognized as a disease caused by mutations in genes encoding sarcomeric proteins, HCM has a wide range of clinical expression and disease penetrance. Many individuals with HCM have a normal life expectancy and are relatively free of symptoms, while an important minority suffers debilitating symptoms and/or premature mortality.<sup>2,6</sup> Symptoms can be related to a range of pathophysiologic mechanisms including diastolic dysfunction,<sup>7,8</sup> heart failure with preserved or reduced ejection fraction (EF),<sup>9,10</sup> left ventricular outflow tract (LVOT) obstruction<sup>11,12</sup> with or without significant mitral regurgitation (MR),<sup>13</sup> autonomic dysfunction,<sup>14</sup> ischemia,<sup>15,16</sup> and arrhythmias.<sup>17,18</sup>

Appropriate understanding and utilization of multimodality imaging is fundamental to accurate diagnosis as well as longitudinal care of patients with HCM. Novel echocardiographic and cardiac magnetic resonance (CMR) imaging techniques have improved differentiation of HCM from other causes of LVH.<sup>19-22</sup> Such refinements in conjunction with serial imaging have broadened our perspective of the penetrance of disease expression in HCM mutation carriers.<sup>23</sup> Resting and stress imaging provides both comprehensive and complementary information to help clarify mechanism(s) responsible for nonspecific symptoms such that appropriate and timely treatment strategies may be implemented. Advanced imaging is relied upon to guide certain treatment options including septal reduction therapy (SRT) and mitral valve repair. Using both clinical and imaging parameters, enhanced algorithms for sudden cardiac death (SCD) risk stratification facilitate selection of HCM patients most likely to benefit

from implantable cardioverter-defibrillators (ICD), resulting in dramatically improved prognosis.<sup>6,24</sup>

## SECTION 1: MULTIMODALITY IMAGING FOR THE EVALUATION OF SUSPECTED OR CONFIRMED HCM

### A. Assessment of Left Ventricular Hypertrophy

Accurate quantification of the magnitude, location, and pattern of LVH is essential for the diagnosis and management of patients. Wall thickness  $\geq 15$  mm in the absence of other causes of hypertrophy in a non-dilated left ventricle (LV) defines HCM.<sup>2</sup> End diastolic wall thickness  $\geq 13$  mm can be diagnostic if there is a family history of HCM or a known disease-causing genetic mutation. Risk of SCD correlates with the magnitude of hypertrophy. Massive LVH ( $\geq 30$  mm, which occurs in about 10% of individuals with HCM) has been used as a threshold for ICD implantation, although the relationship between the degree of hypertrophy and the risk of SCD is a continuous one. In addition, the location and pattern of increased wall thickness can predict the probability of a positive genetic test.<sup>25</sup>

In the pediatric population, it is essential to consider that because of somatic growth, a single cut-off value cannot be applied across patients of different ages and sizes. Cardiac measurements are expressed as z-scores, representing standard deviations from a patient size-specific mean value, with hypertrophy diagnosed at z score  $>2$ .<sup>26,27</sup>

The development of hypertrophy is a dynamic process. An abnormal increase in LV wall thickness in childhood is uncommon and should prompt consideration of phenocopies (Table 1) or double gene mutations. Hypertrophy usually accelerates in adolescence. While there are many different phenotypic expressions of HCM, hypertrophy is usually asymmetric, affecting non-contiguous LV segments, and occasionally the right ventricle (RV).<sup>28</sup> Focal asymmetric hypertrophy of the basal anterior septum, defined as septal/posterior wall thickness  $>1.3$  in a normotensive patient, is the most common pattern of hypertrophy. Variants include a sigmoid septum, reversed septal curvature, concentric, mid-wall, and apical hypertrophy (Figure 1 and Video 1). The positivity rate of genetic testing differs with each pattern of increased wall thickness, with the lowest yield occurring in patients with sigmoid septum and highest in patients with a reversed septal curvature pattern.<sup>25</sup> Furthermore, patients with a pathogenic mutation have greater wall thickness compared with mutation-negative individuals, which may partially account for the higher rate of adverse events in this cohort.<sup>29</sup> All imaging modalities should report the pattern and distribution of hypertrophy along with the location and magnitude of maximal wall thickness at end-diastole.

**1. Echocardiography.** Transthoracic echocardiography (TTE) is the initial imaging modality of choice in HCM. Care should be taken to avoid LV foreshortening in the apical views, especially in cases with apical hypertrophy. The apical, anterior, and anterolateral walls can be challenging to visualize and accurately measure their thickness. Thus, there should be a low threshold to use ultrasound enhancing agents (UEA) if visualization is not optimal. This is particularly important if the pre-test probability is high, such as when screening family members of gene-positive individuals or in the presence of concerning electrocardiographic (ECG) patterns such as deep lateral T-wave inversion. Wall measurements obtained with UEA may be more reproducible than those obtained without and are more closely aligned to measurements obtained by CMR.<sup>30</sup> Additionally, UEA may facilitate identification of myocardial crypts, apical aneurysms, and ventricular thrombi, and can facilitate myocardial target localization for alcohol septal ablation. Systematic identification and exclu-

sion of RV structures (including trabeculation, moderator band, and crista supraventricularis) is advised when measuring the interventricular septum (IVS). Long-axis views can overestimate wall thickness due to tangential cuts through the wall and potential inclusion of other structures such as trabeculations or papillary muscles in the measurements (Figure 2). Therefore, it is important to integrate and cross-reference short- and long-axis views to optimally align measurements.<sup>31,32</sup> High-quality three-dimensional (3D) echocardiography is superior to 2D in the evaluation of LV mass and more closely correlated with CMR assessment.<sup>33,34</sup> The RV free wall should be measured in subcostal views at end-diastole with care to avoid inclusion of epicardial fat.<sup>32</sup>

**2. Cardiac Magnetic Resonance.** CMR's contribution is of particular importance because of high spatial resolution and tissue characterization.<sup>35</sup> Still, care should be taken to avoid erroneous measurements from long-axis views (Figure 3). These capabilities confer diagnostic sensitivity when LVH is near diagnostic or therapeutic thresholds, atypical or complex in distribution, and in patients with technically challenging echocardiographic studies. As a component of the wider clinical and imaging assessment, tissue characterization (late gadolinium enhancement [LGE], T1 and T2 mapping) can help differentiate between increased wall thickness due to HCM and other conditions such as athletic remodeling, hypertension, inflammation, and infiltration (Table 1).<sup>36,37</sup>

**3. Cardiac Computed Tomography.** Claustrophobic patients and/or patients with CMR-incompatible cardiac devices may not be suitable for CMR. In these cases, cardiac CT should be considered. Because of its high 3D resolution, cardiac CT can accurately depict morphological features of HCM, including regional wall thickness, LV mass, and global LV contractile function.<sup>38,39</sup> In addition, cardiac CT visualizes the size and course of septal perforators within the myocardium, which is of potential interest in preparation for percutaneous SRT.<sup>40</sup> Of note, standard coronary CT angiograms acquired during mid-diastole will overestimate wall thickness compared to images acquired at end-diastole.

**4. Cardiac Nuclear Imaging.** Nuclear imaging is not needed for the evaluation of wall thickness given its low spatial resolution and exposure to radiation, in comparison with the high spatial resolution and the lack of exposure to radiation with echocardiography and CMR.

### B. Differentiating HCM from Phenocopies

While clinical context is key, there are many situations where features on the echocardiogram alone can raise suspicion of specific disease processes or narrow the differential diagnosis and guide downstream testing. Features such as asymmetric hypertrophy or dynamic LVOT obstruction (LVOTO) are more commonly seen in HCM than in other pathologies but are not pathognomonic. Correlation with the 12-lead ECG and clinical history is recommended to narrow the differential diagnosis and guide selection of further advanced imaging (Figure 4).

**1. Athlete's Heart Versus HCM.** Most of the literature aimed at distinguishing these entities compares athletes to sedentary HCM patients with clear phenotypic expression. These data are limited in separating physiology from pathology in the true "gray-zone" athlete. In such clinical scenarios it is important to appreciate the pretest probability where, for example, an athlete who has a family history of HCM or presents with concerning symptoms requires a higher degree

**Table 1** Typical Features and Findings in Phenocopies of HCM

Most Common Phenocopies	Clinical Features	Typical ECG Findings	Typical Echo Findings	Typical CMR Findings	Genetics and Additional Features
<b>Children/Adolescents</b>					
Danon Disease	Mild skeletal myopathy, May reveal pre-ophthalmic abnormalities, intellectual disability.	May reveal pre-excitation syndrome.	Massive concentric LVH, occasionally dilated cardiomyopathy.	LVH is often severe. LGE can be extensive, but often conspicuously sparing of the mid septum	X-linked dominant disorder, although isolated cardiac form can present in older females. Diagnosis based on elevated CK, muscle biopsy, genetic testing (LAMP2 gene mutation)
<b>Adults &lt;40 years</b>					
PRKAG2	Proximal myopathy, myalgia, epilepsy, early-onset hypertension	Pre-excitation syndrome, bundle branch block, high voltages. Atrial fibrillation, atrial flutter. Advanced atrioventricular blocks, marked sinus bradycardia, or sinus block	Variable degree of increased LV wall thickness. Diastolic and systolic dysfunction	Highly variable findings from minimal asymmetric hypertrophy without LGE in early stages to severe hypertrophy with extensive LGE in advanced stages	Autosomal dominant, PRKAG2 gene mutation
Friedrichs Ataxia	Progressive ataxia, loss of deep tendon reflexes, motor weakness, cerebral dysarthria, diabetes mellitus	Lateral T wave flattening or inversion. Supraventricular and ventricular arrhythmia	Mild concentric remodeling, followed by hypertrophy, less often eccentric, hypertrophy. Impaired relaxation. Ultimately dilatation with systolic dysfunction. Sparkling texture.	In early and intermediate disease: concentric remodeling or hypertrophy. In late disease: replacement fibrosis.	Autosomal recessive, serum alpha-tocopherol level, brain MRI
Anderson- Fabry Disease	Multi-system disease: peripheral neuropathy, cutaneous lesions, progressive renal insufficiency with proteinuria, coronary small vessel disease.	LVH with repolarization abnormalities, conduction abnormalities, preexcitation, atrial and ventricular arrhythmia.	Concentric, asymmetric, and eccentric hypertrophy. Impaired relaxation. Normal ejection fraction. Thinned basal inferolateral LV wall in advanced disease. RV hypertrophy. Prominent papillary muscle. Aortic dilatation.	LGE typically involves the mid segments of the lateral wall with subendocardial sparing. Involvement of the basal third of other LV walls in severe cases. Short T1 relaxation time may be present in the septum.	X-linked recessive, deficiency of alpha-galactosidase A activity. Males present at a younger age.
Athlete's Heart	Asymptomatic	Sinus bradycardia, LVH, early repolarization, first degree heart block, Wenckebach, ectopic atrial or junctional rhythm.	End-diastolic wall thickness typically below 15 mm. Balanced four chambers dilation. Normal/low-normal biventricular ejection fraction with normal/supranormal diastolic function.	LGE absent except occasionally at the RV insertion points. Normal ECV.	Supranormal functional capacity.

(Continued)

**Table 1** (Continued)

Most Common Phenocopies	Clinical Features	Typical ECG Findings	Typical Echo Findings	Typical CMR Findings	Genetics and Additional Features
Adults > 40					
Hypertensive Heart Disease	May be asymptomatic or develop heart failure symptoms related to diastolic dysfunction	LVH (low sensitivity for detecting anatomic LVH), repolarization abnormalities, prolonged QTc and QRS duration	Most commonly concentric hypertrophy or remodeling with varying degrees of diastolic dysfunction depending on the severity and duration of hypertension	Patchy LGE can be seen. Increased extracellular volume fraction in some patients	
Cardiac Amyloidosis	Clinical features include heart failure, peripheral neuropathy, atrial arrhythmias, and carpal tunnel syndrome	Low QRS voltages relative to LV wall thickness. Conduction abnormalities, supraventricular arrhythmias.	Concentric increase in LV wall thickness, sometimes with septal predominance. Restrictive LV filling pattern with more advanced disease. Normal to progressively reduced systolic function. Reduced global longitudinal strain with apical sparing. Bi-atrial dilatation. Thickening of valve leaflets. Small pericardial effusion.	Subendocardial and transmural late gadolinium enhancement with relative apical sparing. Characteristic simultaneous myocardial and blood nulling or suboptimal myocardial nulling. Prolonged native myocardial T1 relaxation time. Increased extracellular volume fraction.	Technetium-based bone scintigraphy for ATTR amyloidosis. Monoclonal proteins assay in blood and urine in patients with AL amyloidosis. Tissue biopsy may be needed.

*Alpha Gal-A*, alpha galactosidase A; *CK*, creatine kinase; *LAMP2*, lysosome-associated membrane protein 2; *LGE*, Late Gadolinium Enhancement; *LVH*, Left Ventricular Hypertrophy; *PRKAG2*, gamma 2 regulatory subunit of AMP-activated protein kinase.

of suspicion than an asymptomatic athlete who presents via pre-participation screening. An understanding of the electrical adaptations seen on the 12-lead ECG in athletes is required to differentiate normal from pathological changes seen in HCM such as inferolateral T wave inversion, ST-segment depression or Q waves. It is important to note that between 5 and 10% of individuals with HCM will have a normal electrocardiogram.<sup>41,42</sup> The magnitude of exercise-induced hypertrophy is dependent on multiple factors including the duration, type and intensity of exercise pursued as well as the athlete's age, body mass index (BMI), race, and gender.<sup>43</sup> Physiologic hypertrophy is more commonly seen in athletes involved in sports with both high dynamic and static components and in black male athletes. It is rare for LV wall thickness to exceed 12 mm in Caucasian athletes while the upper threshold of normal in elite black male athletes may be close to 15 mm.<sup>43,44</sup> Concentric hypertrophy is usually considered abnormal in female athletes yet can be seen in up to a third of black male athletes.<sup>43,45,46</sup> Therefore, a knowledge of the expected range and pattern of wall thickness for that individual athlete is useful. A history of hypertension and use of anabolic steroids should also be explored.

Features more consistent with physiologic hypertrophy include ventricular dilation with a uniform pattern of thickening (<2 mm difference in wall thickness between contiguous segments), normal diastolic function, normal mitral valve anatomy without obstruction, either at rest or with exercise, and preserved functional capacity. It

is increasingly appreciated that normal diastolic function and functional capacity can also be seen in athletes with HCM.<sup>42,47</sup> Compared to age-matched sedentary controls with HCM, athletes with HCM appear to have less severe disease expression with milder degrees of LVH, a higher prevalence of apical HCM, and lower prevalence of LVOTO.<sup>42</sup> It remains unclear what role longitudinal strain plays in differentiating athletic HCM patients from athletes with physiologic hypertrophy, as published studies mostly compared athletes with sedentary HCM patients. LV mechanical dispersion and left atrial (LA) strain may hold promise in the future.<sup>20</sup> Exercise stress echocardiography may also have a role in differentiating HCM patients from athletes in the pediatric age group, as they develop LVOT obstruction during submaximal exercise, which is different from athletes.<sup>48</sup>

CMR should be pursued in any athlete if there is ongoing concern after the initial evaluation. The presence of LGE, abnormalities in the mitral valve and subvalvular anatomy, abnormally prolonged T1 time, and abnormally increased extracellular volume fraction favor the diagnosis of HCM.<sup>49</sup> In addition, there are emerging data showing LGE at RV insertion points in athletes.<sup>50,51</sup>

Regression of hypertrophy with detraining has been promulgated as a means of distinguishing these entities. However, there are limited normative data on the expected rate of regression. Furthermore, there are reports that regression may also occur in detrained athletes with HCM.<sup>52</sup>

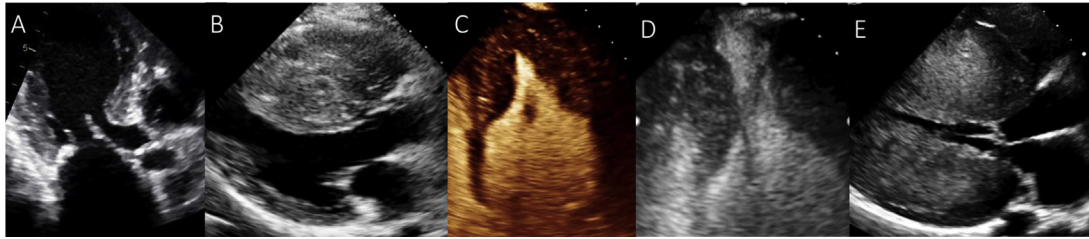


**Figure 1** Transthoracic echocardiographic images representing various phenotypic expressions of hypertrophic cardiomyopathy. A = Sigmoid septum; B = Reversed septal curvature; C = Apical; D = Mid cavity; E = Concentric/neutral. Images courtesy of Dr John Symanski, Sanger Heart & Vascular Institute, Atrium Health, Charlotte, NC.

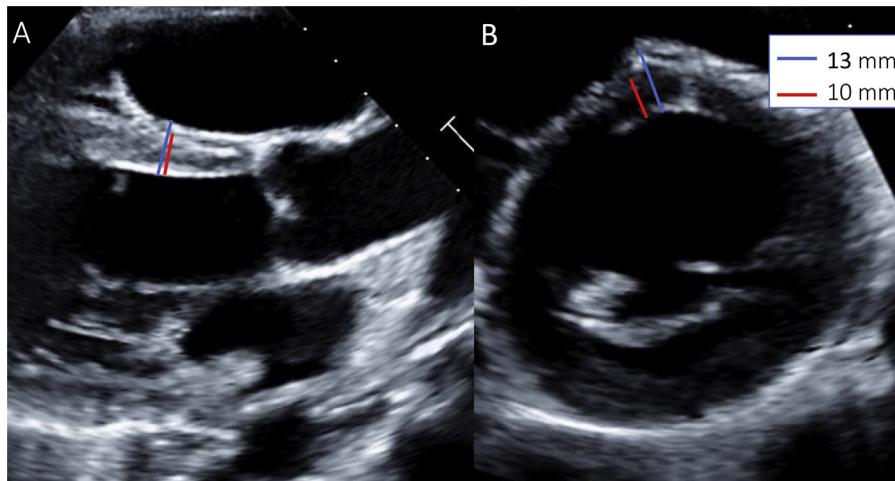


**Figure 2** Challenges in measuring septal wall thickness with echocardiography. Female endurance athlete referred for evaluation of possible hypertrophic cardiomyopathy based on interventricular septal wall (IVS) measurement of 13 mm. Panels A and B are representative parasternal long-axis (PLAX) and short-axis (PSAX) images, respectively, which demonstrate inaccurate IVS measurement (*blue line*) that included right ventricular (RV) trabeculation. Comparison of the PLAX and PSAX views can help differentiate the true contractile IVS (*red line*) from RV trabeculation.

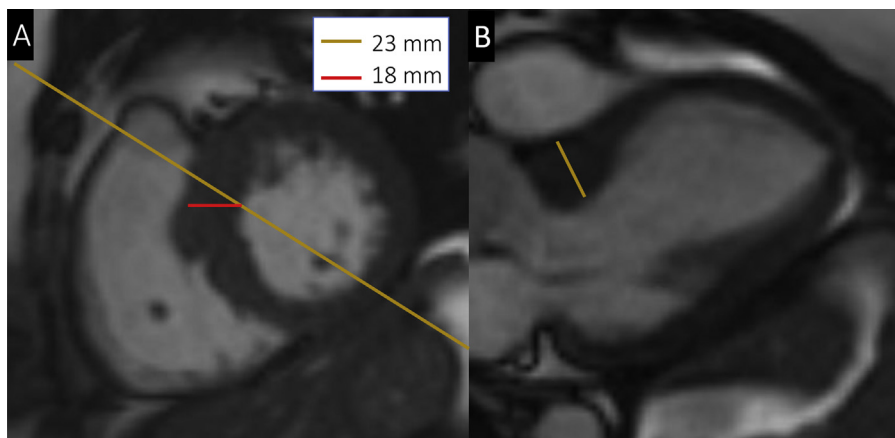


**Figure 3** Challenges in measuring wall thickness with CMR. Cardiac magnetic resonance imaging demonstrating how tangential cuts through septum can overestimate interventricular septal (IVS) thickness on long-axis views. In the short-axis view (**A**), the *yellow line* represents the plane used to obtain the long-axis view (**B**). This line clearly cuts the muscle tangentially, which will overestimate the septal thickness, while the *red line* represents a more accurate nontangential plane through the compacted IVS thickness.

**2. Cardiac Amyloidosis versus HCM.** Echocardiographic and CMR similarities between cardiac amyloidosis and HCM may include increased LV wall thickness, biatrial enlargement, and dia-

stolic dysfunction. Wall thickness may be similar, as the mean septal and posterior wall thicknesses in the ATTR-ACT trial in ATTR (transthyretin) amyloidosis was 17 mm. AL (immunoglobulin light chain)

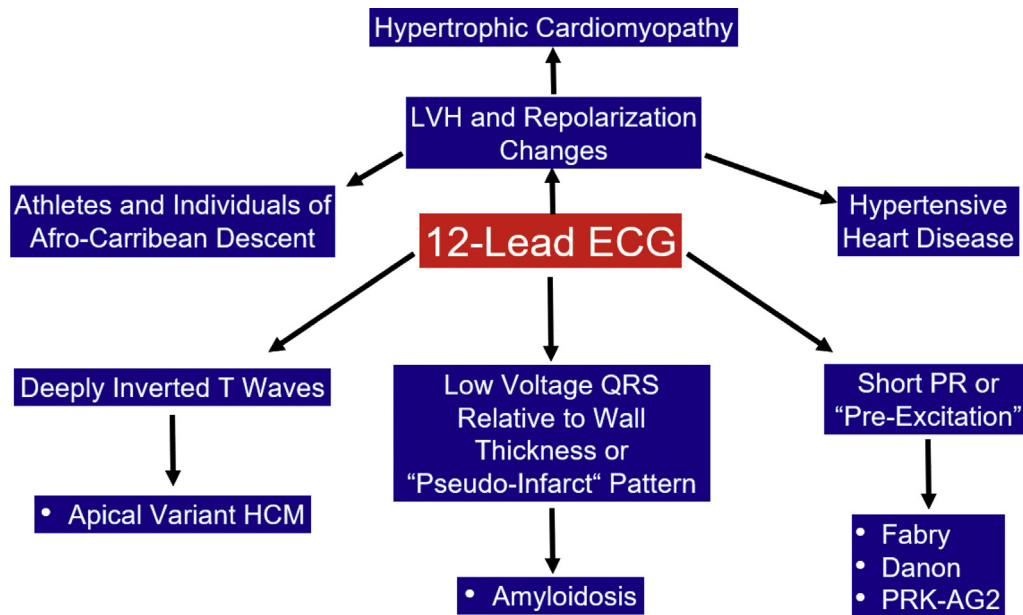


**Figure 4** Integration of the 12-lead ECG in individuals with increased LV wall thickness to aid in the differential diagnosis. Image courtesy of Dr John Symanski, Sanger Heart & Vascular Institute, Atrium Health, Charlotte, NC.

cardiac amyloidosis usually has slightly lower wall thickness compared with ATTR amyloidosis at the time of diagnosis.<sup>53,54</sup> Additional common echocardiographic findings in cardiac amyloidosis include low tissue Doppler  $e'$  and  $s'$  velocities and abnormal global longitudinal strain (GLS) with an apical sparing pattern.<sup>22,55</sup> Longitudinal strain assessment is paramount in patients with increased LV wall thickness, as regional strain patterns have been shown to help reclassify 22% of patients correctly with the largest improvement seen in patients with cardiac amyloidosis.<sup>22</sup> CMR findings characteristic of cardiac amyloidosis include diffuse subendocardial or transmural LGE, abnormal myocardial nulling, and extracellular volume expansion (Table 1). Technetium-based bone scintigraphy (technetium pyrophosphate in the United States) has high accuracy for the diagnosis of ATTR amyloidosis. Other diseases that should be considered in the differential diagnosis are shown in Table 1.<sup>56,57</sup>

## Recommendations and Key Points

- 1- Echocardiography is the initial imaging modality for evaluation of the presence, magnitude, and pattern of LV hypertrophy and UEA should be used whenever needed.
- 2- CMR is indicated in patients with suboptimal echocardiographic images, and patients with borderline LV hypertrophy.
- 3- If CMR is contraindicated or could not be performed, cardiac CT is considered next.
- 4- Irrespective of which imaging modality is used, the report should comment on the pattern and extent of LV hypertrophy including maximum wall thickness.

### C. Assessment of Left Ventricular Systolic Function

Left ventricular ejection fraction (LVEF) is normal to hyperdynamic in the majority of patients with HCM.<sup>58</sup> LV dysfunction, defined as an  $EF < 50\%$ , has been noted in 4-9% of reported

cohorts, and is associated with high rates of all-cause mortality, cardiac transplantation and left ventricular assist device implantation.<sup>59</sup> Echocardiography remains the predominant method of assessing LV systolic function with EF being the most commonly reported quantitative measure. Assessment of LV systolic function can be challenging in patients with large apical aneurysms. Variability in EF measurements can be substantial even with quantitative biplane techniques, and the use of UEA improves concordance with EF measured by CMR. Lower limits of normal LV EF depend on the method used (2D versus 3D). However, these data were obtained from normal subjects and not patients with HCM and thus are not necessarily applicable to HCM patients. The writing group endorses 50% as the lower limits of normal, be it with 2D or 3D echocardiographic imaging given the absence of data in this patient population. In patients with suboptimal echocardiographic imaging, despite the use of UEA, CMR plays an important role. Multiphase cardiac CT correlates well with CMR quantification of LVEF and can be considered in patients in whom CMR is not possible.<sup>60</sup>

Unlike EF, systolic strain (including global longitudinal strain) and strain rate demonstrate a range of regional and global abnormalities in HCM (Figure 5), even in patients with normal wall motion and EF.<sup>61-63</sup> Systolic strain and strain rate abnormalities appear to collocate mostly, but not exclusively, with regions of hypertrophy and are noted in the septum in classic septal hypertrophy and in the apex in the apical variant. Systolic global longitudinal strain predicts event-free survival in HCM patients with normal EF. Measures such as systolic strain rate are also useful in characterizing the myocardial mechanical response with exercise stress.<sup>64</sup> Systolic strain rates are lower in HCM than in normal healthy individuals and the augmentation of systolic strain rate with exercise is significantly blunted in obstructive and non-obstructive HCM patients. Moreover, peak systolic strain rate correlates with exercise capacity and is

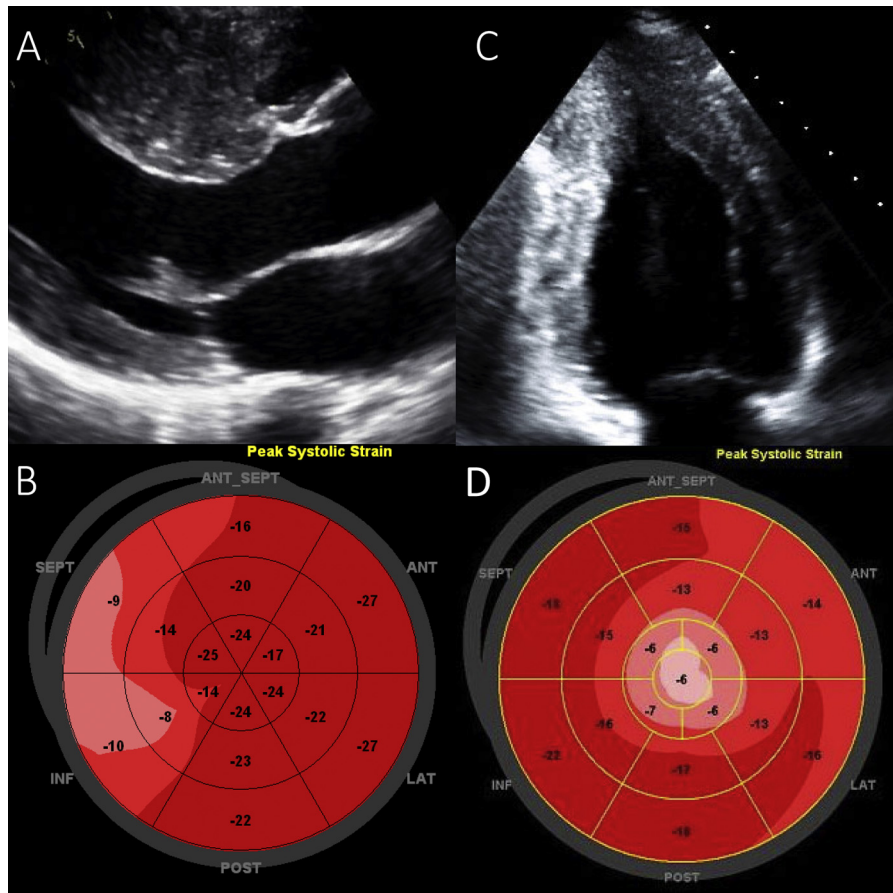


**Figure 5** Typical patterns of regional strain in hypertrophic cardiomyopathy (HCM). Parasternal long-axis view of a patient with septal HCM (**A**) with corresponding longitudinal strain polar map (**B**) showing reduction in strain at the septum. (**C**): An apical 2-chamber view of a patient with apical HCM with corresponding longitudinal strain polar map (**D**) showing reduction in strain at the apex.

inversely related to the burden of scar as quantified by percent LGE by CMR.<sup>64</sup>

Similarly, feature-tracking cardiac magnetic resonance (FT-CMR) is one of several CMR imaging techniques used to assess myocardial strain. It tracks features of interest along contour lines on routinely acquired cine images, following the same basic premise of speckle tracking echocardiography. Its main advantage, relevant for clinical adoption, is that, as a postprocessing CMR technique of routinely acquired steady-state free precision sequences, there is no need for additional image acquisition. It has been shown to aid in differentiation between HCM and hypertensive heart disease,<sup>65</sup> and detection of abnormal strain in preclinical (prior to development of hypertrophy) and pediatric patients.<sup>66,67</sup>

As in the adult population, in children with HCM, LVEF is normal to hyperdynamic in most patients. There are some differences when looking at deformation parameters, with reduced longitudinal strain and strain rates when assessed segmentally but with global values remaining within normal range in a larger proportion of pediatric cases.<sup>68</sup> With regard to torsion, some pediatric studies have shown altered basal rotation but with preserved and even increased apical rotation.<sup>69</sup>

## Recommendations and Key Points

- 1- Assessment of LVEF should be performed in all HCM patients using echocardiography, with or without UEA, at the time of diagnosis and when there is a significant change in clinical condition. There should be a low threshold for using imaging modalities such as CMR or CT for LV systolic function assessment when echocardiographic images are suboptimal.
- 2- Assessment of global longitudinal strain adds important prognostic data and may be performed in centers with experience and expertise with using strain echocardiography.

### D. Assessment of Left Ventricular Diastolic Function

Diastolic dysfunction occurs in HCM patients due to impaired LV relaxation and increased myocyte and chamber stiffness. In addition, abnormal LA function, in part due to an atrial myopathy, can be an important cause of impaired LV filling. Diastolic dysfunction accounts, in part, for the symptomatic status of patients with and without obstruction. It is not practical to perform cardiac catheterization to assess LV diastolic function in most patients, and thus noninvasive

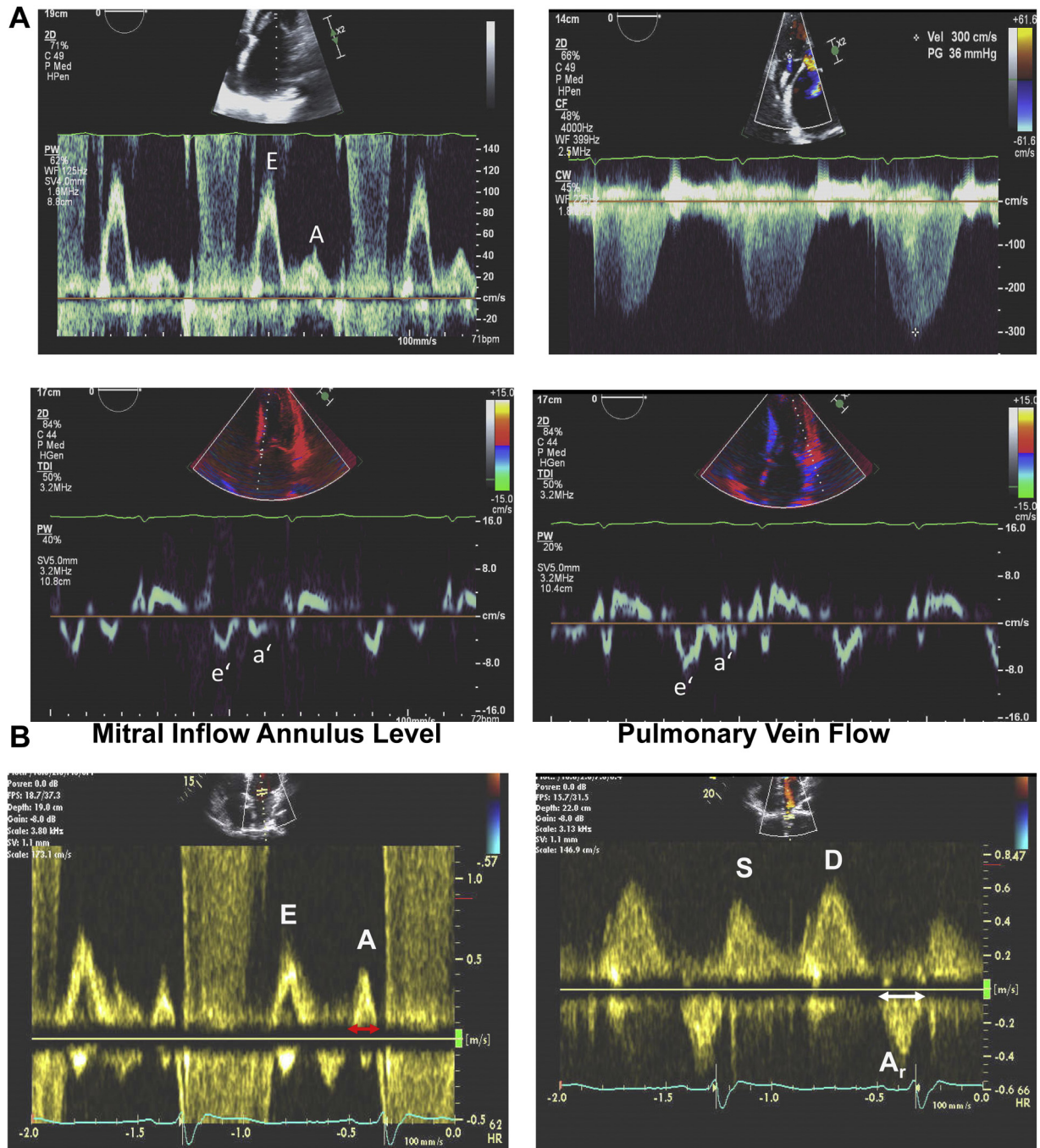


**Figure 6** (A) Mitral inflow velocity measured at the leaflet tips (upper left), peak tricuspid regurgitation velocity recorded by CW Doppler (upper right), and tissue Doppler velocities measured at the septal (lower left), and lateral (lower right) aspects of the mitral annulus from a symptomatic patient with obstructive hypertrophic cardiomyopathy and dilated left atrium. Peak TR velocity at 3 m/s and the increased average E/e' ratio (>14) are consistent with increased mean left atrial pressure. E = mitral inflow early diastolic velocity, A = mitral inflow atrial diastolic velocity, e' = mitral annulus early diastolic velocity, and a' = mitral annulus atrial diastolic velocity. (B) Prolonged Ar -A duration from an HCM patient with increased LV end diastolic pressure. Ar (white arrow) atrial reversal velocity recorded from the right pulmonary vein and A (red arrow) mitral A velocity with the sample volume placed at level of mitral annulus.

imaging has become the standard approach to diagnose and identify the presence of abnormally elevated LV filling pressures.<sup>70-72</sup> Assessment of abnormal LV filling patterns is affected by both LV relaxation and transmitral pressure gradient. Echocardiography allows for the dissection of hemodynamic determinants of LV filling and is usually the only test utilized for that objective. Notwithstanding, there are emerging data showing the feasibility of measurement of mitral annulus velocities by CT and CMR, albeit not tested specifically in patients with HCM.<sup>73,74</sup>

Identification of diastolic dysfunction, similar to other cardiovascular conditions, requires a comprehensive approach.<sup>75</sup> It includes mitral inflow velocities recorded at the annulus (for mitral A duration) and leaflet tips, early diastolic velocity by tissue Doppler at the septal and lateral sides of the mitral annulus, peak tricuspid regurgitation (TR) velocity measured by CW Doppler from multiple windows, biplane LA maximum volume index, and pulmonary vein velocities. Mitral regurgitation (MR) of at least moderate severity can affect LA volumes and E/e' ratio, irrespective of LA pressure. Thus, in the absence of  $\geq$ moderate MR, LA maximum volume index, average E/e' ratio, and peak TR velocity should be considered in reaching conclusions about LA pressure. In the presence of significant MR, peak TR velocity and pulmonary vein atrial reversal velocity are the more reliable indices of LV filling pressures. In particular, Ar-A duration  $>30$  ms is consistent with increased LV end diastolic pressure (Figures 6 and 7). A number of studies have associated a restrictive LV filling pattern and increased E/e' ratio in HCM patients with heart failure hospitalizations, reduced exercise tolerance in children and adults, and SCD.<sup>76-80</sup> In patients with atrial fibrillation, the specific measurements recommended in the ASE 2016 diastolic function guideline should be considered.<sup>75</sup> Thus, a short deceleration time is indicative of increased LA pressure when EF is depressed. For normal LVEF, isovolumic relaxation time, peak acceleration of mitral E velocity, septal E/e' ratio, deceleration time of pulmonary vein diastolic velocity, and peak TR velocity are the variables that should be considered, although data in HCM patients with atrial fibrillation are very limited.

There are growing data showing the association of LA reservoir, conduit, and pump (contractile) strain with reduced exercise tolerance, and subsequent development of atrial fibrillation.<sup>81-83</sup> However, there is a paucity of data on the hemodynamic determinants of LA strain in HCM and the impact of inter-vendor differences in LA strain measurements and whether these are equivalent or not.<sup>84</sup> At the present time, it is reasonable to record and report LA strain values when serial analysis is performed by the same software for a given patient. Interestingly, CMR studies have shown a high burden of atrial fibrosis in HCM patients, which likely accounts for the abnormal LA function.<sup>85</sup>

More recently, the speed of propagation of extrinsically generated shear waves was shown to be higher in children and adults with HCM when compared to normal controls, likely reflecting higher myocardial stiffness.<sup>7</sup> While promising, these studies are few and lack validation with invasive measurements. The speed of propagation is affected not only by intrinsic stiffness but also loading conditions and wall thickness. In addition, shear wave propagation speed is measured only in the septum and given the heterogeneity of myocardial structure and function in HCM, it remains to be seen if a local measurement can be reflective of global function.

The assessment of diastolic dysfunction in children remains a challenge. The adult guidelines should not be applied to the pediatric population, including the cutoff values for the different diastolic parameters.<sup>86</sup> While there are published normal data by age groups for all parameters, the normal range is very wide. The assessment of left atrial strain and function as well as stiffness analysis by shear wave imaging show promising results in the pediatric population but require further studies and validation.<sup>87,88</sup>

## Recommendations and Key Points

- 1- A comprehensive approach is recommended for the evaluation of diastolic function in HCM.
- 2- Diastolic function assessment includes mitral inflow velocities recorded at annulus and leaflet tip levels, early diastolic velocity by tissue Doppler

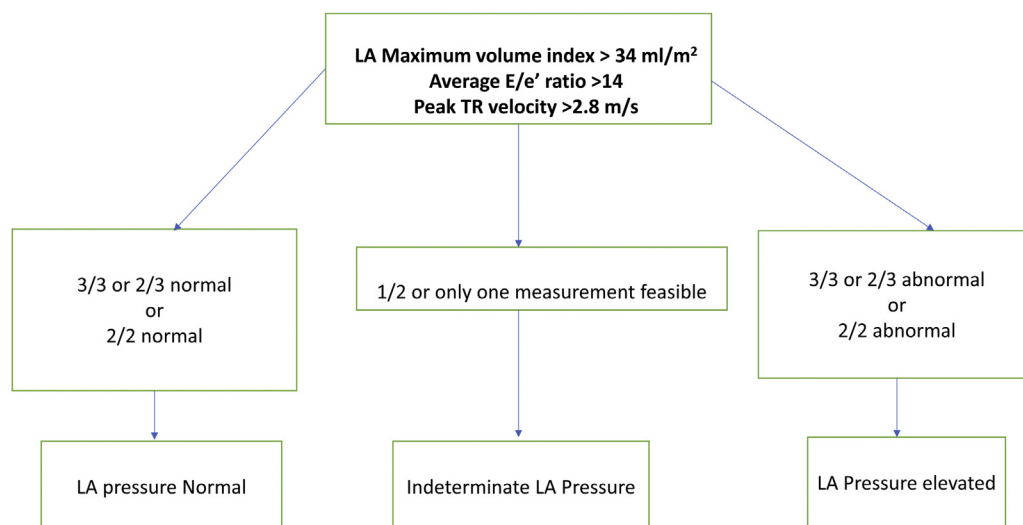


**Figure 7** Algorithm for estimation of mean LA pressure in HCM patients without significant mitral regurgitation.<sup>75</sup>

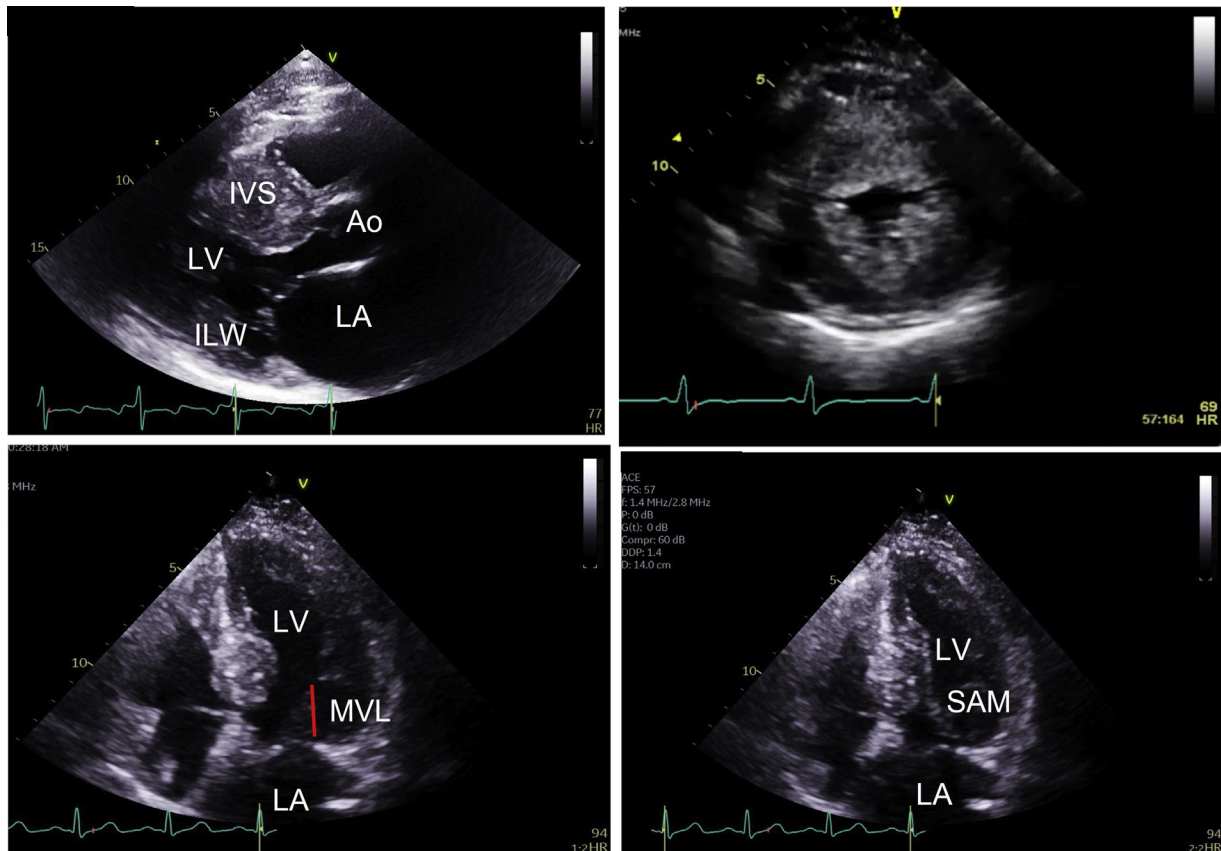


**Figure 8** (Upper left) Parasternal long-axis view (PLAX). Severe asymmetric septal hypertrophy. Septum measures 3.2 cm. (Upper right) Parasternal short-axis view (PSAX). Asymmetric septal hypertrophy involving anterior septum and anterior wall. (Lower left) Apical 4-chamber view (A4C). The tips of the elongated leaflets protrude into the left ventricle and coapt in the body of the leaflets (red line). (Lower right) A4C. Elongated anterior mitral leaflet coming in contact with the septum (SAM). *IVS*, interventricular septum; *LV*, left ventricle; *ILW*, inferolateral wall; *AO*, aorta; *LA*, left atrium; *MVL*, mitral valve leaflets; *SAM*, systolic anterior motion of the mitral valve.

measured at septal and lateral sides of the mitral annulus, peak TR velocity obtained by CW Doppler from multiple windows, biplane LA maximum volume index, and pulmonary vein velocities.

- 3- A restrictive LV filling pattern and increased E/e' ratio in HCM patients is associated with heart failure hospitalizations, reduced exercise tolerance in children and adults, and SCD.

### E. Assessment of Dynamic Obstruction and Mitral Valve Anatomy

Left ventricular outflow tract obstruction (LVOTO) commonly occurs in patients with HCM. Resting LVOTO, considered significant with a peak gradient  $\geq 30$  mm Hg, is present in about 30-35% of symptomatic patients with HCM. In another 30-35%, obstruction is latent and only inducible by provocative maneuvers (e.g., Valsalva or amyl nitrite inhalation). If bedside maneuvers fail to induce LVOTO then exercise echocardiography is recommended.<sup>89</sup> The remaining 30% of patients do not have either a resting or provoked LVOT gradient and are classified as having non-obstructive HCM.<sup>90,91</sup>

The presence of a resting peak LVOT gradient  $\geq 30$  mm Hg is associated with increased risk of SCD and progression to New York Heart Association Class III or IV symptoms of heart failure.<sup>92</sup> Resting or provoked gradients of  $\geq 50$  mm Hg are considered a threshold for invasive therapy in patients who exhibit drug-refractory symptoms.<sup>2,93</sup> Notably, LVOTO in HCM is a labile and dynamic phenomenon that can vary depending on LV afterload, preload, and contractility.<sup>94,95</sup>

The main structural abnormalities contributing to LVOTO are septal hypertrophy, narrowing of the LVOT, and mitral valve (MV) and subvalvular apparatus abnormalities. Many patients with obstructive HCM have elongation of both mitral valve leaflets, and patients with obstructive cardiomyopathy have longer leaflets than patients with non-obstructive HCM. Elongated leaflets extend further into the LV cavity and coapt at the body of the leaflets rather than at the leaflet tips.<sup>96,97</sup> The residual portion of the anterior leaflet extends past the coaptation point, which contributes to the predisposition toward systolic anterior motion (SAM) of the mitral valve<sup>13,98</sup> (Figure 8). Uncommonly, isolated elongation of the posterior mitral valve leaflet can lead to SAM.<sup>13</sup>

Furthermore, abnormalities of papillary muscles frequently contribute to development of SAM and dynamic LVOTO. Anterior

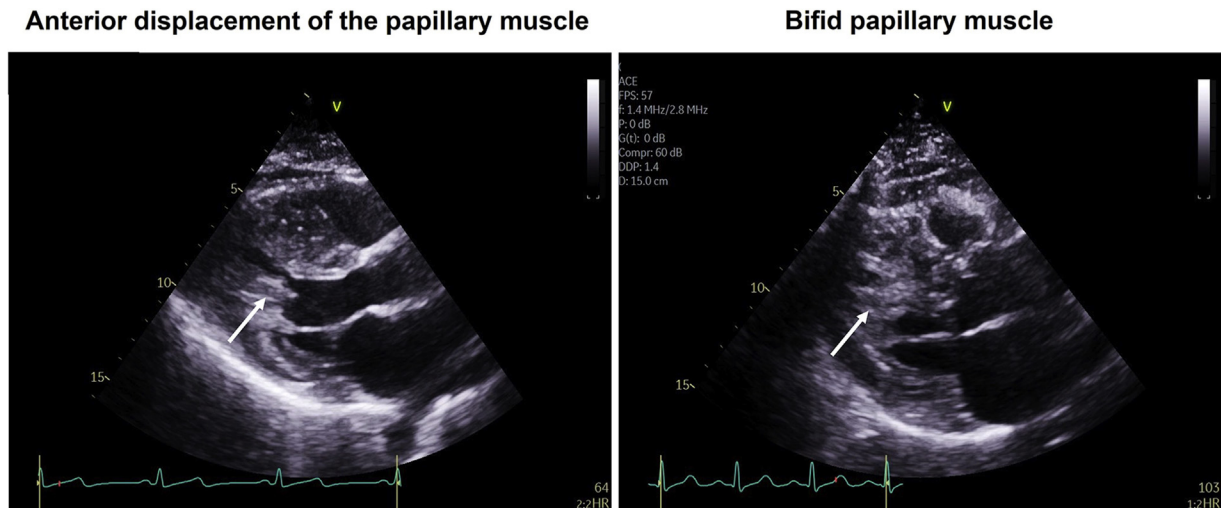


**Figure 9** (Left) Parasternal long-axis view (PLAX). Anteriorly displaced hypertrophied papillary muscle (*white arrow*) with a lax chord prolapsing into the left ventricular outflow tract (LVOT). (Right) PLAX. Bifid papillary muscle (*white arrow*) inserting directly to the underbelly of the anterior mitral valve leaflet leading to LVOT obstruction.

or apical displacement of the papillary muscle results in chordal-leaflet laxity, which in turn contributes to SAM.<sup>97</sup> Other papillary muscle abnormalities identified in patients with HCM include bifid papillary muscle (70% of HCM patients on CMR) (Figure 9), anomalous insertion of papillary muscle directly into the anterior leaflet (13% of patients), hypertrophy of the papillary muscles,<sup>99,100</sup> hypermobile accessory papillary muscles<sup>101</sup> and, less commonly, presence of accessory chords to the body of A2 segment of the anterior mitral leaflet. Descriptions of these variations should be included in the imaging report to help guide surgical planning.

SAM is the result of drag forces on the anterior mitral valve leaflet, pushing it toward the LVOT. The development of SAM can begin at normal LVOT velocity, preceding systolic flow acceleration in the LVOT. In addition to drag forces on the mitral leaflets, Venturi forces created as flow enters the narrowed LVOT may contribute to obstruction. Although Venturi forces are present in the LVOT, they are not the primary cause of SAM. Rather, a larger leaflet area and length predispose the mitral valve leaflets to be swept anteriorly, closer to the septum by drag forces.<sup>102</sup> Although SAM is commonly described in patients with HCM, it is not specific to this disease. It can occur in other conditions provoked by reduced afterload, increased inotropic state, or reduced preload.<sup>103-108</sup> An example of this is the postoperative repair of a myxomatous mitral valve in a patient with basal septal hypertrophy or sigmoid septum, in which the LV is underfilled coming off bypass. In this situation, a number of factors converge and produce SAM along with LVOTO. These include elongated mitral leaflets, a narrow LVOT, a small LV cavity, and hyperdynamic ventricle. In general, these can be reversed with volume loading, afterload increase, and cessation of inotropic agent administration. Similarly, SAM with dynamic obstruction can be seen in patients on inotropic drugs who are volume depleted, particularly if elderly with basal septal hypertrophy. Careful clinical assessment and supplemental information are needed to establish the etiology of SAM/LVOTO. Conditions other than HCM resulting in SAM and LVOTO are listed in Table 2.

### 1. Echocardiographic Techniques in the Evaluation of Left Ventricular Outflow Tract Obstruction

The echocardiographic report, in addition to quantification of LVOTO and mitral valve regurgitation, should contain a clear statement about anatomy of the mitral valve, the degree of SAM, the effect of provocative maneuvers on the degree of obstruction, and papillary muscle morphology.<sup>1</sup> Thorough evaluation requires utilization of multiple echocardiographic techniques.

**i. M Mode.** Prior to the development of Doppler echocardiography, the degree of LVOTO was evaluated by determining the presence and duration of SAM by M-mode echocardiography.<sup>109</sup> The severity of SAM was categorized by SAM-septal distance and the duration of leaflet-septal contact: (1) mild: SAM-septal distance >10 mm; (2) moderate: SAM-septal distance ≤10 mm, or brief mitral leaflet-septal contact (<30% of systolic duration); and (3) severe: prolonged SAM-septal contact, lasting ≥30% of systole.<sup>110</sup> In addition, M mode may depict mid-systolic notching of the aortic valve, which is caused by the attenuation in blood flow as obstruction develops.<sup>111</sup> (Figure 10).

**ii. Color Flow and Pulsed-Wave Doppler.** Once SAM is identified by M-mode and 2D imaging, color flow (CF) Doppler is used to localize turbulent, aliased flow indicating increased velocity (Figure 11). Pulsed-wave (PW) Doppler can be utilized to interrogate velocities sequentially and systematically from the LV apex all the way to the LVOT in order to confirm the anatomical level of obstruction; however, this is also usually apparent with color Doppler, which is less time consuming. Localization of obstruction using PW Doppler is done in the apical 5-chamber view (A5C) and/or apical three-chamber view (A3C). In the body of the LV, PW Doppler has a typical shape of a low-velocity, late-peaking envelope (Figure 12). If LVOTO is severe, usually >60 mm Hg at rest, a phenomenon called “lobster-claw” abnormality can be seen.<sup>98,112</sup> (Figure 12) This characteristic Doppler envelope has two low

**Table 2** Differential Diagnosis of SAM and LVOTO

Elderly with hypertension, sigmoid septum and hyperdynamic LV function
Compensatory basal septal hypercontractility following acute myocardial infarction with apical dysfunction
Takotsubo cardiomyopathy with hyperdynamic basal LV function
Massive posterior mitral annulus calcification
After surgical and percutaneous mitral valve repair
After aortic valve replacement in patients with LVH and hyperdynamic LV
Elderly patients in ICU with anemia, volume depletion, tachyarrhythmias, sepsis
Medications eg: inotropes, vasodilators and sympathomimetics
Right ventricular pressure overload like acute COPD exacerbation and/or ARDS
Phenocopies of HCM such as cardiac amyloidosis or Anderson-Fabry disease

velocity systolic components; the first one early in systole, which rapidly decelerates due to afterload mismatch, and the second one late in systole when flow resumes after LVOT obstruction is relieved. The onset of rapid deceleration of the early systolic flow corresponds to the initial leaflet-septal contact and a notch in the aortic valve, as described above. The nadir of flow deceleration corresponds to peak of the LVOT gradient.

When a localized sudden increase in velocity and aliasing are present, a change to high pulse repetition frequency (HPRF) Doppler could be considered to further evaluate flow velocities and the shape of the velocity waveform.<sup>113</sup>

**iii. Continuous-Wave Doppler.** Typically, in HCM, outflow velocities increase slowly in early systole, then rise abruptly and peak in mid-to-late systole, resulting in a characteristic “dagger-shaped” envelope (Figure 13). Maximal instantaneous gradient, reflecting severity of the obstruction, is determined by measuring the peak LVOT velocity using CW Doppler and calculated with the simplified Bernoulli equation ( $LVOT\ gradient = 4 \times [LVOT\ velocity]^2$ ). There is excellent correlation between the pressure gradient determined by CW Doppler and the LVOT gradient obtained by cardiac catheterization. Variations in waveform configuration in HCM can be encountered. Occasionally, the rate of increase in velocities in early systole is more rapid and the peak velocity is achieved earlier in systole, producing a more symmetrically shaped envelope<sup>114</sup> (Figure 14). However, the shape of both envelopes, mid- and late-peaking, is distinctly different from the Doppler spectral profile of fixed valvular aortic stenosis.

**iv. Transesophageal Echocardiography.** Transesophageal echocardiography is recommended in patients with poor transthoracic echocardiographic windows and/or difficulty in establishing the etiology of LVOTO, mitral valve and papillary muscle abnormalities, and/or mechanism of mitral valve regurgitation (Figure 15). In particular, the mid-esophageal and transgastric long axis views can provide detailed assessment of the mitral valve apparatus.

**v. Three-Dimensional echocardiography.** Three-dimensional technology has been successfully applied in imaging of SAM and associated abnormalities during TTE and TEE examinations (Video 2).<sup>115</sup>

## 2. Pitfalls and Challenges in the Evaluation of Left Ventricular Outflow Tract Obstruction

**i. Mitral Regurgitation.** Because of the close anatomic proximity, it can be hard to distinguish high-velocity LVOT flow from that of MR, which is usually present in patients with SAM. Efforts should be made to isolate, record, and label the MR signal by sweeping the CW Doppler beam away from the LVOT and directly into the MR jet. Anteriorly directed jets of MR can be particularly difficult to differentiate from the LVOT signal and can require steep probe tilting and off-axis imaging to align the Doppler beam out of the LA. Although the MR envelope in HCM can have slight acceleration of flow at the time of SAM, and both flows can peak in mid-systole, the MR velocity waveform usually peaks earlier than that of LVOT flow. The duration of MR may be longer, often beginning during isovolumic contraction although, in HCM, MR may only begin with SAM-induced leaflet separation in mid-to-late systole. Overall, the MR envelope is more rounded, and the velocity is always higher than LVOT velocity (Figure 16). Caution is advised when interpreting a flow velocity higher than 5.5 m/s as representing the LVOT signal, when this high-velocity flow could be consistent with MR.<sup>114</sup> The LVOT gradient also can be estimated using the systolic blood pressure and the MR velocity, as illustrated in Figure 17. As a general rule, the difference in peak gradient between the MR jet (LV systolic pressure) and LVOTO jet should be close to the systolic blood pressure (ignoring left atrial pressure results in a lower estimate of LV outflow tract gradient). The stand-alone CW Doppler probe may be useful and sometimes, depending on the degree of anterior angulation of the LVOT, an accurate gradient may be obtained from a high right parasternal or suprasternal view.

**ii. Discrete Subvalvular Stenosis.** Discrete subvalvular stenosis (DSS) can be encountered as an isolated abnormality or as a component of a more complicated congenital condition, most notably Shone complex. Findings that favor the diagnosis of DSS include an early peaking LVOT signal and the presence of associated aortic regurgitation. TTE may be sufficient to make a diagnosis by visualizing a membrane or circumferential narrowing of LVOT commonly involving the base of the anterior mitral leaflet, but DSS can be associated with septal hypertrophy and turbulence with flow acceleration in the LVOT and may be mistaken for HCM. M-mode depiction of systolic notching of the aortic valve is not a specific finding for HCM and it may occur in a variety of other conditions where a drop in LV ejection velocity may be encountered.<sup>116</sup> The absence of SAM suggests the presence of fixed rather than dynamic obstruction<sup>117,118</sup> (Figure 18).

**iii. Hyperdynamic LV Function.** In patients with a hyperdynamic LV and concomitant cavity obliteration, CW Doppler can demonstrate very late-peaking systolic flow acceleration.<sup>105,114</sup> Color and PW Doppler can localize the origin of this flow to the area of cavity obliteration.<sup>119</sup> This is distinctly different from the mid-to-late-peaking, dagger-shaped high-velocity flow characteristic of HCM. Careful assessment of the associated clinical presentation is necessary to appropriately

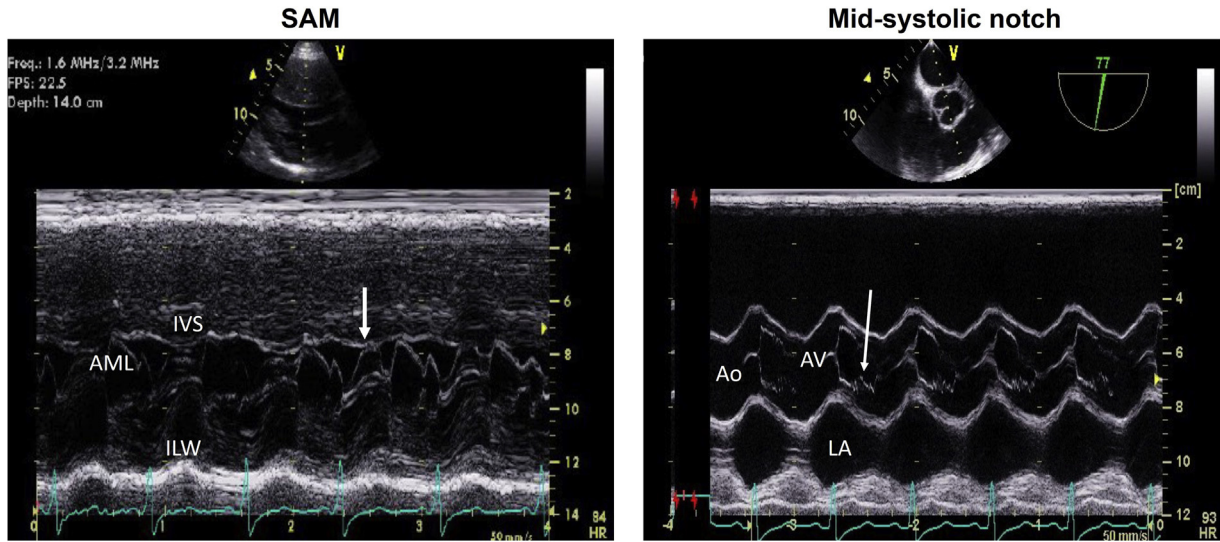


**Figure 10** M-mode echocardiographic traces of the mitral and aortic valves. (Left): Anterior mitral valve leaflet (AML) contacting the septum (IVS), identified by *white arrow*. (Right): Mid-systolic notch (*white arrow*) due to premature closure of the aortic valve (AV), correlating with the peak left ventricular outflow tract gradient.

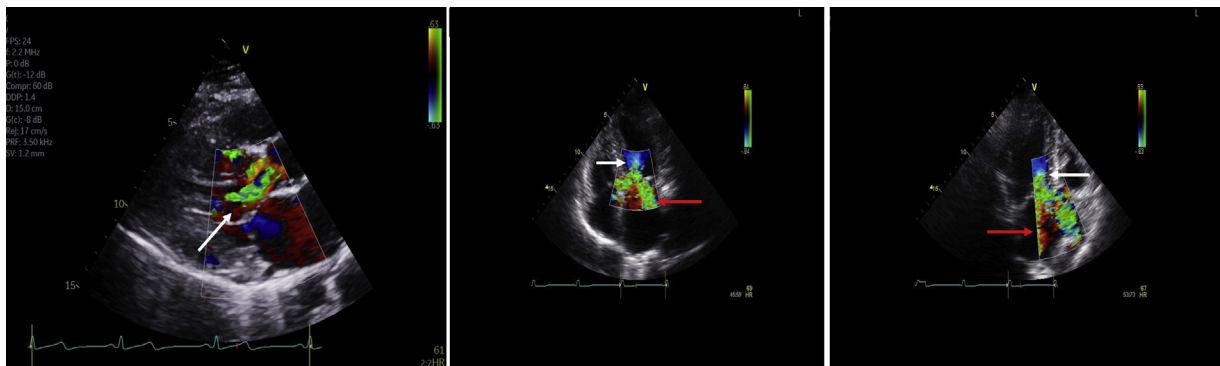


**Figure 11** (Left): Parasternal long-axis view. Color flow (CF) Doppler shows the beginning of turbulent flow in the left ventricular outflow tract (LVOT) identifying the level of obstruction (*white arrow*). (Middle): Apical 4-chamber view. Turbulent flow in the LVOT (*white arrow*) with simultaneous turbulent flow in the left atrium from an eccentric, posteriorly directed mitral valve regurgitant jet (*red arrow*). (Right): The same flows in the apical 3-chamber view.

**Low-velocity flow in the body of LV**

**“Lobster claw” abnormality**

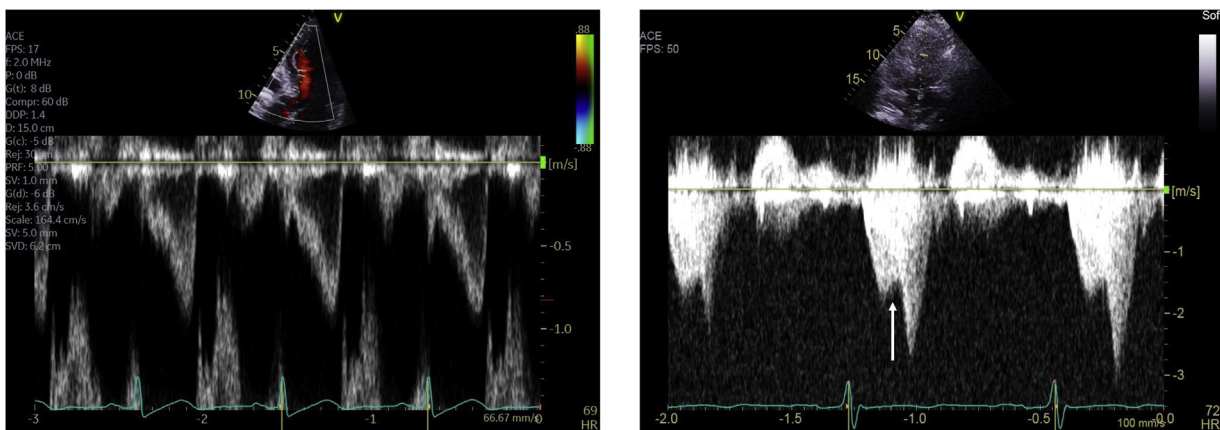


**Figure 12** (Left): Apical 5-chamber view (A5C). Pulsed-wave (PW) Doppler of a low-velocity late-peaking flow in the body of the left ventricle (LV) proximal to the left ventricular outflow tract (LVOT) obstruction. (Right): A5C. CW Doppler. “Lobster claw” abnormality in the LV cavity prior to SAM. Note mid-systolic drop in left ventricular velocity due to sudden rise in afterload (*white arrow*).

### Late-peaking, dagger-shaped LVOT velocity waveform at rest and with Valsalva

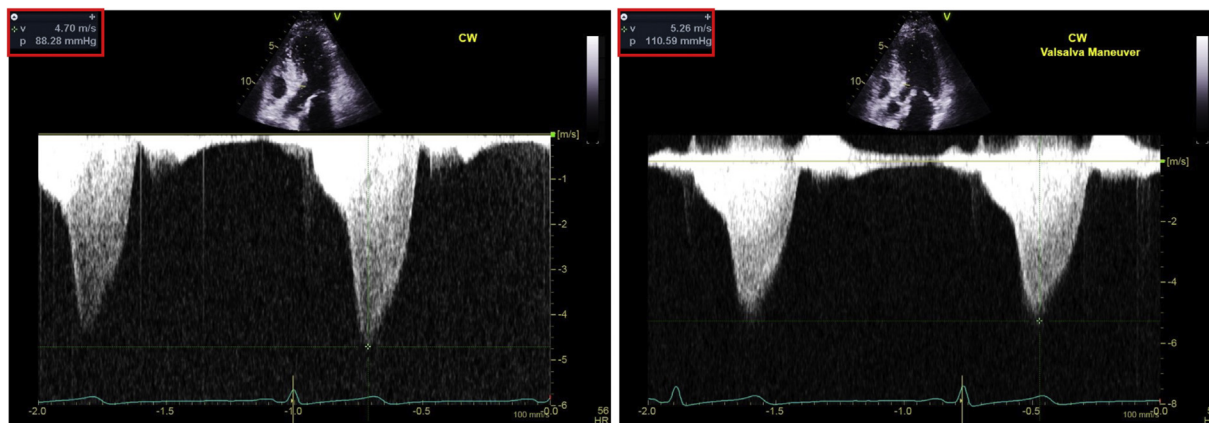


**Figure 13** (Left): Apical 5-chamber view (A5C). Continuous-wave (CW) Doppler recording of a dagger shape or concave-to-the-left contour of a typical left ventricular outflow tract (LVOT) velocity waveform in obstructive hypertrophic cardiomyopathy. The mid-systolic flow acceleration peaks at 4.7 m/s, yielding a peak dynamic LVOT gradient of 88 mm Hg (red box). (Right): A5C. CW Doppler waveform indicating accentuated LVOT dynamic obstruction in the same patient (5.26 m/s = 110 mm Hg) after Valsalva maneuver (red box). Note that peak gradient was calculated from peak velocity using the modified Bernoulli equation ( $4V^2$ ).

diagnose patients, as many conditions with a hyperdynamic LV can be associated with mid-cavitary gradients in the absence of HCM.

**iv. Concomitant Aortic Valve Stenosis.** The presence of aortic stenosis (AS) coexisting with obstructive HCM is a diagnostic challenge that requires meticulous echocardiographic assessment to establish the correct diagnosis. It is particularly important to evaluate the severity of each condition to recommend the appropriate therapeutic plan. Careful 2D imaging of the valve, assessing leaflet thickening/calcification and restricted leaflet motion, is important in identifying intrinsic aortic valve pathology. In addition, color Doppler can identify the area of turbulence and PW Doppler confirms the level of obstruction by localizing flow acceleration. AS is a fixed obstruction, hence the shape of the CW Doppler envelope is usually early peaking and triangular in mild stenosis and rounded, peaking in mid-systole, in more severe stenosis. It differs from dynamic LVOTO where a mid-to-late-peaking dagger-shaped envelope is encountered. Both envelopes might be superimposed since they are tandem stenoses<sup>120</sup> (Figure 19). Furthermore, the severity of dynamic obstruction can be uncovered after aortic valve replacement which decreases afterload.

In a patient with concomitant AS and HCM, use of the continuity equation is not recommended to calculate aortic valve area. Direct planimetry by TEE, CT, or CMR should be considered. The simplified Bernoulli equation to calculate peak AS gradient cannot be used in serial stenoses. When peak velocity in the LVOT exceeds 1.5 m/s, the peak aortic gradient can be calculated using the formula:  $4(V_2^2 \text{ max} - V_1^2 \text{ prox})$ . Invasive hemodynamic evaluation is recommended if a definitive diagnosis cannot be established by imaging.<sup>121</sup>

### Recommendations and Key Points

- 1- LVOT obstruction occurs in 70-75% of patients, where there is either a resting or provoked LVOT gradient. A systematic approach using provocative maneuvers can differentiate non-obstructive from obstructive phenotype. (Figure 20).
- 2- Most patients with HCM and LVOTO have abnormalities of the mitral valvular and subvalvular apparatus. SAM is a result of drag forces on elongated mitral valve leaflets.

- 3- SAM/LVOTO is not specific for HCM and can occur in other conditions provoked by reduced afterload, reduced preload, and increased LV contractility.
- 4- CW Doppler shows a mid-to-late-systolic peaking, dagger-shaped spectral pattern characteristic of dynamic LVOTO. The LVOT gradient can be determined using the modified Bernoulli equation:  $\text{LVOT gradient} = 4 \times (\text{LVOT velocity})^2$
- 5- Dynamic LVOTO obstruction should be differentiated from fixed subvalvular, valvular, or supra-valvular stenosis. The CW Doppler envelope in these latter conditions is usually early peaking.
- 6- The echocardiographic report, in addition to blood pressure, quantification of LVOT gradient, and mitral valve regurgitation severity, should contain a clear statement about the anatomy of the mitral valve, the presence of SAM, the effect of provocative maneuvers on LVOT gradient, and papillary muscle abnormalities if present.

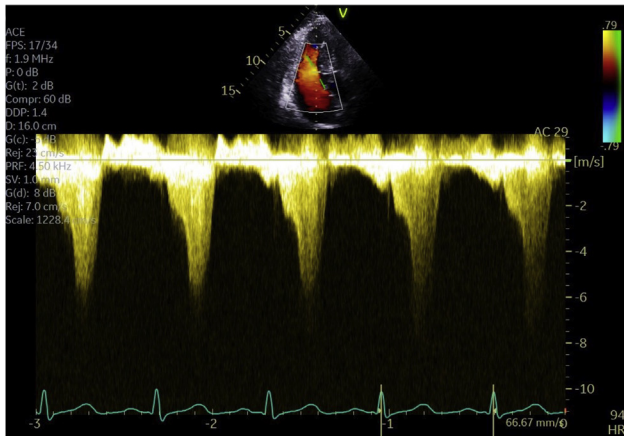
### 3. Provoking Obstruction

LVOTO is dynamic and dramatically influenced by loading conditions. In patients who do not meet gradient thresholds for consideration of SRT, it is imperative to perform various provocative maneuvers. Imaging in a post-prandial state may also reveal latent obstruction. There are several maneuvers, described below, used to assess for a provokable LVOT gradient.

**i. Strain phase of the Valsalva maneuver.** The strain phase of the Valsalva maneuver, during which there is forced exhalation against a closed airway, results in increased intrathoracic pressure and a decrease in venous return, which can precipitate LVOTO. A limitation to the Valsalva maneuver is the subjective nature of the effort and thus variable response. In general, a Valsalva-induced gradient is less than that induced by exercise.<sup>12</sup> A “goal-directed” approach can be considered, where an aneroid manometer (blood pressure cuff) is connected to a disposable 10-mL syringe and the patient instructed to blow into the syringe and maintain a pressure of  $>40$  mm Hg for  $>10$  seconds.<sup>122</sup>

**ii. Squat to Stand.** Squat to stand also decreases venous return with a resultant decrease in preload and LV size with worsening

**Dagger-shaped LVOT velocity**



**Symmetric LVOT velocity**

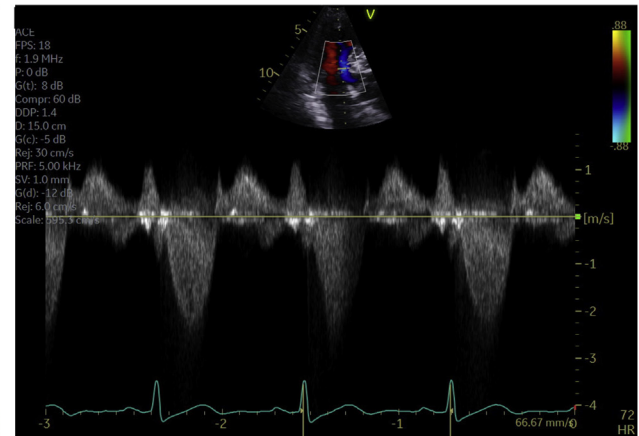


**Figure 14** Apical 3-chamber view. Two continuous-wave Doppler left ventricular outflow tract obstruction (LVOT) velocities from 2 patients with obstructive HCM: one (left) typical, late-peaking, concave to the left, and another (right) less common, more symmetric, slow rising and peaking in mid-systole.

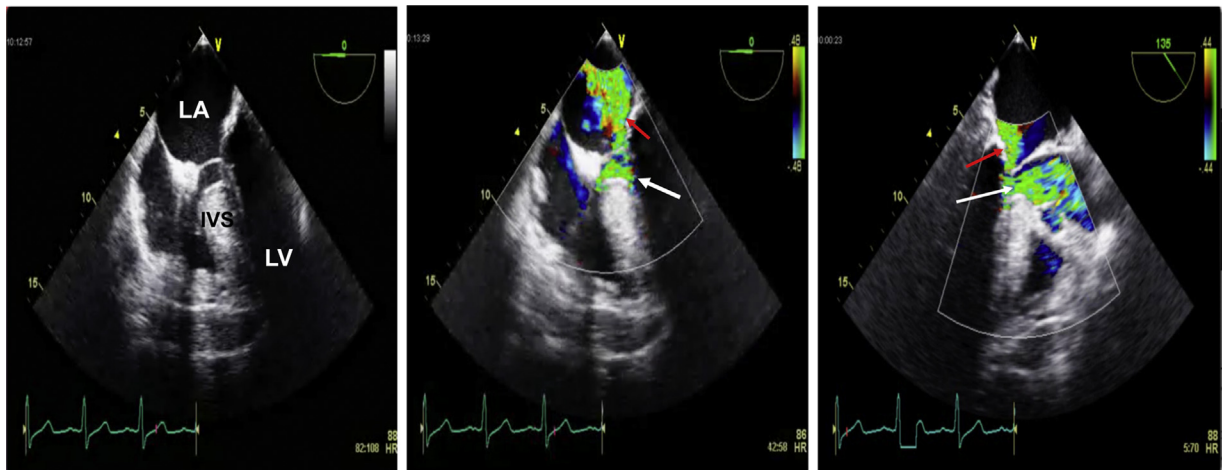


**Figure 15** TEE. (Left): Midesophageal 4-chamber view (ME4C). Elongated anterior mitral valve leaflet and systolic anterior motion of the mitral valve (SAM). Note hypertrophy of the interventricular septum. (Middle): ME4C. Color Doppler of two separate turbulent flows in mid-systole in two directions: one due to left ventricular outflow tract obstruction at the site of SAM (white arrow) and another due to the eccentric, posteriorly directed mitral regurgitation (red arrow). (Right): The same flows seen in the ME long-axis view.

**Late-peaking LVOTO velocity**



**LVOTO velocity and superimposed MR velocity**

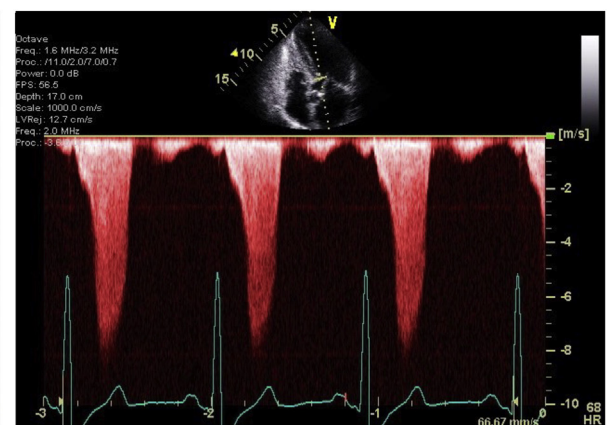


**Figure 16** (Left): Apical 3-chamber view. Continuous-wave (CW) Doppler high-velocity late-peaking left ventricular outflow tract (LVOT) flow separated from the mitral regurgitation (MR) flow. (Right): Apical 4-chamber view. CW Doppler waveform containing superimposed velocities: LVOT and MR (peak velocity at 7.5 m/s). When LVOT and MR velocities are superimposed, the highest velocity overestimates the LVOT gradient.

LVOTO. If able, the patient is instructed to squat for 3 seconds and then stand. This maneuver is repeated for approximately 5 cycles.

**iii. Amyl Nitrite.** Amyl nitrite is a vasodilator that decreases afterload and increases heart rate and can provoke latent LVOTO. Amyl nitrite comes in a glass capsule covered by a protective cloth and is administered by having an individual crush the glass capsule between their fingers and the patient is instructed to inhale the vapors. Amyl nitrite is of limited supply and is not available in many hospitals.

**iv. Exercise Stress Echocardiography.** Exercise is the most physiologic way to provoke LVOTO. Upright exercise (treadmill or upright bicycle) reflects a more physiologic form of exercise and is expected to provoke higher gradients than supine exercise. Exercise in the supine position leads to increased preload and afterload and a lower heart rate response, predisposing to lower provokable gradients.

Although the gradient measured immediately post exercise in a recumbent position may be attenuated when compared to gradients measured in the upright position simultaneously at peak exercise, technical challenges and practical limitations make it reasonable to measure gradients immediately post exercise in the supine position. Dobutamine stress echocardiography is not recommended since it is not a physiologic approach and can result in dynamic gradients even in some normal subjects.

Currently the primary indication to pursue invasive SRT in individuals with obstructive HCM is the persistence of severe symptoms with LVOT gradient  $\geq 50$  mm Hg, despite maximum medical therapy. Therefore, beta blocker and non-dihydropyridine calcium channel blocker therapy should not be withheld prior to exercise.

In the younger pediatric population, it is often difficult to obtain good cooperation for provocative maneuvers (Valsalva or squat to stand). Exercise stress echocardiography is preferred in the pediatric HCM population and can be adequately performed in children over 8 years of age who are cooperative and capable of performing an exercise stress test. It can be used as a tool to identify low risk patients.<sup>123</sup>

## Recommendations and Key Points

- 1- In symptomatic patients, if a peak instantaneous gradient  $\geq 50$  mm Hg is not obtained, then provocative maneuvers should be pursued. (Figure 20)

### 4. Mitral regurgitation in HCM

Because the anterior leaflet is longer than the posterior leaflet, an inter-leaflet gap often occurs during systole, resulting in a posteriorly directed jet of MR, which can be significant (moderate or greater severity). The severity of MR is related to the extent of mismatch of anterior and posterior leaflet lengths, and the decreased mobility of the posterior leaflet.<sup>124</sup> In addition, the factors that influence the severity of dynamic obstruction can also influence the severity of MR.<sup>125</sup>

Not all MR associated with HCM is related to SAM. Patients with HCM can have intrinsic valvular abnormalities, such as mitral valve prolapse, leaflet thickening secondary to injury from repetitive septal contact or flow turbulence, chordal rupture, chordal elongation or thickening, and leaflet destruction due to infective endocarditis.<sup>125</sup> The presence of a central or an anteriorly directed jet should prompt careful evaluation of the mitral valve apparatus to identify intrinsic valvular abnormalities, although SAM can be associated with central

and anterior jets in the absence of intrinsic leaflet pathology. If the mechanism cannot be defined with TTE, TEE should be considered before invasive therapy.

Variability in the length of the posterior leaflet can influence the direction of SAM-induced MR.<sup>126</sup> In addition, due to the eccentricity of the MR jet, quantitative assessment using the proximal isovelocity surface area (PISA) method can lead to erroneous estimation of MR severity. MR regurgitant volume can be calculated in these patients as the difference between LV stroke volume by 2D (LV end diastolic volume - end systolic volume) and systolic RVOT (right ventricular outflow tract) flow by PW Doppler (RVOT area multiplied by time velocity integral of flow through RVOT), in the absence of significant aortic regurgitation. Alternatively, it can be determined as the difference between diastolic flow across mitral annulus (mitral annulus area multiplied by time velocity integral of flow across the mitral annulus) and systolic RVOT flow.

Echocardiography is the initial imaging modality used to assess the mitral valve as well as the LVOT pressure gradient. CMR is of value in determining the severity of MR by measuring regurgitant volume and fraction. In addition, CMR can provide a detailed assessment of the papillary muscles, which can influence the surgical approach for symptomatic patients undergoing surgery to treat dynamic LVOT obstruction.

## Recommendations and Key Points

- 1- In most patients with obstructive HCM, mitral regurgitation is related to dynamic obstruction with a posteriorly and laterally directed eccentric jet.
- 2- In some patients, mitral valve prolapse or flail is the etiology of mitral regurgitation.
- 3- In some patients, TEE or CMR is needed for better evaluation of the mechanism of MR.

### 5. Midventricular Obstruction and Apical Aneurysm

Hypertrophic cardiomyopathy with midventricular obstruction (MVO) is an uncommon but important morphologic subtype of HCM. MVO can be identified in the presence of two imaging criteria: systolic obliteration of the LV that is unrelated to SAM, and a systolic pressure gradient at midventricular level  $\geq 30$  mm Hg at rest.<sup>127</sup> Anatomic substrates of MVO include systolic apposition of the hypertrophied septum with a hypercontractile LV free wall,<sup>127</sup> apposition of hypertrophied papillary muscles,<sup>128</sup> and midventricular narrowing due to middle-to-apical wall hypertrophy and an apical aneurysm.<sup>127</sup> Notably, SAM-related LVOTO and midventricular obstruction may co-exist and can complicate assessment and therapy.<sup>127,129</sup> In the prospective multi-center international study (HCM Registry) of over 2600 patients who underwent CMR, MVO with an apical aneurysm was detected in 3%.<sup>130</sup> Although MVO is occasionally seen in the pediatric population, the development of an apical aneurysm is very rare in children.

**i. Doppler Findings.** Patients with isolated MVO have color Doppler-demonstrating turbulence at the midventricular level. CW Doppler may demonstrate high velocities persisting through late systole.<sup>127</sup> Alternatively, the spectral Doppler pattern of some patients with MVO shows intracavitary velocities peaking in mid-systole, ending abruptly with rapid deceleration, often not extending into late systole.<sup>129,131</sup> For patients with isolated MVO under resting conditions, good correlations usually exist between pressure gradients obtained invasively and by CW Doppler. However, peak Doppler gradients can be lower than those obtained by cardiac catheterization

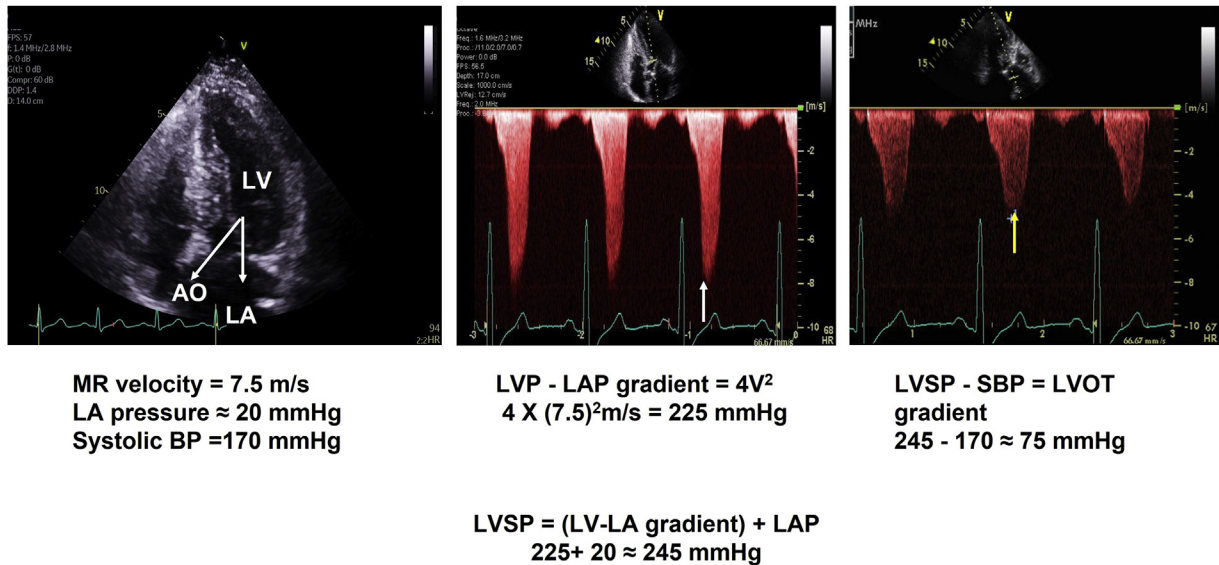


**Figure 17** Estimation of the left ventricular outflow tract (LVOT) gradient from mitral regurgitation (MR) velocity using an assumed elevated left atrial (LA) pressure of approximately 20 mm Hg. Applying the modified Bernoulli equation ( $4V^2$ ) to MR velocity of 7.5 m/s (*white arrow*), the gradient between left ventricle (LV) and LA is calculated to be 225 mm Hg. Adding assumed LA pressure to the LV/LA gradient leads to the estimation of LV peak systolic pressure. Once systolic blood pressure is known, in this case 170 mm Hg, it can be subtracted from the LV systolic pressure, yielding the LVOT gradient of approximately 75 mm Hg, corresponding with the LVOT velocity of approximately 4.3 m/s (*yellow arrow*).

### Discrete subaortic stenosis

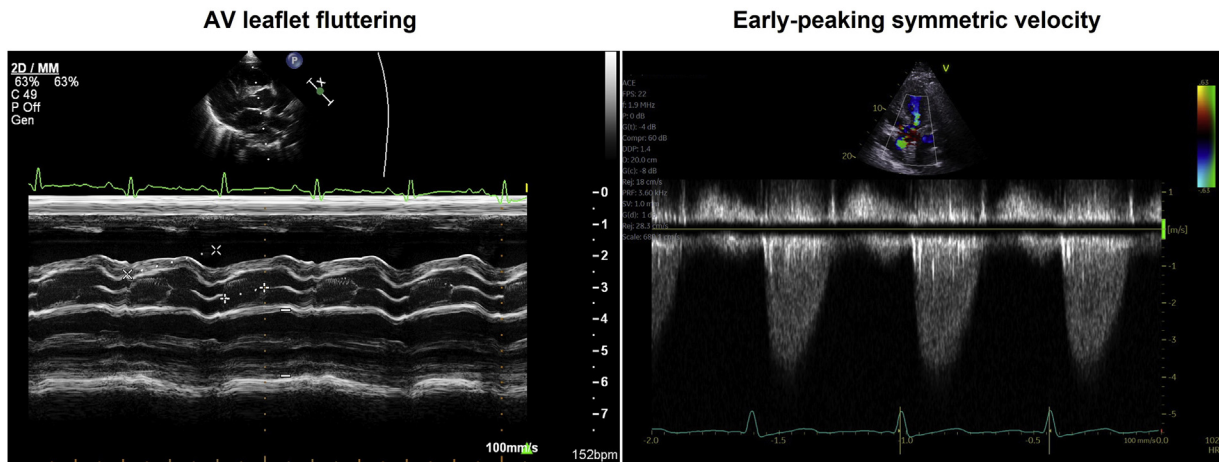


**Figure 18** (Left): M-mode echocardiographic trace of the aortic valve (AV). Systolic fluttering of the aortic valve leaflets is seen. Valve closure usually occurs earlier than in patients with hypertrophic cardiomyopathy. (Right): Apical 5-chamber view. Symmetric continuous-wave Doppler early peaking velocity due to the fixed obstruction in DSS.

in patients with isolated MVO when the Doppler spectral tracing indicates abrupt cessation of flow across the mid-ventricle in mid-systole, rendering the pressure gradient inaccessible to Doppler measurement.<sup>131</sup> In such cases, a jet in early diastole directed from the apical chamber to the basal LV cavity may also be seen, reflecting emptying of the apical cavity through the narrowed mid-LV cavity at the onset of diastole.<sup>132</sup> This 'paradoxical' early diastolic jet can also be detected as an isolated finding in a small subset of patients with apical-variant HCM and severe hypokinesia of the apex, where it reflects a higher pressure in the sequestered apical cavity being released in early diastole. This early diastolic flow toward the base

may also reflect heterogeneity in regional relaxation with more rapid relaxation in the mid ventricle, compared to the apex, creating a diastolic gradient. (Figure 21, and Videos 3 and 4).<sup>132</sup>

**ii. CMR and CT Diagnosis.** CMR imaging can help confirm the presence of apical aneurysms when ECG and echocardiographic findings, raise the possibility of this diagnosis. In addition, CMR can identify small aneurysms that may not have been suspected following echocardiographic examination.<sup>133</sup> Post-contrast (gadolinium) imaging can also reveal apical thrombi, as well as delineate the presence and pattern of myocardial scarring in the aneurysm and its contractile

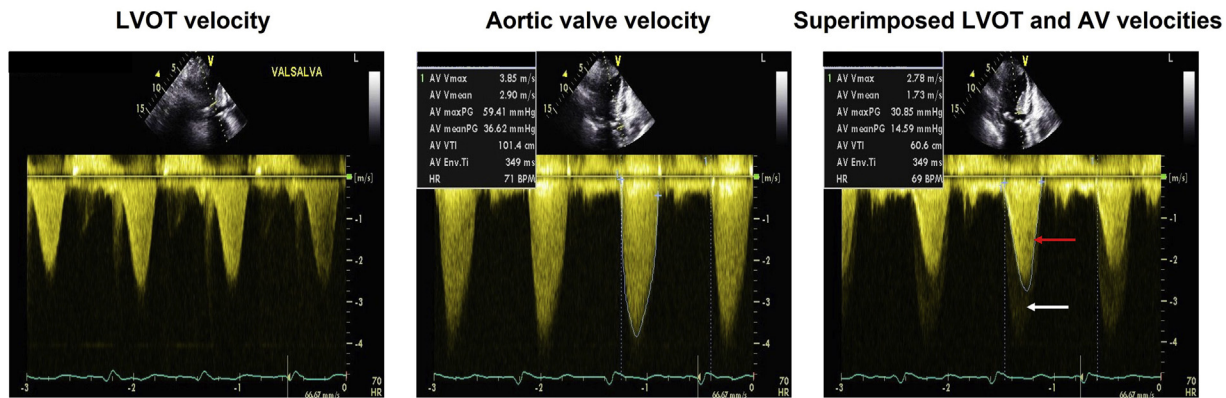


**Figure 19** (Left): Apical 3-chamber view. Continuous-wave (CW) Doppler of a mid-to-late peaking left ventricular outflow tract (LVOT) velocity waveform, indicating dynamic obstruction, measuring 2.8 m/s. (Middle): Early-peaking CW Doppler flow velocity that is rounded and reflective of a fixed obstruction, measuring 3.9 m/s. (Right): Superimposed CW Doppler waveforms of LVOT (*red arrow*) and aortic valve (*white arrow*). To estimate approximate transaortic gradient the LVOT gradient has to be subtracted from the aortic valve gradient. In this case the peak gradient calculates to 29 mm Hg and mean gradient is 22 mm Hg.

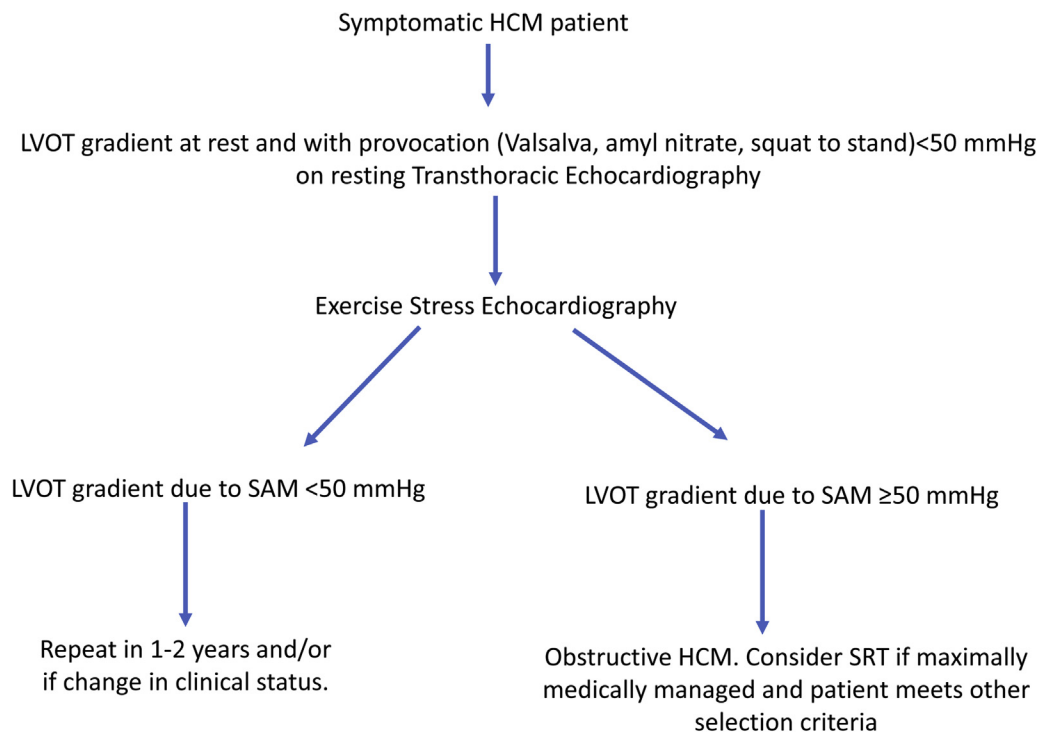


**Figure 20** Algorithm for evaluation of dynamic obstruction in patients with known or suspected diagnosis of hypertrophic cardiomyopathy (HCM). LVOT, left ventricular outflow tract; SAM, systolic anterior motion; SRT, septal reduction therapy.

neck. Stress imaging often identifies profound perfusion defects localized at the site of the mid-ventricular aneurysm, and the importance of these defects remains uncertain. Retrospectively gated CT can provide important anatomical and functional information in patients with mid-cavity obstruction in patients with intracardiac devices, and/or in patients who also require CT coronary imaging.

**iii. Clinical Implications of MVO.** MVO is often under-recognized, and is associated with refractory symptoms, as well as

increased risks for ventricular arrhythmias and premature mortality.<sup>127</sup> LV thrombi may form within the aneurysmal sac and increase the risk of thromboembolic events.<sup>134</sup> An apical aneurysm is now included in risk assessment algorithms for SCD and is a Class 2a indication for implantation of a prophylactic ICD.<sup>2</sup> When associated with symptoms, the majority of patients are managed with negative inotropic agents. Favorable surgical results have been reported in patients with MVO, where the obstruction was relieved by means of a myectomy via a transaortic approach, a transapical approach, or

combined transaortic and transapical incisions.<sup>135</sup> In some patients, invasive septal reduction (either surgical or ablative) for SAM-related LVOT obstruction may precipitate or exacerbate MVO, by a mechanism thought to reflect the effects of afterload reduction (i.e., reduction of the outflow gradient) on a susceptible mid-cavity substrate. When anticipated, the risk of this outcome may weigh in favor of recommending an extended surgical myectomy.

## Recommendations and Key Points

- 1- MVO is diagnosed with mid-cavitary obliteration and a systolic gradient  $\geq 30$  mm Hg at rest.
- 2- Echo with ultrasound enhancing agents or CMR can identify the presence of small apical aneurysms and apical clots. CTA can be used if needed.
- 3- MVO is associated with higher risk of ventricular arrhythmias and mortality.

### F. Tissue Characterization

Tissue characterization by CMR plays a critical role in HCM assessment. In addition to the established role of LGE in risk stratification and prognostication in HCM (Figure 22), CMR provides additional techniques that can aid in tissue characterization such as T1 mapping. T1 relaxation time is measured for each individual pixel of the myocardium and extracellular volume fraction (ECV) is calculated based on the comparison of native T1 values with those obtained following gadolinium-chelate contrast agents, allowing for further tissue characterization and the detection of diffuse interstitial expansion.<sup>136</sup> Regional increased native T1 times have been shown to correlate with areas of increased wall thickness and LGE in HCM.<sup>137</sup> Moreover, T1 mapping and ECV can help differentiate HCM from hypertensive heart disease, athlete's heart, Fabry disease, and cardiac amyloidosis,<sup>19,49,138</sup> and are associated with adverse outcomes.<sup>139</sup> Increased signal intensity on T2 imaging is associated with edema/inflammation and potentially increased risk for SCD.<sup>140</sup> However, the incremental utility of all these techniques, in terms of prognostic value and risk stratification, remains to be determined.

Current echocardiographic techniques are not accurate in detecting myocardial fibrosis, as quantified by LGE, in children with HCM. But there are data suggesting good negative predictive value of standard imaging.<sup>141-143</sup> On the other hand, myocardial stiffness assessment by shear wave imaging has shown a positive correlation with fibrosis markers in LGE-CMR, although additional data in many more patients are needed.<sup>7</sup>

## Recommendations and Key Points

- 1- LGE by CMR identifies areas of replacement fibrosis.
- 2- T1 mapping can be used to determine extracellular volume fraction in HCM patients.
- 3- LGE patterns and T1 mapping are of value in evaluation of patients with increased LV wall thickness.

## SECTION 2: MULTIMODALITY IMAGING FOR RISK STRATIFICATION AND PROGNOSTICATION

The overall risk of SCD in patients with HCM is low and estimated at  $\sim 0.5\%$ /year.<sup>2,144</sup> In addition to a personal history of ventricular

fibrillation or tachycardia, reasons for consideration of ICD implantation include prior resuscitation for SCD, malignant family history of SCD, unexplained syncope, massive LV wall thickness  $\geq 30$  mm, apical aneurysm, additional imaging features of extensive late LGE on CMR, and LV systolic dysfunction.<sup>2</sup> The 2014 European Society of Cardiology (ESC) guidelines devised and recommended using an HCM Risk-SCD calculator to assess the 5-year risk of SCD. Using the results, an ICD is recommended with a 5-year risk score  $\geq 6\%$  (high risk) and can be considered in those with a 5-year risk  $\geq 4\%$  and  $< 6\%$  (intermediate risk).<sup>144,145</sup> The algorithm for the HCM Risk-SCD calculator incorporates age, maximal wall thickness (MWT), LA diameter, and maximal LVOT gradient (either resting or with Valsalva) as continuous variables, along with family history of SCD, NSVT on Holter, and unexplained syncope as binary conditions.<sup>145</sup> Recent studies call into question the sensitivity of the algorithm, perhaps due to the lack of inclusion of LGE and apical aneurysms. Inclusion of these features results in a higher sensitivity and smaller numbers needed to treat.

A validated model for SCD risk prediction in pediatric HCM has been recently published and includes age at diagnosis, documented NSVT, unexplained syncope, septal diameter z-score, LV posterior wall diameter z-score, LA diameter z-score, peak LVOT gradient, and presence of a pathogenic variant, with  $> 70\%$  prediction accuracy.<sup>146</sup>

In the section below, we address the established as well as potential risk modifiers of SCD from the perspective of cardiac imaging.

### A. Left Ventricular Wall Thickness

The importance of the magnitude of LVH as a risk factor for SCD is well established,<sup>147</sup> with maximum wall thickness  $\geq 30$  mm denoting a high risk for SCD while the AHA/ACC 2020 HCM Guideline also proposes that consideration be given to borderline values of  $\geq 28$  mm at the discretion of the treating cardiologist.<sup>2</sup> Notwithstanding, it is important to recognize that the association between the severity of LVH and risk is linear. Furthermore, data linking the degree of LVH and risk has largely been based on echocardiographic measurements, and wall thickness determined by CMR may refine this association further.<sup>31,147</sup>

### B. Left Atrial Diameter

LA diameter (anteroposterior) was included as a continuous variable in the HCM Risk-SCD calculator, based on one study demonstrating increased risk for SCD with increasing LA diameter.<sup>145,148</sup> Other studies have provided conflicting results on whether LA diameter is associated with increased risk of SCD or heart failure admissions.<sup>80,149,150</sup> LA volume is considered a more accurate assessment of LA size, although only a few small studies have examined its association with outcomes.<sup>81,151</sup>

### C. Left Ventricular Outflow Tract Obstruction

Several studies have demonstrated an association between resting LVOTO and SCD.<sup>92,152,153</sup> The association between latent obstruction and SCD is not as well described, with some data suggesting that patients with a provoked gradient ( $\geq 90$  mm Hg) have worse outcomes than those with less severe provoked gradients (30-89 mm Hg).<sup>154</sup> A recent study also demonstrated that, in obstructed HCM patients, SRT was associated with better longer-term outcomes (including SCD) vs. watchful waiting.<sup>155</sup> The HCM Risk-SCD calculator includes peak LVOT gradient at rest or with Valsalva regardless

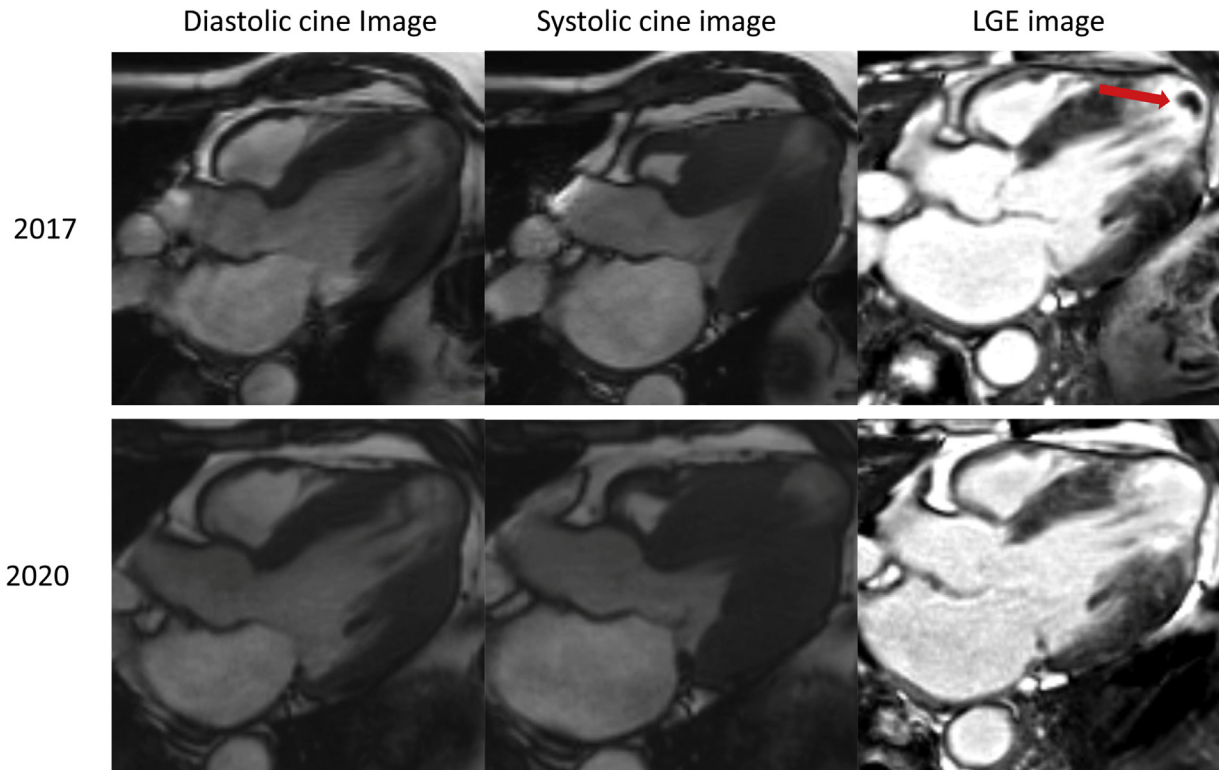


**Figure 21** Serial cardiac magnetic resonance imaging in a patient with hypertrophic cardiomyopathy at baseline (top row of images) and 3 years later (bottom row of images) showing the diastolic frame of a cine image (left), the systolic frame (middle) and late gadolinium enhancement (LGE) images (right). The patient has mid-ventricular obstruction with an apical aneurysm that has enlarged over time. An apical thrombus that was noted (*red arrow*) in the first scan resolved with anticoagulation 3 years later. Figure courtesy of Dr. James Malcolmson, Barts Heart Centre, London.

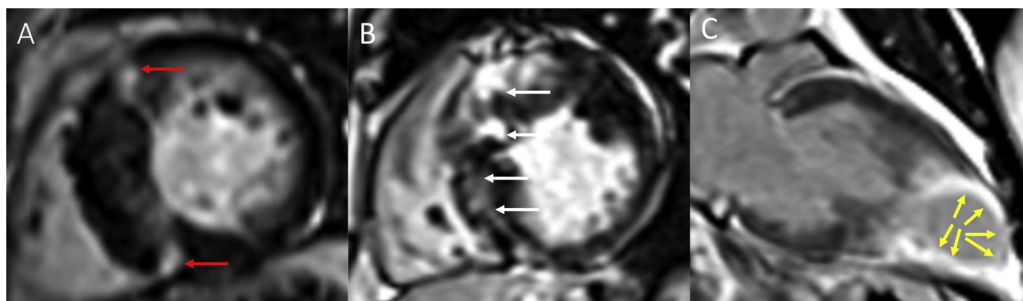


**Figure 22** Patterns of late gadolinium enhancement (LGE) in hypertrophic cardiomyopathy. **(A)** LGE primarily in the right ventricular insertion points (*red arrows*); **(B)** Severe LGE of the hypertrophied septum with non-ischemic patchy mid-ventricular pattern (*white arrows*); **(C)** Apical aneurysm in a patient with mid-cavity obstruction and transmural LGE of the apex (*yellow arrows*).

of concurrent medical therapy. Criticisms of this method include the paucity of data regarding the association of provokable gradients with SCD, whether other methods of provocation should have been included, and the dynamic nature of LVOT obstruction.

#### D. Apical Aneurysm

The ability to echocardiographically identify the region of hypertrophy and presence of apical aneurysm and thrombus can be improved

by administering UEA and avoiding foreshortening the LV apex. Therefore, we advocate for the use of UEA in all patients with a possible diagnosis of apical HCM. UEA should also be considered in any patient where there is suspicion of an apical aneurysm, including those with mid-cavity obstruction and apical HCM. CMR may still be necessary to distinguish these features. LGE imaging can also demonstrate transmural myocardial fibrosis and scar,<sup>133</sup> and may be additionally useful for identifying an apical thrombus. Major adverse event rates in patients with an apical aneurysm have

**Table 3** Summary of Key Imaging Markers and Approach in SCD Risk Stratification

Imaging Parameter	SCD risk threshold	Imaging Approach	Practical Points and/or Caveats
<b>Established markers</b>			
LV maximal wall thickness*	Highest risk in those with LVH $\geq 30$ mm, although relationship between wall thickness and SCD is continuous	Echo or CMR	Limited negative predictive value of 30 mm threshold, most SCD occurs below this threshold
Late gadolinium enhancement**	Highest risk in those with LGE $> 15\%$ , although relationship between LGE and SCD is continuous	CMR	Abnormal threshold of $>6SD$ above normal myocardium
LVOT obstruction	$>30$ mm Hg	Echo	Varies according to loading conditions and activities
LV apical aneurysm*	Presence associated with increased risk even in those $> 60$ years old	Echo or CMR	CMR more sensitive, suspect in those with mid cavity obliteration
Left atrial size	LA volume ( $> 34$ ml/m <sup>2</sup> ) using biplane LA volumes or anteroposterior diameter ( $>48$ mm)	Echo	Single 2-D measurement may erroneously estimate size
LV ejection fraction*	LV ejection fraction $<50\%$	Echo or CMR	Consider use of contrast echo or CMR to optimally assess LVEF
<b>Emerging marker</b>			
LV global longitudinal strain	No clear threshold value, abnormal results portend a worse prognosis	Echo (CMR approaches emerging)	Further standardization needed between platforms

\*Major risk factor for SCD and if present, is considered class IIA indication for ICD implantation.

\*\*In HCM patients without major risk factors for SCD and uncertain on whether to implant ICD, decision on ICD implantation may be reached based on late gadolinium enhancement findings.

been estimated to be between 5 and 15% per year.<sup>133,134,156,157</sup> Apical aneurysm, independent of its size, is a risk factor for SCD.

### E. Late Gadolinium Enhancement by CMR

Following their administration, gadolinium contrast agents redistribute from the intravascular space to the extracellular space with accumulation in areas with expansion of extracellular space due to either edema or fibrosis, resulting in increased signal intensity on T1 weighted imaging.<sup>136</sup> LGE is noted in approximately half of patients with HCM and is commonly described as patchy and mid-myocardial within segments of maximal hypertrophy.<sup>158-160</sup> Several studies have demonstrated an increased burden of ventricular arrhythmias, SCD, and all-cause mortality in patients who have LGE on CMR.<sup>158-161</sup> LGE is also associated with increased heart failure symptoms and admissions, and reduced LVEF in patients with HCM.<sup>161,162</sup> Isolated LGE at the RV insertion points does not appear to be associated with increased risk.<sup>158</sup>

Although LGE is present in  $>50\%$  of patients with HCM, the overall prevalence of SCD in these patients is far lower.<sup>144,163</sup> Thus, recent studies have focused on identifying a cut point for the extent of LGE beyond which there would be a benefit from an ICD. Although multiple studies have been conducted, the heterogeneity of the imaging sequences and postprocessing techniques have made it difficult to implement a precise LGE cutoff.<sup>144,163,164</sup> LGE quantification techniques include a visual assessment or automatic software quantification of signal intensity of affected areas compared to those selected as normal myocardium by visual assessment with cutoffs at 2-6 standard deviations (SD) or full width half maximum (FWHM: region of

interest is manually drawn in the region with hyperenhancement, and enhancement calculated as pixels where signal intensity is  $> 50\%$  of the automatically determined maximum intensity).<sup>165</sup> Although currently no specific technique is recommended by the Society for Cardiovascular Magnetic Resonance,<sup>165</sup> prior studies comparing the various techniques have found that either 6 SD or FWHM are preferred in HCM.<sup>166,167</sup> Large studies used a threshold of 15% LGE of the LV mass using the 6-SD technique and showed LGE  $\geq 15\%$  was associated with increased risk of SCD. Repeat CMR may be considered every 3-5 years to evaluate for changes in the magnitude of wall thickness and LGE, and to identify new apical aneurysms or reduction in LVEF.<sup>2</sup>

We advocate for the incorporation of LGE into the risk assessment for SCD for patients in the "gray zone" (without major American College of Cardiology (ACC)/American Heart Association (AHA) risk factors who have other mitigating risk factors, or low-to-intermediate risk by the HCM Risk-SCD calculator) to aid in shared decision making since the presence of extensive LGE ( $\geq 15\%$ ) is associated with an increased risk of SCD compared to patients with minimal LGE (Table 3 presents a comprehensive summary of risk markers).

### F. Left Ventricular systolic dysfunction.

The 2020 ACC/AHA HCM guidelines recommend (Class 2a) consideration of ICD implantation in individuals with LV ejection fraction  $\leq 50\%$  (2). Although prophylactic ICD implantation is an accepted therapy for primary prevention in HCM patients with systolic dysfunction, these patients were not included in primary

prevention ICD trials. If needed, assessment of LVEF using CMR should be considered in this context.

### G. Ischemia

Autopsy findings from individuals with HCM-related SCD found a high prevalence of histological changes consistent with acute/sub-acute myocardial ischemia, possibly forming the substrate for arrhythmogenesis. Flow heterogeneity using positron emission tomography (PET) has been associated with ventricular arrhythmias,<sup>168</sup> suggesting a potential role for PET in SCD risk assessment. Given the limited data and associated radiation, we cannot recommend its routine adoption until confirmed with larger studies.

## Recommendations and Key Points

- 1- Imaging provides key data needed for risk stratification for SCD.
- 2- Maximum wall thickness  $\geq 30$  mm, apical aneurysm, LVEF  $\leq 50\%$ , LGE  $\geq 15\%$ , LVOT obstruction, and enlarged LA are imaging findings associated with higher risk of SCD.
- 3- An UEA is recommended for patients with MVO or apical HCM to evaluate for apical aneurysms.

## SECTION 3: MULTIMODALITY IMAGING IN COMMON CLINICAL SCENARIOS

### A. Assessment of Ischemia

Chest pain is a common symptom in patients with HCM and may not be related to epicardial coronary artery disease (CAD), with multiple potential factors contributing to inadequate oxygen supply and a higher susceptibility for myocardial ischemia. Oxygen demand is increased because of larger myocardial mass and increased filling pressures, while oxygen supply is decreased by microvascular dysfunction and medial hypertrophy of the intramural arterioles.<sup>169-171</sup> Myocardial bridges are commonly seen in HCM and may contribute to ischemia by prolonged coronary compression and reduced blood flow in the early diastolic phase.<sup>172-174</sup> Myocardial blood flow reserve is often reduced, particularly in the endocardial layer, and myocardial ischemia with measurable cardiac troponin can be demonstrated in daily activities.<sup>175</sup> Regional blood flow may be further reduced by concomitant atherosclerotic coronary disease, which is associated with worse clinical outcome in HCM.<sup>176</sup>

**1. Echocardiography.** Myocardial ischemia in HCM is frequently related to abnormal coronary flow reserve (CFR).<sup>177,178</sup> CFR can be evaluated using PW Doppler in the middle left anterior descending (LAD) coronary artery, and when reduced it is associated with worse outcomes.<sup>179,180</sup> The ability of echocardiography (rest or stress) to define epicardial CAD is limited. The pathophysiology of exercise-induced wall motion abnormalities (WMA) in HCM is complex and multifactorial,<sup>180</sup> and while exercise-induced WMA may have prognostic significance, they are not a good predictor of epicardial CAD.<sup>181</sup>

**2. SPECT and PET myocardial perfusion imaging.** Myocardial perfusion imaging with either single-photon-emission computed tomography (SPECT) or PET can define the presence and severity of ischemia. Stress with either exercise or vasodilators is most commonly used, and typically demonstrates one of three patterns: 1) normal

perfusion; 2) a reversible perfusion defect in the area of greatest hypertrophy; or 3) diffuse subendocardial ischemia from microvascular disease leading to ischemic dilation of the LV and a decrease in EF. Pattern #3 is typically seen with concentric HCM, while focal areas of hypertrophy may demonstrate reversible perfusion defects (Figure 23). Underlying the assessment of all of these patterns is the fact that standard nuclear techniques identify relative myocardial perfusion when compared with areas of normal myocardium. Absolute myocardial blood flow can be quantified, typically using PET, and may show blunted augmentation of flow during stress when compared with rest, either globally or in the areas of greatest hypertrophy.

Studies using SPECT imaging with thallium-201 have introduced the concept of ischemia in HCM<sup>182,183</sup> and its relation to adverse events including cardiac arrest and syncope.<sup>184</sup> Moreover, the common treatments for HCM, including calcium channel blockers<sup>185</sup> and surgical myectomy,<sup>186</sup> have been shown to improve or normalize myocardial perfusion patterns. In general practice, the preferred SPECT radiotracer is now technetium-99m due to a significantly shorter half-life (6 hours versus 73 hours for thallium-201) and lower radiation exposure. Due to the long half-life of both agents, stress images are actually acquired 15-60 minutes after peak stress and maximum hyperemia. At that point, stunned myocardium may have recovered, making SPECT assessment of stress-induced wall motion abnormalities suboptimal.

PET myocardial perfusion imaging is superior to conventional SPECT due to its precise built-in attenuation correction that improves image quality and provides for accurate quantitative analysis of myocardial blood flow. Additionally, test duration is shorter due to the relatively short half-lives of the most common radiotracers (rubidium-82: 75 seconds and N-13 ammonia: 10 minutes). Vasodilator injection is performed while the patient is under the camera and images are acquired during hyperemia. This allows for more accurate quantification of stress EF, transient ischemic dilatation, and myocardial blood flow reserve.<sup>187</sup> About half of the patients with HCM have an abnormal EF response to stress,<sup>188</sup> with some showing transient ischemic dilatation.<sup>189</sup> Resting blood flow is typically normal, although areas with significant scar may demonstrate decreased flow.<sup>190</sup> Peak stress flow may be blunted due to microvascular disease, leading to decreased blood flow reserve. Maximum wall thickness is one of the strongest predictor of impaired flow reserve,<sup>191</sup> although abnormal flow reserve may be seen in both hypertrophied and non-hypertrophied areas of the LV.<sup>192</sup> With respect to outcomes, PET-derived blood flow reserve in HCM showing microvascular dysfunction is an independent predictor of clinical deterioration and death<sup>193</sup> although, as mentioned previously, these data need to be replicated in larger cohorts.

**3. CMR Myocardial Perfusion Imaging.** CMR perfusion imaging utilizes a one-pass technique, with a series of images acquired during stress and rest.<sup>194,195</sup> Imaging comprises basal, mid, and apical short-axis slices of the LV, but long-axis perfusion imaging may also be useful (Figure 24) across a number of cardiac cycles; a perfusion defect is detected when a regional delay and/or decrease in relative myocardial signal intensity is evident as the contrast bolus passes through the LV myocardium.

Pharmacological stress with intravenous regadenosine or adenosine is the usual method of stress, though exercise stress can be performed with MR-compatible equipment.<sup>196</sup> Both semi-quantitative and quantitative techniques are also available,<sup>197</sup> with the latter providing pixel-level assessments of myocardial blood flow (MBF)

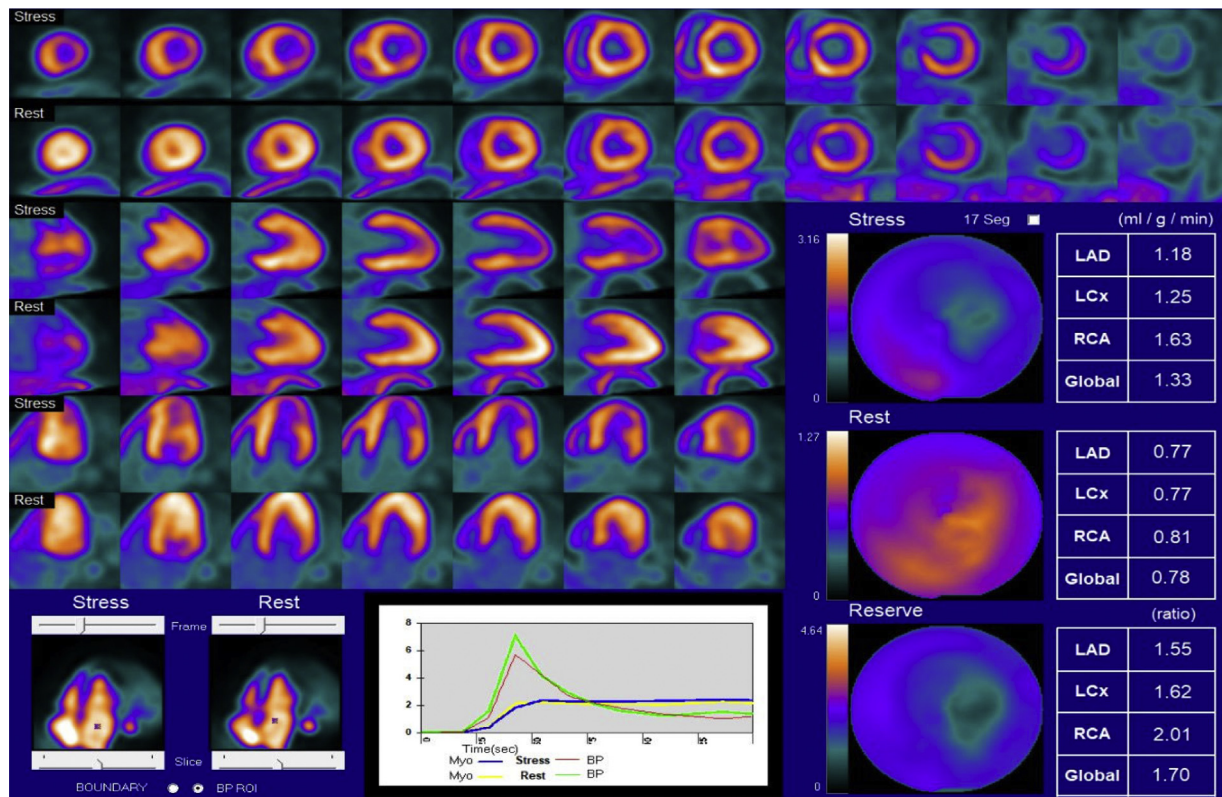


**Figure 23** Example of a patient with apical hypertrophic cardiomyopathy. Note the brighter areas of myocardium in the distal lateral wall and apex on the rest images, with decreased perfusion during stress, representing ischemia. There is transient ischemic dilation of the left ventricle with stress, and flow reserve is severely impaired in the distal lateral wall and apex. This pattern often mimics distal left anterior descending coronary artery ischemia.

that correlate with PET-derived MBF but with greater spatial resolution.<sup>198</sup> As in PET, utilization of MBF may be able to help differentiate epicardial from microvascular coronary disease. CMR's 'multiparametric' assessment has facilitated identifying the association of perfusion defects/reduced MBF reserve with increased LV mass, LGE, and ECV.<sup>199</sup> Reduced MBF reserve with CMR has also been reported in normal appearing segments and in genotype-positive/phenotype-negative hearts in some cases, suggesting that it may be a marker of early disease.<sup>194</sup>

While subendocardial patterns of LGE are accurate indicators of prior myocardial infarction (MI) in almost all clinical settings, its absence does not exclude coronary disease, and subendocardial LGE can occur in HCM despite culprit-free coronary angiograms; for example, in apical or mid-cavity HCM and following thromboembolic disease. Coronary imaging and contemporaneous myocardial perfusion CMR has been used to establish baseline abnormalities. In this setting, prospective changes in perfusion, function, or LGE imaging may serve as a helpful and safe screening tool, although this strategy remains formally untested.

**4. Cardiac CT.** Contrast-enhanced, ECG-synchronized computed tomography (CT) of the heart is useful in patients with HCM to non-invasively detect obstructive epicardial coronary artery disease, which is present by CT in 7-19% of patients.<sup>173,174,200</sup> Cardiac computed tomographic angiography (CCTA) has been regarded as the reference standard for imaging anomalous coronary anatomy and myocardial

bridges, the latter being detected in up to half of patients (Figure 25).<sup>174</sup> Although radiation exposure is a relative drawback of CCTA in younger HCM patients, the use of contemporary CT technology combined with heart rate modulation can keep doses well below 5mSv. Iodine contrast medium is required, but not recommended in patients with reduced renal function (eGFR <30). HCM does not pose a specific technical challenge for cardiac CT, although preprocedural nitroglycerin should be avoided when severe LVOTO is present. The diagnostic performance of CCTA for the detection of CAD in HCM is good, and in the same range as reported for general cohorts.<sup>201</sup> CCTA performance varies with available CT technology and is best in cooperative patients with a low heart rate and regular rhythm. The ability to rule out obstructive coronary disease decreases in the presence of severe calcification or coronary stents. Challenges can occur in patients with metal artifacts, coronary stents, and markedly elevated calcium scores.

CT-based fractional flow reserve (CT-FFR) can estimate the functional severity of intermediate-severity coronary lesions detected on CCTA. Commercially available CT-FFR applications have not been validated specifically in HCM patients. Even in the absence of severe CAD, patients with HCM appear to have slightly lower CT-FFR values in the distal vessels, which may be caused by a disproportionate increase in myocardial mass compared to the coronary capacity.<sup>202</sup> In patients with higher myocardial mass, more discrepancy has been noted when comparing an investigational CT-FFR algorithm with invasive FFR.<sup>203</sup>

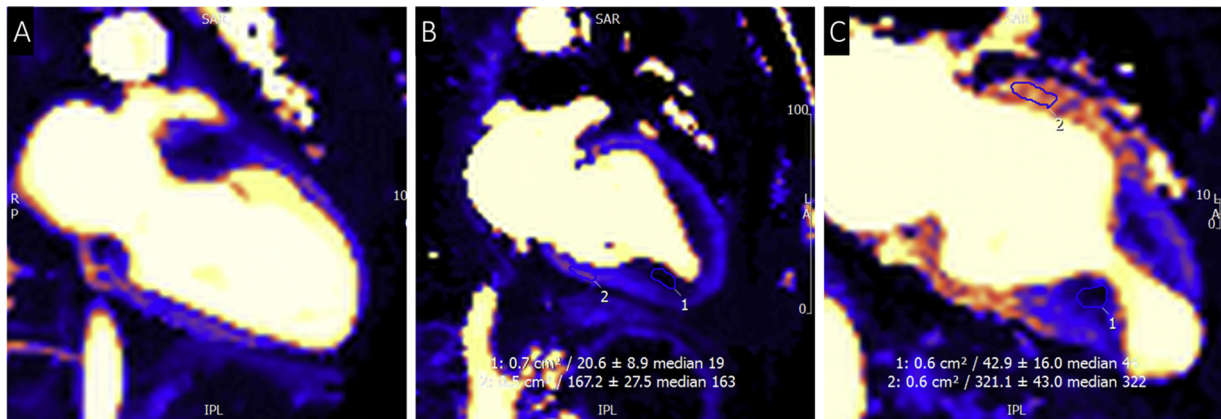


**Figure 24** Patterns of perfusion defect in hypertrophic cardiomyopathy (HCM): In-line quantitative perfusion with cardiac magnetic resonance. Standard short-axis imaging may miss some noncoronary perfusion defect patterns. **(A)** HCM with reduced mid-wall perfusion co-localizing with mild isolated basal anterior wall left ventricular hypertrophy. **(B)** Apical HCM with reduced sub-endocardial perfusion in the hypertrophic apical segments. **(C)** Mid-cavity obstructive HCM with reduced perfusion confined to the strangulating muscular aneurysmal neck.

## B. Assessment of Coronary Artery Disease

Chest discomfort and perfusion abnormalities in the absence of CAD are common in patients with HCM and are not well correlated or understood mechanistically; the presence of CAD is, however, associated with adverse outcomes. There is limited prospective data on CAD testing in HCM, or specific comparisons between different techniques. Recommendations in this guideline parallel the recent chest pain guidelines based on evidence in the general population but adapted to the context of HCM based on expert consensus.

### 1. HCM patient with chest discomfort and clinical need to evaluate CAD.

The initial step in evaluating a patient with suspected CAD is a comprehensive clinical evaluation. Challenges in patients with HCM include baseline ECG abnormalities and noncoronary causes for symptoms of chest pain and dyspnea. Randomized trials and registries have consistently demonstrated that traditional prediction rules based on age, sex and symptoms, such as the Diamond & Forrester rule, grossly overestimate CAD prevalence in contemporary chest pain cohorts.<sup>204-206</sup> For convenience, we recommend an approach that has not been validated in HCM patients, with the expectation of additional overestimation of CAD because of more frequent myocardial ischemia in the absence of epicardial coronary artery stenosis. Heart failure with a possible ischemic etiology lowers the threshold for diagnostic testing.

For patients with a low probability of CAD (<15%), the diagnostic yield of testing is low and a conservative initial approach without testing is appropriate (Figure 26). Other causes of chest discomfort should be considered, but persistent symptoms may necessitate further testing. Because clinically relevant CAD is very rare in the absence of detectable coronary calcium, a calcium scan may be a reasonable first test in low-probability patients with nonacute chest discomfort.<sup>207-210</sup>

For most patients with a low-to-intermediate probability (15-50%), CCTA is an effective approach to evaluate for epicardial CAD or myocardial bridging. Randomized controlled trials in general chest pain populations have demonstrated that cardiac CT is safe, and in some studies is associated with improved outcomes, at the expense of increased coronary angiography rates. To avoid negative invasive

angiograms or revascularizations of low clinical relevance, it is important to note that CCTA tends to overestimate severity compared to invasive angiography, and that moderate angiographic stenosis by CT or cardiac catheterization is in many cases not functionally significant.

Furthermore, some patients are not good candidates for CCTA. In case of a high probability or known CAD, a functional test may be more efficient to establish management. In the event of safety concerns for radiation or iodine contrast exposure, or circumstances that decrease CCTA performance such as arrhythmia, functional tests may be more appropriate. Because of previously detailed technical limitations of SPECT myocardial perfusion imaging (MPI) and stress echocardiography for the detection of CAD in patients with HCM, quantitative PET or MRI perfusion techniques are preferable when available (Figure 26).

In HCM patients, CAD is associated with adverse outcomes, although no outcome benefit has been prospectively demonstrated from either testing or revascularization. Based on available data, it is reasonable to reserve invasive angiography for cases of severe CAD on CCTA (left main or triple vessel disease) or functional imaging or for patients with persistent symptoms despite medical therapy. Functional assessment of CAD severity is recommended before intervention, either by invasive means (FFR) in the catheterization laboratory, a noninvasive functional test, or CT-FFR in case a CCTA of adequate quality is available. Functional testing is particularly useful if there is discrepancy between symptoms and disease severity.

### 2. HCM patient with abnormal myocardial perfusion test.

If abnormal myocardial perfusion is detected following functional evaluation in symptomatic patients, or in asymptomatic patients as part of a comprehensive imaging evaluation, the question of epicardial CAD should be considered. Patients considered low risk and for whom further testing can be deferred include those without symptoms, low pre-test risk (<15%), normal LVEF, and small ischemic burden (<5% of LV volume, or a defect not well defined by a coronary distribution) (Figure 27). High-risk patients include those with symptoms and a large territorial ischemic defect (>10%) and should be considered for catheter-based coronary angiography or CCTA (with FFR if available) if a noninvasive strategy is preferred. Intermediate-risk patients may be further risk-stratified noninvasively by CCTA.

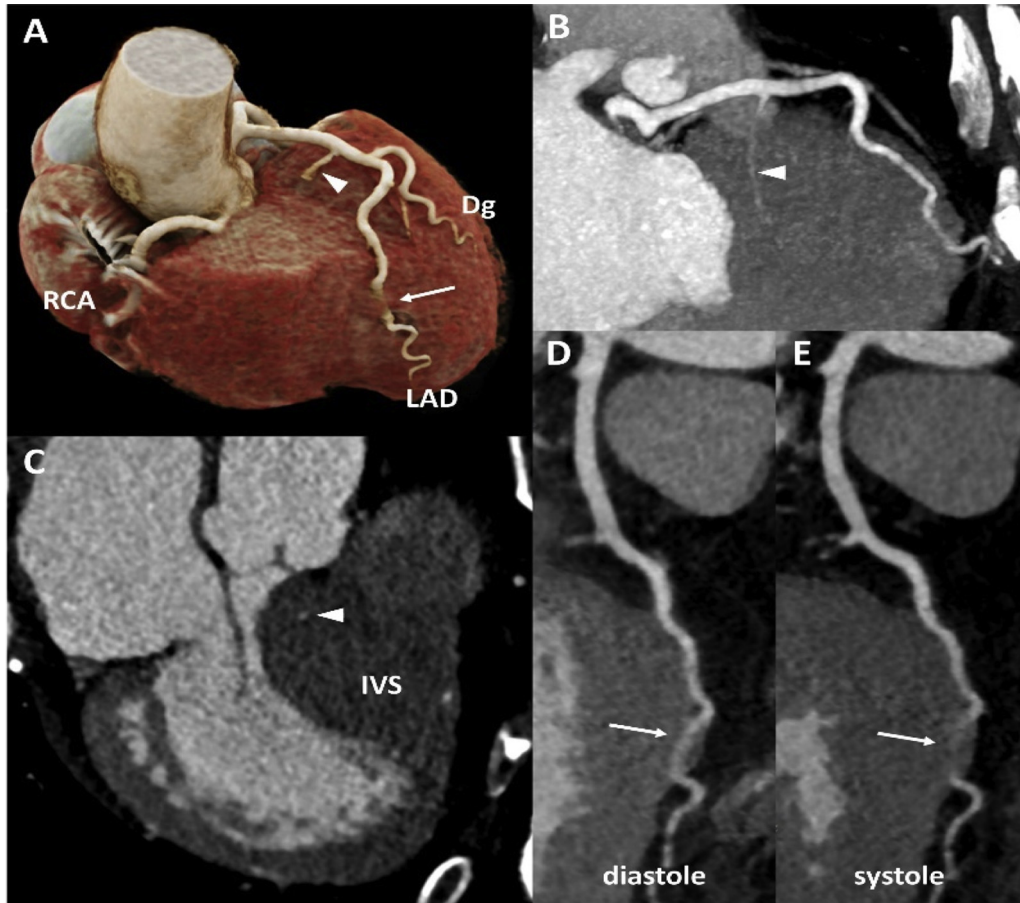


**Figure 25** Coronary computed tomography angiogram in a patient with hypertrophic cardiomyopathy demonstrating no atherosclerotic coronary disease. There is myocardial bridging (*arrow*) of the distal left anterior descending coronary artery (LAD) and compression of the vessel during systole (panels **A**, **D**, **E**). A large septal branch (*arrow head*) perforates the proximal hypertrophic interventricular septum (IVS) (**A**, **B**, **C**). An atrial lead electrode causes limited streak artifacts in the proximity of the right coronary artery (RCA)(**A**). *Dg*, diagonal branch.

## Recommendations and Key Points

- 1- CCTA can be used to noninvasively evaluate the coronary arteries in HCM patients.
- 2- PET and CMR are the preferred techniques for stress perfusion imaging.
- 3- Epicardial CAD in HCM patients is associated with worse outcomes.

### C. Screening

Echocardiography is the best initial imaging modality for HCM screening, in conjunction with clinical evaluation and ECG. For asymptomatic family members of HCM patients, the frequency of screening depends on the age of the family member, whether a pathogenic variant is identified, and if there is early-onset disease. For children and adolescents from families with known pathogenic variant and/or early onset disease, screening should be performed every 1-2 years. However, in the absence of these 2 conditions, children and adolescents should be screened every 2-3 years. For adults, screening is recommended every 3-5 years, and at the onset of symptoms suggestive of cardiac disease.<sup>2</sup>

All myocardial segments should be carefully examined for evidence of hypertrophy. CMR should be considered in patients with technically challenging echocardiograms, and in patients in whom abnormal electrocardiographic findings are present despite an apparently normal echocardiogram. There are several observational studies in patients who are genotype positive but who have not yet developed LV hypertrophy, noting the presence of crypts, increased ratio of LV wall thickness to LV end-diastolic dimension, increased ECV by CMR, and abnormal segmental systolic and diastolic function.<sup>1,211-214</sup> Despite these intriguing findings, there are few studies relating these abnormalities to the subsequent development of pathological LVH.<sup>215</sup>

## Recommendations and Key Points

- 1- Echocardiography is the initial imaging modality for HCM screening.
- 2- Periodic screening is recommended at intervals that depend on age, presence of a known pathogenic variant, and whether disease is early onset.
- 3- CMR should be considered in patients with technically challenging echocardiograms, and in patients in whom abnormal electrocardiographic findings are present despite an apparently normal echocardiogram.

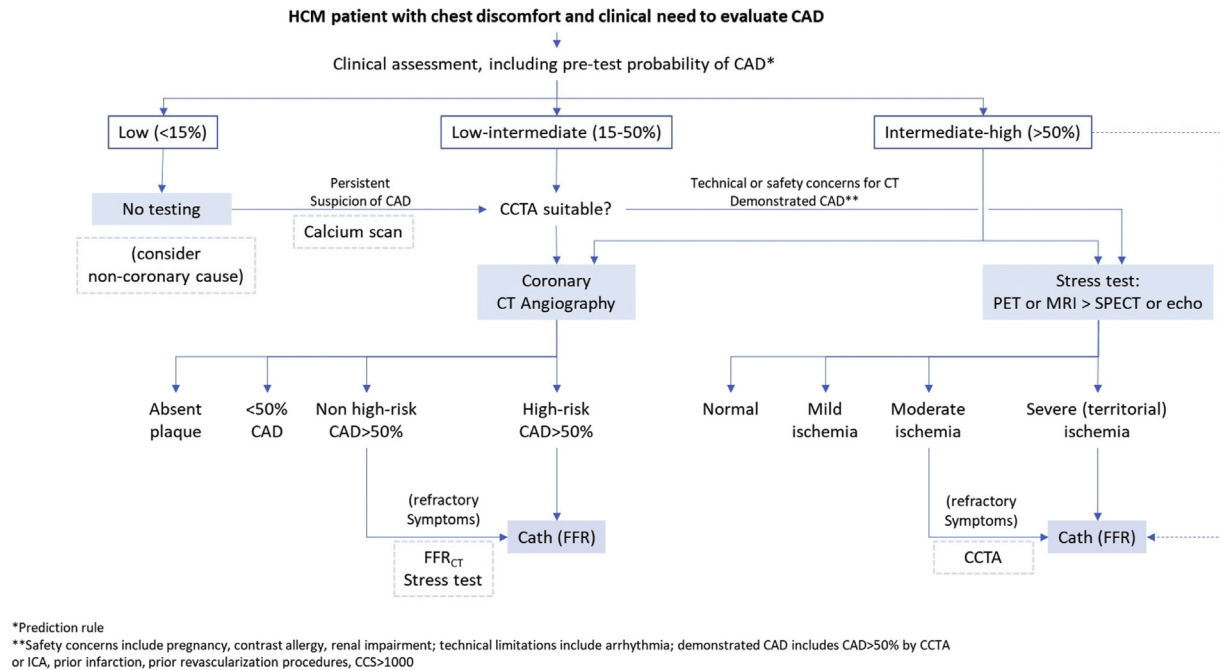


**Figure 26** Algorithm for chest pain workup in the evaluation of patients with HCM. *FFR*, fractional flow reserve.

## D. Role of Imaging in Treatment Selection and Monitoring

**1. Monitoring Medical therapy.** Medical therapy for symptomatic HCM with either the obstructive or nonobstructive phenotype is directed at the relief of symptoms and therefore the primary outcome of treatment is symptom-based. Titration of beta blockers and non-dihydropyridine calcium channel blockers is based on clinical response, with monitoring for bradycardia or atrioventricular conduction block.

In patients with obstructive HCM who remain symptomatic despite maximally tolerated dose of a beta blocker and/or non-dihydropyridine calcium channel blocker with or without the use of disopyramide, repeat echocardiography to evaluate for the presence of a resting and/or provokable peak instantaneous LVOT gradient of  $\geq 50$  mm Hg is appropriate. If this gradient threshold is identified, discussion and shared decision-making with the patient regarding SRT is appropriate.

For patients with reduced EF on treatment with guideline-directed medical therapy, repeat echocardiography to evaluate for reverse remodeling and changes in LV filling and pulmonary artery pressures is reasonable. In the absence of a change in clinical status, repeat TTE every 1 to 2 years is recommended.<sup>2</sup>

A new class of oral allosteric inhibitors of cardiac  $\beta$ -myosin is emerging. This class of drugs resets the equilibrium between the on and off state of myosin heads, causing reversible inhibition of actin-myosin cross bridging. As a result, when these therapies become clinically available, monitoring of LVEF will be required. The frequency of examinations, and clinically relevant LVEF thresholds, remain to be determined.

**2. Pacing.** Dual-chamber pacing is not recommended for the majority of patients with HCM for treatment of LVOTO. It may be useful in a select group of patients, specifically those with a significant resting

or provoked LVOT gradient with drug-refractory symptoms who are not candidates for septal reduction therapies.<sup>144,216</sup> Pacing may also be necessary in patients who develop high degree conduction system disease with heart block after septal reduction therapies as these interventions can damage the conduction system.

Apical RV lead placement is optimal for patients with obstructive HCM to ensure maximal benefit from RV pacing (reducing LVOT gradient and preserving cardiac output), and TEE guidance can be used.<sup>217</sup> In patients who meet criteria for cardiac resynchronization therapy-defibrillator (CRT-D), echocardiography is supportive for the evaluation and follow up of response to this intervention, and selection of the most optimal atrioventricular delay.<sup>103,218</sup>

**3. Surgery.** TEE imaging is important for intraoperative surgical planning and guidance of septal myectomy. The optimal surgical approach depends on the location and extent of maximum septal thickness, mitral valve pathology, and coexisting lesions, such as valvular aortic stenosis. The preprocedural evaluation should evaluate the interventricular septum, the mitral valve apparatus, and any other factors contributing to LVOT obstruction. Concomitant intrinsic valve disease should be noted.

The interventricular septum is best evaluated in the mid-esophageal 4-chamber and long-axis views. The location of maximal thickness should be measured in both the anterosseptal and inferoseptal walls at end-diastole. It is important when making these measurements to optimize border definition of the ventricular walls and be conservative with measurements when the borders are not clearly defined. In addition, the longitudinal extent of thickness needs to be determined. A useful measurement to guide the surgeon's resection includes the distance from the base of the right coronary cusp of the aortic valve to the contact point of the anterior mitral valve leaflet with the septum (Figure 28).

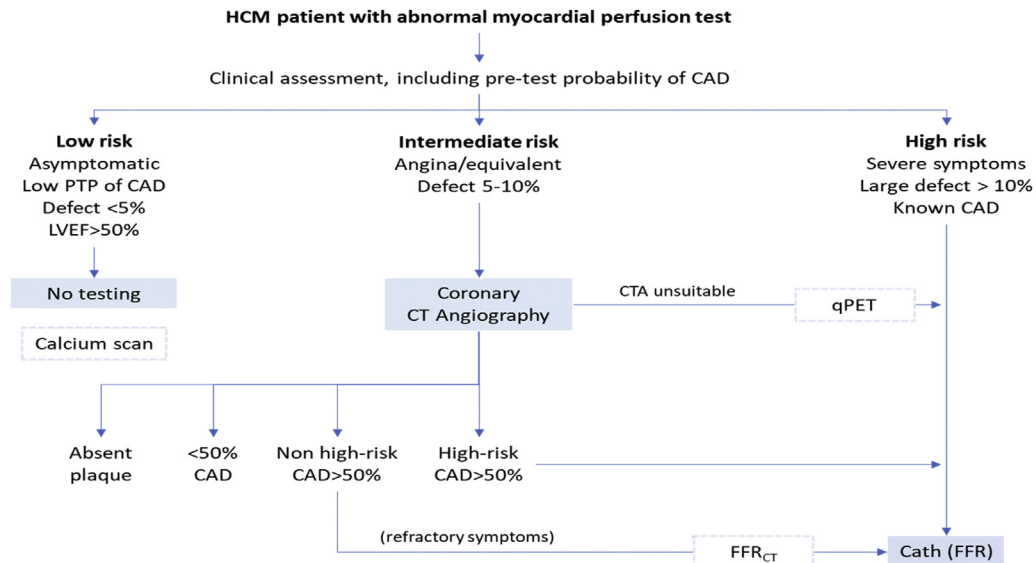


**Figure 27** Algorithm for workup of HCM patients with abnormal myocardial perfusion on stress testing. *qPET*, quantitative positron emission tomography; *PTP*, pre-test probability.

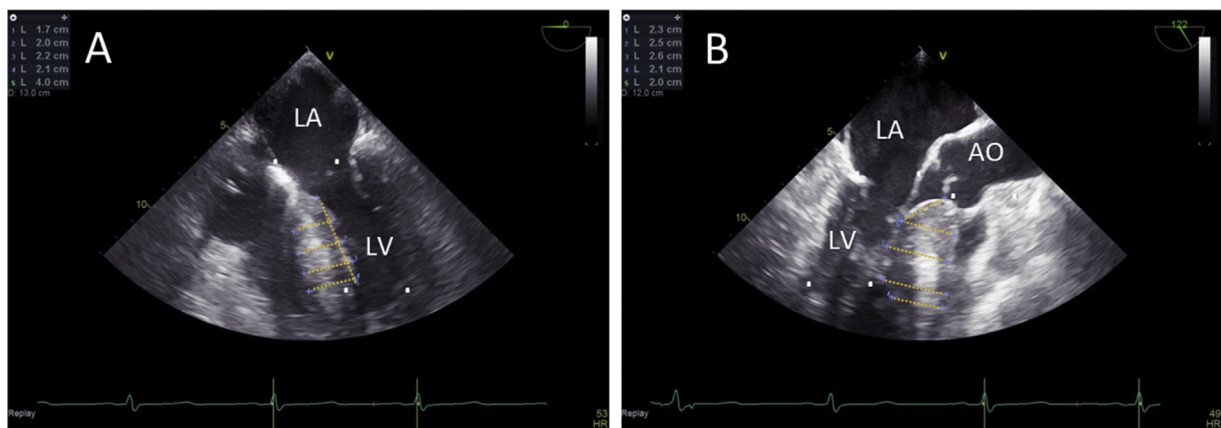


**Figure 28** Transesophageal echocardiogram of intra-operative septal measurements. Left panel: Pre-bypass mid-esophageal 4-chamber view; longitudinal extent of interventricular septum thickness = 4.0 cm. Right panel: Pre-bypass mid-esophageal long-axis view; interventricular septum maximum thickness is 2.6 cm, distance between coaptation point of anterior leaflet mitral valve with septum to right coronary cusp is 2.3 cm.

The mitral valve should be carefully evaluated. MR related to SAM of the mitral valve is typically posteriorly oriented<sup>126</sup> and septal myectomy alone is adequate to resolve the MR. However, MR related to intrinsic mitral valve disease has to be addressed separately. The length of the anterior leaflet of the mitral valve should be measured, as a leaflet  $>16$  mm/m<sup>2</sup> is considered elongated, may contribute to obstruction, and may require leaflet plication.<sup>219,220</sup> In addition, imaging should be performed to determine if anomalous insertion of the papillary muscle is present, as it needs unique treatment, with papillary muscle release and resection of the abnormal attachments to the mitral valve, or papillary muscle realignment.<sup>221</sup> Mitral valve replacement should only be performed in patients with intrinsic mitral valve pathology not amenable to repair and its routine use with septal myectomy should be discouraged.

Finally, the LVOT needs to be evaluated to confirm dynamic obstruction and rule out aortic stenosis or a subaortic membrane. Dynamic gradients are best obtained in a deep transgastric view but

may not be as high as on pre-procedural imaging due to limitations of Doppler alignment and the hemodynamic effects of anesthesia.

After weaning from cardiopulmonary bypass, postprocedural assessment is important, including for cases with extended myectomy.<sup>220</sup> It usually includes a pharmacological challenge (most commonly with isoproterenol or dobutamine) to evaluate for residual obstruction.<sup>222</sup> An elevated LVOT velocity ( $>3$  m/s) or the presence of significant SAM during provocation may require a return to bypass for additional surgical intervention. Although it is common to obtain measurements of the interventricular septum during this period, the measurements may not be accurate due to tissue edema. Finally, complications related to myectomy, such as aortic regurgitation, ventricular septal defect, and coronary cameral fistula, need to be excluded (Figure 29).

The application of intraoperative TEE in the management of surgical myectomy has been detailed in the ASE Guidelines for the Use of Transesophageal Echocardiography to Assist with Surgical Decision-

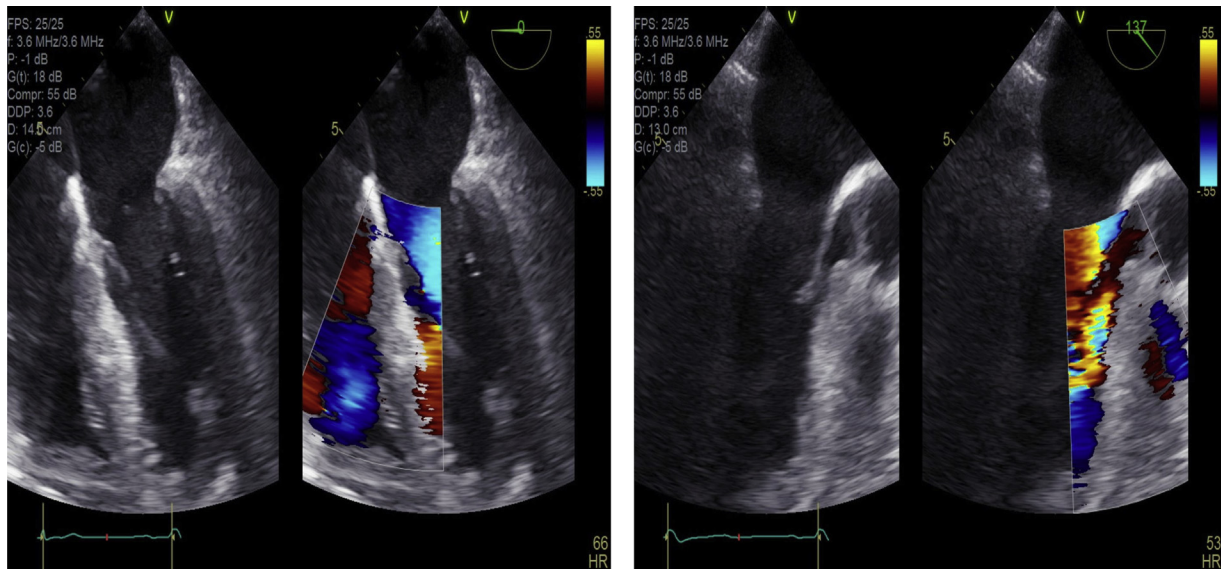


**Figure 29** Two-dimensional (2D) and color Doppler echocardiographic evaluation for ventricular septal defect (VSD). Left panel: Mid-esophageal 4-chamber view; Right panel: Post-bypass mid-esophageal long-axis view. There is no VSD.

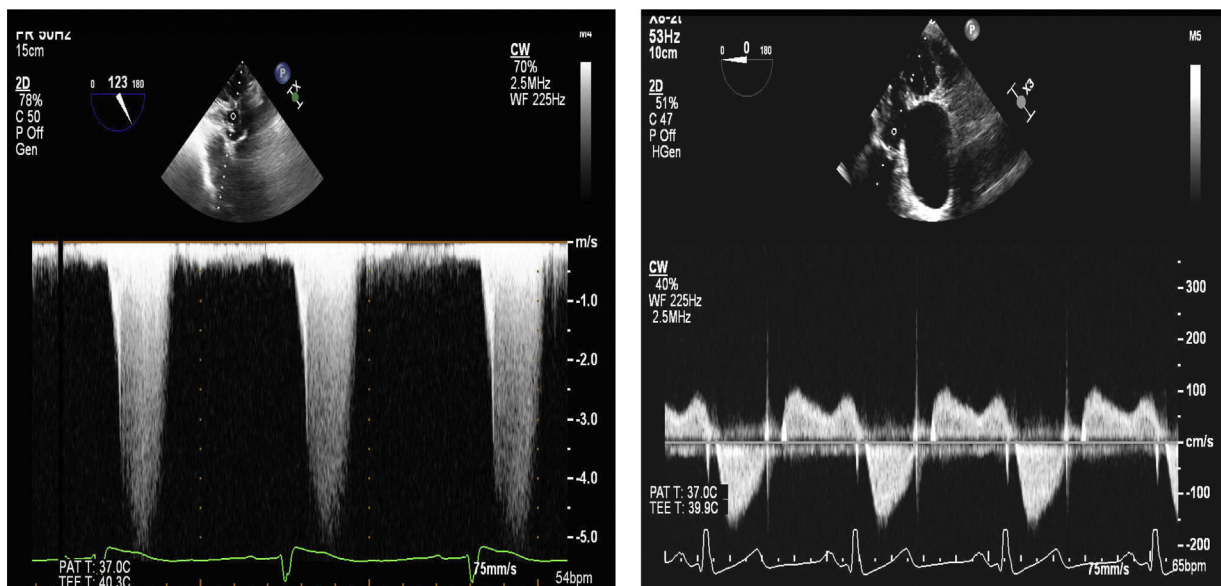


**Figure 30** Left ventricular outflow tract gradient at baseline before (left), and after (right) transcatheter edge-to-edge repair (TEER) of the mitral valve. Signals acquired by transesophageal echocardiography using deep transgastric view. Notice the elimination of the 100-mm Hg gradient after TEER.

Making in the Operating Room: A Surgery-Based Approach.<sup>221</sup> Further details are outlined in that document.

**4. Alcohol Septal Ablation.** Imaging plays an important role in patient selection for alcohol (ethanol) septal ablation, with the goal of determining location of the increased septal thickness, dynamic obstruction, and presence of coexisting abnormalities that can indicate a preference for surgical intervention. These include the need for corrective mitral/papillary surgery as well as for extended myectomy when hypertrophy extends into the middle LV.

Echocardiography is essential for procedural guidance of alcohol septal ablation.<sup>223-226</sup> Ethanol is injected into one of the proximal septal perforator branches (which usually arises from the left anterior

descending coronary artery) to produce localized myocardial infarction of the proximal anterior septum thereby reducing dynamic obstruction (Videos 5 to 8). The use of myocardial contrast echocardiography (MCE) with the injection of echocardiographic contrast agent into the target septal artery (or arteries) to delineate the vascular distribution of the individual perforator branches is important to the success of the procedure. After the target septal perforator is identified and cannulated, a balloon catheter is advanced into the vessel and inflated to prevent backflow. Subsequently, 1 to 2 mL of a diluted contrast agent is injected through the balloon catheter followed by a 1-2-mL saline flush during continuous imaging. The contrast agent should be diluted with normal saline to optimize myocardial opacification and minimize attenuation. Most operators now use agitated radiographic contrast

instead of UEA. MCE produces a demarcated area with increased echocardiographic density in the basal septum. It is important to document the absence of perfusion of myocardial segments remote from the targeted areas for ablation, including the LV anterolateral wall, RV free wall, and papillary muscles. Observational studies have shown that the use of MCE results in shorter intervention time, fluoroscopy duration, a smaller number of occluded vessels, a smaller volume of injected ethanol, lower likelihood of heart block, and higher likelihood of success. This is due to the selection of different vessels for ethanol injection based on the segments opacified by MCE, and in some cases aborting the procedure altogether.

At most centers, TTE is used for intraprocedural guidance, relying on apical 4-, 3-, and 2-chamber views and parasternal short-axis and long-axis views to delineate opacification of target and nontarget regions (if present). Sometimes, TEE is needed because of challenging TTE images. If TEE is used, the 4-chamber (deep gastric at 0°) and longitudinal (mid-esophageal, aortic valve level, 120–130°) views should be used. These views may be supplemented by the transgastric short-axis view to assess for possible perfusion of the papillary muscles or the RV. After the procedure, cardiac imaging (usually only echocardiography is needed) is used to evaluate changes in septal thickness, LV dimensions, mass, systolic and diastolic functions, MR, and possible complications such as ventricular septal defect.<sup>2,27</sup>

**5. Transcatheter Edge-to-Edge Repair.** Although there are no formal guideline recommendations for the use of transcatheter edge-to-edge repair (TEER), in patients who remain symptomatic despite guideline-directed medical therapy and are deemed to have an unacceptable risk for septal reduction therapy, including septal thickness <1.5 cm, an off-label approach of percutaneous mitral plication may be considered.<sup>2</sup> Favorable baseline findings include SAM resulting in LVOT obstruction, absence of calcification in the grasping zone, and suitable mitral valve area (mean transmitral gradient <5 mm Hg and mitral valve area ≥4 cm<sup>2</sup>) to exclude significant post-procedure mitral valve stenosis (Figure 30 and Videos 9 to 11).

## Recommendations and Key Points

- 1- For patients on oral allosteric modulators of cardiac  $\beta$ -myosin, monitoring of LVEF is essential to avoid the development of heart failure due to reduced EF.
- 2- Intraoperative TEE plays a critical role in guiding the management of HCM patients undergoing surgical myectomy.
- 3- Myocardial contrast echocardiography plays a critical role in intraprocedural guidance of alcohol septal ablation.
- 4- TEE is critical for intraprocedural guidance of TEER to treat obstructive HCM patients who are not candidates for septal reduction therapy.

## SUMMARY

Multimodality imaging plays a crucial role in the initial evaluation of patients with known or suspected HCM. In conjunction with clinical findings, imaging can confirm or refute the diagnosis. Imaging should be performed at clinical sites/centers of excellence with experience in the diagnosis and management of HCM. Imaging is central to risk stratification for sudden cardiac death as well as the evaluation of patients with chest pain and possible CAD. Along with ECG, imaging

with echocardiography and/or CMR is needed for screening. In addition, imaging can guide treatment for obstructive HCM, be it with negative inotropic drugs, septal reduction therapy, or TEER of the mitral valve. The imaging staff should have a clear understanding of the strengths and limitations of the different imaging modalities and the clinical implications of the findings ascertained by imaging. Importantly, the results should be communicated clearly with the clinical team taking care of the patient.

**NOTICE AND DISCLAIMER:** This report is made available by ASE as a courtesy reference source for members. This report contains recommendations only and should not be used as the sole basis to make medical practice decisions or for disciplinary action against any employee. The statements and recommendations contained in this report are primarily based on the opinions of experts, rather than on scientifically-verified data. ASE makes no express or implied warranties regarding the completeness or accuracy of the information in this report, including the warranty of merchantability or fitness for a particular purpose. In no event shall ASE be liable to you, your patients, or any other third parties for any decision made or action taken by you or such other parties in reliance on this information. Nor does your use of this information constitute the offering of medical advice by ASE or create any physician-patient relationship between ASE and your patients or anyone else.

## Reviewers

This document was reviewed by members of the 2021–2022 ASE Guidelines and Standards Committee, ASE Board of Directors, ASE Executive Committee, and designated representatives from the American Society of Nuclear Cardiology, Society for Cardiovascular Magnetic Resonance, and Society of Cardiovascular Computed Tomography. Reviewers included David M. Dudzinski, MD, FASE, Jared Feinman, MD, FASE, Lanqi Hua, ACS, APCA, RDCS, FASE, Judy Hung, MD, FASE, Noreen Kelly, MD, FASE, Kan Liu, MD, FASE, Anuj Mediratta, MD, FASE, David Orsinelli, MD, FASE, Alan S. Pearlman, MD, FASE, Andrew Pellett, PhD, RDCS, Anita Sadeghpour, MD, FASE, Vincent Sorrell, MD, FASE, Kenan Stern, MD, FASE, Melissa A. Wasserman, RDCS, RCCS, FASE, David H. Wiener, MD, FASE.

## SUPPLEMENTARY DATA

Supplementary data to this article can be found online at <https://doi.org/10.1016/j.echo.2022.03.012>.

## REFERENCES

1. Nagueh SF, Bierig SM, Budoff MJ, Desai M, Dilsizian V, Eidem B, et al. American Society of Echocardiography clinical recommendations for multimodality cardiovascular imaging of patients with hypertrophic cardiomyopathy: Endorsed by the American Society of Nuclear Cardiology, Society for Cardiovascular Magnetic Resonance, and Society of Cardiovascular Computed Tomography. *J Am Soc Echocardiogr* 2011;24: 473-98.
2. Ommen SR, Mital S, Burke MA, Day SM, Deswal A, Elliott P, et al. 2020 AHA/ACC Guideline for the Diagnosis and Treatment of Patients With Hypertrophic Cardiomyopathy: A Report of the American College of

- Cardiology/American Heart Association Joint Committee on Clinical Practice Guidelines. *J Am Coll Cardiol* 2020;162:e23-106.
3. Maron BJ, Gardin JM, Flack JM, Gidding SS, Kurosaki TT, Bild DE. Prevalence of hypertrophic cardiomyopathy in a general population of young adults. Echocardiographic analysis of 4111 subjects in the CARDIA Study. Coronary Artery Risk Development in (Young) Adults. *Circulation* 1995;92:785-9.
  4. Maron BJ, Mathenge R, Casey SA, Poliac LC, Longe TF. Clinical profile of hypertrophic cardiomyopathy identified de novo in rural communities. *J Am Coll Cardiol* 1999;33:1590-5.
  5. Semsarian C, Ingles J, Maron MS, Maron BJ. New perspectives on the prevalence of hypertrophic cardiomyopathy. *J Am Coll Cardiol* 2015;65:1249-54.
  6. Maron BJ, Rowin EJ, Casey SA, Maron MS. How hypertrophic cardiomyopathy became a contemporary treatable genetic disease with low mortality: shaped by 50 years of clinical research and practice. *JAMA Cardiol* 2016;1:98-105.
  7. Villemain O, Correia M, Mousseaux E, Baranger J, Zarka S, Podetti I, et al. Myocardial stiffness evaluation using noninvasive shear wave imaging in healthy and hypertrophic cardiomyopathic adults. *JACC Cardiovasc Imaging* 2019;12:1135-45.
  8. Soullier C, Obert P, Doucende G, Nottin S, Cade S, Perez-Martin A, et al. Exercise response in hypertrophic cardiomyopathy: blunted left ventricular deformational and twisting reserve with altered systolic-diastolic coupling. *Circ Cardiovasc Imaging* 2012;5:324-32.
  9. Pasqualucci D, Fornaro A, Castelli G, Rossi A, Arretini A, Chiriatti C, et al. Clinical spectrum, therapeutic options, and outcome of advanced heart failure in hypertrophic cardiomyopathy. *Circ Heart Fail* 2015;8:1014-21.
  10. Rowin EJ, Maron BJ, Carrick RT, Patel PP, Koethe B, Wells S, et al. Outcomes in patients with hypertrophic cardiomyopathy and left ventricular systolic dysfunction. *J Am Coll Cardiol* 2020;75:3033-43.
  11. Sorajja P, Nishimura RA, Gersh BJ, Dearani JA, Hodge DO, Wiste HJ, et al. Outcome of mildly symptomatic or asymptomatic obstructive hypertrophic cardiomyopathy: a long-term follow-up study. *J Am Coll Cardiol* 2009;54:234-41.
  12. Maron MS, Olivetto I, Zenovich AG, Link MS, Pandian NG, Kuvin JT, et al. Hypertrophic cardiomyopathy is predominantly a disease of left ventricular outflow tract obstruction. *Circulation* 2006;114:2232-9.
  13. Sherrid MV, Balam S, Kim B, Axel L, Swistel DG. The mitral valve in obstructive hypertrophic cardiomyopathy: a test in context. *J Am Coll Cardiol* 2016;67:1846-58.
  14. Patel V, Critoph CH, Finlay MC, Mist B, Lambiase PD, Elliott PM. Heart rate recovery in patients with hypertrophic cardiomyopathy. *Am J Cardiol* 2014;113:1011-7.
  15. Raphael CE, Cooper R, Parker KH, Collinson J, Vassiliou V, Pennell DJ, et al. Mechanisms of myocardial ischemia in hypertrophic cardiomyopathy: insights from wave intensity analysis and magnetic resonance. *J Am Coll Cardiol* 2016;68:1651-60.
  16. Sharzehee M, Chang Y, Song JP, Han HC. Hemodynamic effects of myocardial bridging in patients with hypertrophic cardiomyopathy. *Am J Physiol Heart Circ Physiol* 2019;317:H1282-91.
  17. van Velzen HG, Theuns DA, Yap SC, Michels M, Schinkel AF. Incidence of device-detected atrial fibrillation and long-term outcomes in patients with hypertrophic cardiomyopathy. *Am J Cardiol* 2017;119:100-5.
  18. Wilke I, Witzel K, Munch J, Pecha S, Blankenberg S, Reichenspurner H, et al. High incidence of de novo and subclinical atrial fibrillation in patients with hypertrophic cardiomyopathy and cardiac rhythm management device. *J Cardiovasc Electrophysiol* 2016;27:779-84.
  19. Hinojar R, Varma N, Child N, Goodman B, Jabbour A, Yu CY, et al. T1 mapping in discrimination of hypertrophic phenotypes: hypertensive heart disease and hypertrophic cardiomyopathy: findings from the international T1 multicenter cardiovascular magnetic resonance study. *Circ Cardiovasc Imaging* 2015;8:e003285.
  20. Schnell F, Matelot D, Daudin M, Kervio G, Mabo P, Carre F, et al. Mechanical dispersion by strain echocardiography: a novel tool to diagnose hypertrophic cardiomyopathy in athletes. *J Am Soc Echocardiogr* 2017;30:251-61.
  21. Williams LK, Forero JF, Popovic ZB, Phelan D, Delgado D, Rakowski H, et al. Patterns of CMR measured longitudinal strain and its association with late gadolinium enhancement in patients with cardiac amyloidosis and its mimics. *J Cardiovasc Magn Reson* 2017;19:61.
  22. Phelan D, Thavendiranathan P, Popovic Z, Collier P, Griffin B, Thomas JD, et al. Application of a parametric display of two-dimensional speckle-tracking longitudinal strain to improve the etiologic diagnosis of mild to moderate left ventricular hypertrophy. *J Am Soc Echocardiogr* 2014;27:888-95.
  23. Lorenzini M, Norrish G, Field E, Ochoa JP, Cicerchia M, Akhtar MM, et al. Penetrance of hypertrophic cardiomyopathy in sarcomere protein mutation carriers. *J Am Coll Cardiol* 2020;76:550-9.
  24. Maron BJ, Rowin EJ, Maron MS. Evolution of Risk Stratification and Sudden Death Prevention in Hypertrophic Cardiomyopathy: 20 Years with the Implantable Cardioverter-Defibrillator. *Heart Rhythm* 2021;18:1012-23.
  25. Bos JM, Towbin JA, Ackerman MJ. Diagnostic, prognostic, and therapeutic implications of genetic testing for hypertrophic cardiomyopathy. *J Am Coll Cardiol* 2009;54:201-11.
  26. Colan SD. Normal echocardiographic values for cardiovascular structures. *Echocardiography in Pediatric and Congenital Heart Disease: From Fetus to Adult*. John Wiley & Sons Ltd; 2016. pp. 883-901.
  27. Lopez L, Colan S, Stylianou M, Granger S, Trachtenberg F, Frommelt P, et al. Relationship of Echocardiographic Z Scores Adjusted for Body Surface Area to Age, Sex, Race, and Ethnicity: The Pediatric Heart Network Normal Echocardiogram Database. *Circ Cardiovasc Imaging* 2017;10:e006979.
  28. Klues HG, Schiffers A, Maron BJ. Phenotypic spectrum and patterns of left ventricular hypertrophy in hypertrophic cardiomyopathy: morphologic observations and significance as assessed by two-dimensional echocardiography in 600 patients. *J Am Coll Cardiol* 1995;26:1699-708.
  29. Ho CY, Day SM, Ashley EA, Michels M, Pereira AC, Jacoby D, et al. Genotype and lifetime burden of disease in hypertrophic cardiomyopathy: insights from the sarcomeric human cardiomyopathy registry (SHaRe). *Circulation* 2018;138:1387-98.
  30. Urbano-Moral JA, Gonzalez-Gonzalez AM, Maldonado G, Gutierrez-Garcia-Moreno L, Vivancos-Delgado R, De Mora-Martin M, et al. Contrast-enhanced echocardiographic measurement of left ventricular wall thickness in hypertrophic cardiomyopathy: comparison with standard echocardiography and cardiac magnetic resonance. *J Am Soc Echocardiogr* 2020;33:1106-15.
  31. Phelan D, Sperry BW, Thavendiranathan P, Collier P, Popovic ZB, Lever HM, et al. Comparison of ventricular septal measurements in hypertrophic cardiomyopathy patients who underwent surgical myectomy using multimodality imaging and implications for diagnosis and management. *Am J Cardiol* 2017;119:1656-62.
  32. Lang RM, Badano LP, Mor-Avi V, Afilalo J, Armstrong A, Ernande L, et al. Recommendations for cardiac chamber quantification by echocardiography in adults: an update from the American Society of Echocardiography and the European Association of Cardiovascular Imaging. *Eur Heart J Cardiovasc Imaging* 2015;16:233-70.
  33. Chang SA, Kim HK, Lee SC, Kim EY, Hahm SH, Kwon OM, et al. Assessment of left ventricular mass in hypertrophic cardiomyopathy by real-time three-dimensional echocardiography using single-beat capture image. *J Am Soc Echocardiogr* 2013;26:436-42.
  34. Avegliano GP, Costabel JP, Asch FM, Sciancalepore A, Kuschnir P, Huguet M, et al. Utility of real time 3D echocardiography for the assessment of left ventricular mass in patients with hypertrophic cardiomyopathy: comparison with cardiac magnetic resonance. *Echocardiography* 2016;33:431-6.
  35. Hindieh W, Chan R, Rakowski H. Complementary role of echocardiography and cardiac magnetic resonance in hypertrophic cardiomyopathy. *Curr Cardiol Rep* 2017;19:81.

36. Haaf P, Garg P, Messroghli DR, Broadbent DA, Greenwood JP, Plein S. Cardiac T1 Mapping and Extracellular Volume (ECV) in clinical practice: a comprehensive review. *J Cardiovasc Magn Reson* 2016;18:89.
37. Captur G, Manisty C, Moon JC. Cardiac MRI evaluation of myocardial disease. *Heart* 2016;102:1429-35.
38. van der Vleuten PA, Willems TP, Gotte MJ, Tio RA, Greuter MJ, Zijlstra F, et al. Quantification of global left ventricular function: comparison of multidetector computed tomography and magnetic resonance imaging: a meta-analysis and review of the current literature. *Acta Radiol* 2006;47:1049-57.
39. Puesken M, Fischbach R, Wenker M, Seifarth H, Maintz D, Heindel W, et al. Global left-ventricular function assessment using dual-source multi-detector CT: effect of improved temporal resolution on ventricular volume measurement. *Eur Radiol* 2008;18:2087-94.
40. Cooper RM, Binukrishnan SR, Shahzad A, Hasleton J, Sigwart U, Stables RH. Computed tomography angiography planning identifies the target vessel for optimum infarct location and improves clinical outcome in alcohol septal ablation for hypertrophic obstructive cardiomyopathy. *EuroIntervention* 2017;12:e2194-203.
41. Rowin EJ, Maron BJ, Appelbaum E, Link MS, Gibson CM, Lesser JR, et al. Significance of false negative electrocardiograms in preparticipation screening of athletes for hypertrophic cardiomyopathy. *Am J Cardiol* 2012;110:1027-32.
42. Sheikh N, Papadakis M, Schnell F, Panoulas V, Malhotra A, Wilson M, et al. Clinical profile of athletes with hypertrophic cardiomyopathy. *Circ Cardiovasc Imaging* 2015;8:e003454.
43. Baggish AL, Battle RW, Beaver TA, Border WL, Douglas PS, Kramer CM, et al. Recommendations on the use of multimodality cardiovascular imaging in young adult competitive athletes: A report from the American Society of Echocardiography in Collaboration with the Society of Cardiovascular Computed Tomography and the Society for Cardiovascular Magnetic Resonance. *J Am Soc Echocardiogr* 2020;33:523-49.
44. Basavarajaiah S, Boraita A, Whyte G, Wilson M, Carby L, Shah A, et al. Ethnic differences in left ventricular remodeling in highly-trained athletes: relevance to differentiating physiologic left ventricular hypertrophy from hypertrophic cardiomyopathy. *J Am Coll Cardiol* 2008;51:2256-62.
45. Engel DJ, Schwartz A, Homma S. Athletic cardiac remodeling in US professional basketball players. *JAMA Cardiol* 2016;1:80-7.
46. Finocchiaro G, Dhutia H, D'Silva A, Malhotra A, Steriotis A, Millar L, et al. Effect of sex and sporting discipline on LV adaptation to exercise. *JACC Cardiovasc Imaging* 2017;10:965-72.
47. Finocchiaro G, Dhutia H, D'Silva A, Malhotra A, Sheikh N, Narain R, et al. Role of Doppler diastolic parameters in differentiating physiological left ventricular hypertrophy from hypertrophic cardiomyopathy. *J Am Soc Echocardiogr* 2018;31:606-613 e1.
48. Gaitonde M, Jones S, McCracken C, Ferguson ME, Michelfelder E, Sachdeva R, et al. Evaluation of left ventricular outflow gradients during staged exercise stress echocardiography helps differentiate pediatric patients with hypertrophic cardiomyopathy from athletes and normal subjects. *Pediatr Exerc Sci* 2021;1-7.
49. Swoboda PP, McDiarmid AK, Erhayiem B, Broadbent DA, Dobson LE, Garg P, et al. Assessing myocardial extracellular volume by T1 mapping to distinguish hypertrophic cardiomyopathy from athlete's heart. *J Am Coll Cardiol* 2016;67:2189-90.
50. Malek LA, Bucciarelli-Ducci C. Myocardial fibrosis in athletes-Current perspective. *Clin Cardiol* 2020;43:882-8.
51. Clark DE, Parikh A, Dendy JM, Diamond AB, George-Durrett K, Fish FA, et al. COVID-19 myocardial pathology evaluation in athletes with Cardiac Magnetic Resonance (COMPETE CMR). *Circulation* 2021;143:609-12.
52. de Gregorio C, Speranza G, Magliarditi A, Pugliatti P, Ando G, Coglitore S. Detraining-related changes in left ventricular wall thickness and longitudinal strain in a young athlete likely to have hypertrophic cardiomyopathy. *Journal of sports science & medicine* 2012;11:557-61.
53. Maurer MS, Schwartz JH, Gundapaneni B, Elliott PM, Merlini G, Waddington-Cruz M, et al. Tafamidis Treatment for Patients with Transthyretin Amyloid Cardiomyopathy. *N Engl J Med* 2018;379:1007-16.
54. Sperry BW, Vranian MN, Hachamovitch R, Joshi H, Ikram A, Phelan D, et al. Subtype-specific interactions and prognosis in cardiac amyloidosis. *J Am Heart Assoc* 2016;5:e002877.
55. Phelan D, Collier P, Thavendiranathan P, Popovic ZB, Hanna M, Plana JC, et al. Relative apical sparing of longitudinal strain using two-dimensional speckle-tracking echocardiography is both sensitive and specific for the diagnosis of cardiac amyloidosis. *Heart* 2012;98:1442-8.
56. Boucek D, Jirikovic J, Taylor M. Natural history of Danon disease. *Genet Med* 2011;13:563-8.
57. Kampmann C, Baehner F, Whybra C, Martin C, Wiethoff CM, Ries M, et al. Cardiac manifestations of Anderson-Fabry disease in heterozygous females. *J Am Coll Cardiol* 2002;40:1668-74.
58. Haland TF, Hasselberg NE, Almaas VM, Dejgaard LA, Saberniak J, Leren IS, et al. The systolic paradox in hypertrophic cardiomyopathy. *Open Heart* 2017;4:e000571.
59. Marstrand P, Han L, Day SM, Olivotto I, Ashley EA, Michels M, et al. Hypertrophic cardiomyopathy with left ventricular systolic dysfunction: insights from the SHaRe Registry. *Circulation* 2020;141:1371-83.
60. Pickett CA, Cheezum MK, Kassop D, Villines TC, Hulten EA. Accuracy of cardiac CT, radionuclide and invasive ventriculography, two- and three-dimensional echocardiography, and SPECT for left and right ventricular ejection fraction compared with cardiac MRI: a meta-analysis. *Eur Heart J Cardiovasc Imaging* 2015;16:848-52.
61. Liu H, Pozios I, Haileselassie B, Nowbar A, Sorensen LL, Phillip S, et al. Role of global longitudinal strain in predicting outcomes in hypertrophic cardiomyopathy. *Am J Cardiol* 2017;120:670-5.
62. Reant P, Mirabel M, Lloyd G, Peyrou J, Lopez Ayala JM, Dickie S, et al. Global longitudinal strain is associated with heart failure outcomes in hypertrophic cardiomyopathy. *Heart* 2016;102:741-7.
63. Serri K, Reant P, Lafitte M, Berhouet M, Le Bouffos V, Roudaut R, et al. Global and regional myocardial function quantification by two-dimensional strain: application in hypertrophic cardiomyopathy. *J Am Coll Cardiol* 2006;47:1175-81.
64. Pozios I, Pinheiro A, Corona-Villalobos C, Sorensen LL, Dardari Z, Liu HY, et al. Rest and stress longitudinal systolic left ventricular mechanics in hypertrophic cardiomyopathy: implications for prognostication. *J Am Soc Echocardiogr* 2018;31:578-86.
65. Neisius U, Myerson L, Fahmy AS, Nakamori S, El-Rewaidy H, Joshi G, et al. Cardiovascular magnetic resonance feature tracking strain analysis for discrimination between hypertensive heart disease and hypertrophic cardiomyopathy. *PLoS One* 2019;14:e0221061.
66. Vigneault DM, Yang E, Jensen PJ, Tee MW, Farhad H, Chu L, et al. Left ventricular strain is abnormal in preclinical and overt hypertrophic cardiomyopathy: cardiac MR feature tracking. *Radiology* 2019;290:640-8.
67. Li A, Ruh A, Berhane H, Robinson JD, Markl M, Rigsby CK. Altered regional myocardial velocities by tissue phase mapping and feature tracking in pediatric patients with hypertrophic cardiomyopathy. *Pediatr Radiol* 2020;50:168-79.
68. Dorobantu DM, Wadey CA, Amir NH, Stuart AG, Williams CA, Pieles GE. The role of speckle tracking echocardiography in the evaluation of common inherited cardiomyopathies in children and adolescents: a systematic review. *Diagnostics (Basel)* 2021;11.
69. Forsey J, Benson L, Rozenblyum E, Friedberg MK, Mertens L. Early changes in apical rotation in genotype positive children with hypertrophic cardiomyopathy mutations without hypertrophic changes on two-dimensional imaging. *J Am Soc Echocardiogr* 2014;27:215-21.

70. Nishimura RA, Appleton CP, Redfield MM, Ilstrup DM, Holmes DR Jr, Tajik AJ. Noninvasive doppler echocardiographic evaluation of left ventricular filling pressures in patients with cardiomyopathies: a simultaneous Doppler echocardiographic and cardiac catheterization study. *J Am Coll Cardiol* 1996;28:1226-33.
71. Nagueh SF, Lakkis NM, Middleton KJ, Spencer WH 3rd, Zoghbi WA, Quinones MA. Doppler estimation of left ventricular filling pressures in patients with hypertrophic cardiomyopathy. *Circulation* 1999;99:254-61.
72. Geske JB, Sorajja P, Nishimura RA, Ommen SR. Evaluation of left ventricular filling pressures by Doppler echocardiography in patients with hypertrophic cardiomyopathy: correlation with direct left atrial pressure measurement at cardiac catheterization. *Circulation* 2007;116:2702-8.
73. Thavendiranathan P, Guetter C, da Silveira JS, Lu X, Scandling D, Xue H, et al. Mitral annular velocity measurement with cardiac magnetic resonance imaging using a novel annular tracking algorithm: Validation against echocardiography. *Magn Reson Imaging* 2019;55:72-80.
74. Nakahara T, Jinzaki M, Fukuda N, Takahashi Y, Ishihara T, Takada A, et al. Estimation of the left ventricular diastolic function with cardiac MDCT: correlation of the slope of the time-enhancement-curve with the mitral annulus diastolic velocity. *Eur J Radiol* 2012;81:234-8.
75. Nagueh SF, Smiseth OA, Appleton CP, Byrd BF 3rd, Dokainish H, Edvardsen T, et al. Recommendations for the evaluation of left ventricular diastolic function by echocardiography: An Update from the American Society of Echocardiography and the European Association of Cardiovascular Imaging. *J Am Soc Echocardiogr* 2016;29:277-314.
76. Matsumura Y, Elliott PM, Virdee MS, Sorajja P, Doi Y, McKenna WJ. Left ventricular diastolic function assessed using Doppler tissue imaging in patients with hypertrophic cardiomyopathy: relation to symptoms and exercise capacity. *Heart* 2002;87:247-51.
77. McMahon CJ, Nagueh SF, Pignatelli RH, Denfield SW, Dreyer WJ, Price JF, et al. Characterization of left ventricular diastolic function by tissue Doppler imaging and clinical status in children with hypertrophic cardiomyopathy. *Circulation* 2004;109:1756-62.
78. Losi MA, Betocchi S, Barbatì G, Parisi V, Tocchetti CG, Pastore F, et al. Prognostic significance of left atrial volume dilatation in patients with hypertrophic cardiomyopathy. *J Am Soc Echocardiogr* 2009;22:76-81.
79. Woo A, Williams WG, Choi R, Wigle ED, Rozenblyum E, Fedwick K, et al. Clinical and echocardiographic determinants of long-term survival after surgical myectomy in obstructive hypertrophic cardiomyopathy. *Circulation* 2005;111:2033-41.
80. Nistri S, Olivetto I, Betocchi S, Losi MA, Valsecchi G, Pinamonti B, et al. Prognostic significance of left atrial size in patients with hypertrophic cardiomyopathy (from the Italian Registry for Hypertrophic Cardiomyopathy). *Am J Cardiol* 2006;98:960-5.
81. Hiemstra YL, Debonnaire P, Bootsma M, van Zwet EW, Delgado V, Schalij MJ, et al. Global longitudinal strain and left atrial volume index provide incremental prognostic value in patients with hypertrophic cardiomyopathy. *Circ Cardiovasc Imaging* 2017;10.
82. Debonnaire P, Joyce E, Hiemstra Y, Mertens BJ, Atsma DE, Schalij MJ, et al. Left atrial size and function in hypertrophic cardiomyopathy patients and risk of new-onset atrial fibrillation. *Circ Arrhythm Electrophysiol* 2017;10.
83. Vasquez N, Ostrander BT, Lu DY, Ventoulis I, Haileselassie B, Goyal S, et al. Low left atrial strain is associated with adverse outcomes in hypertrophic cardiomyopathy patients. *J Am Soc Echocardiogr* 2019;32:593-603 e1.
84. Tayal B, Malahfi M, Buergler JM, Shah DJ, Nagueh SF. Hemodynamic determinants of left atrial strain in patients with hypertrophic cardiomyopathy: A combined echocardiography and CMR study. *PLoS One* 2021;16:e0245934.
85. Sivalokanathan S, Zghaib T, Greenland GV, Vasquez N, Kudchadkar SM, Kontari E, et al. Hypertrophic cardiomyopathy patients with paroxysmal atrial fibrillation have a high burden of left atrial fibrosis by cardiac magnetic resonance imaging. *JACC Clin Electrophysiol* 2019;5:364-75.
86. Dragulescu A, Mertens L, Friedberg MK. Interpretation of left ventricular diastolic dysfunction in children with cardiomyopathy by echocardiography: problems and limitations. *Circ Cardiovasc Imaging* 2013;6:254-61.
87. Jhaveri S, Komarlu R, Worley S, Shahbah D, Gurumoorthi M, Zahka K. Left atrial strain and function in pediatric hypertrophic cardiomyopathy. *J Am Soc Echocardiogr* 2021;34:996-1006.
88. Villemain O, Correia M, Khraiche D, Podetti I, Meot M, Legendre A, et al. Myocardial stiffness assessment using shear wave imaging in pediatric hypertrophic cardiomyopathy. *JACC Cardiovasc Imaging* 2018;11:779-81.
89. Rowin EJ, Maron BJ, Olivetto I, Maron MS. Role of exercise testing in hypertrophic cardiomyopathy. *JACC Cardiovasc Imaging* 2017;10:1374-86.
90. Maron BJ, Ommen SR, Semsarian C, Spirito P, Olivetto I, Maron MS. Hypertrophic cardiomyopathy: present and future, with translation into contemporary cardiovascular medicine. *J Am Coll Cardiol* 2014;64:83-99.
91. Wigle ED. Cardiomyopathy: The diagnosis of hypertrophic cardiomyopathy. *Heart* 2001;86:709-14.
92. Maron MS, Olivetto I, Betocchi S, Casey SA, Lesser JR, Losi MA, et al. Effect of left ventricular outflow tract obstruction on clinical outcome in hypertrophic cardiomyopathy. *N Engl J Med* 2003;348:295-303.
93. Sherrid MV, Shetty A, Winson G, Kim B, Musat D, Alviar CL, et al. Treatment of obstructive hypertrophic cardiomyopathy symptoms and gradient resistant to first-line therapy with beta-blockade or verapamil. *Circ Heart Fail* 2013;6:694-702.
94. Adams JC, Ommen SR, Klarich KW, Tajik AJ, Nishimura RA. Significance of postprandial symptom exacerbation in hypertrophic cardiomyopathy. *Am J Cardiol* 2010;105:990-2.
95. Geske JB, Sorajja P, Ommen SR, Nishimura RA. Left ventricular outflow tract gradient variability in hypertrophic cardiomyopathy. *Clin Cardiol* 2009;32:397-402.
96. Shah PM, Taylor RD, Wong M. Abnormal mitral valve coaptation in hypertrophic obstructive cardiomyopathy: proposed role in systolic anterior motion of mitral valve. *Am J Cardiol* 1981;48:258-62.
97. Jiang L, Levine RA, King ME, Weyman AE. An integrated mechanism for systolic anterior motion of the mitral valve in hypertrophic cardiomyopathy based on echocardiographic observations. *Am Heart J* 1987;113:633-44.
98. Sherrid MV, Wever-Pinzon O, Shah A, Chaudhry FA. Reflections of inflections in hypertrophic cardiomyopathy. *J Am Coll Cardiol* 2009;54:212-9.
99. Kwon DH, Setser RM, Thamilarasan M, Popovic ZV, Smedira NG, Schoenhagen P, et al. Abnormal papillary muscle morphology is independently associated with increased left ventricular outflow tract obstruction in hypertrophic cardiomyopathy. *Heart* 2008;94:1295-301.
100. Klues HG, Roberts WC, Maron BJ. Anomalous insertion of papillary muscle directly into anterior mitral leaflet in hypertrophic cardiomyopathy. Significance in producing left ventricular outflow obstruction. *Circulation* 1991;84:1188-97.
101. Cavalcante JL, Barboza JS, Lever HM. Diversity of mitral valve abnormalities in obstructive hypertrophic cardiomyopathy. *Prog Cardiovasc Dis* 2012;54:517-22.
102. Silbiger JJ. Abnormalities of the mitral apparatus in hypertrophic cardiomyopathy: echocardiographic, pathophysiologic, and surgical insights. *J Am Soc Echocardiogr* 2016;29:622-39.
103. Nagueh SF, Mahmarian JJ. Noninvasive cardiac imaging in patients with hypertrophic cardiomyopathy. *J Am Coll Cardiol* 2006;48:2410-22.
104. Topol EJ, Traill TA, Fortuin NJ. Hypertensive hypertrophic cardiomyopathy of the elderly. *N Engl J Med* 1985;312:277-83.
105. Chockalingam A, Dorairajan S, Bhalla M, Dellsperger KC. Unexplained hypotension: the spectrum of dynamic left ventricular outflow

- tract obstruction in critical care settings. *Crit Care Med* 2009;37:729-34.
106. Maslow AD, Regan MM, Haering JM, Johnson RG, Levine RA. Echocardiographic predictors of left ventricular outflow tract obstruction and systolic anterior motion of the mitral valve after mitral valve reconstruction for myxomatous valve disease. *J Am Coll Cardiol* 1999;34:2096-104.
  107. Blanke P, Naoum C, Dvir D, Bapat V, Ong K, Muller D, et al. Predicting LVOT obstruction in transcatheter mitral valve implantation: concept of the neo-LVOT. *JACC Cardiovasc Imaging* 2017;10:482-5.
  108. Afonso LC, Bernal J, Bax JJ, Abraham TP. Echocardiography in hypertrophic cardiomyopathy: the role of conventional and emerging technologies. *JACC Cardiovasc Imaging* 2008;1:787-800.
  109. Williams LK, Frenneaux MP, Steeds RP. Echocardiography in hypertrophic cardiomyopathy diagnosis, prognosis, and role in management. *Eur J Echocardiogr* 2009;10:iii9-14.
  110. Gilbert BW, Pollick C, Adelman AG, Wigle ED. Hypertrophic cardiomyopathy: subclassification by m mode echocardiography. *Am J Cardiol* 1980;45:861-72.
  111. Boughner DR, Schuld RL, Persaud JA. Hypertrophic obstructive cardiomyopathy. Assessment by echocardiographic and Doppler ultrasound techniques. *Br Heart J* 1975;37:917-23.
  112. Sherrid MV, Gunsburg DZ, Pearle G. Mid-systolic drop in left ventricular ejection velocity in obstructive hypertrophic cardiomyopathy—the lobster claw abnormality. *J Am Soc Echocardiogr* 1997;10:707-12.
  113. Mitchell C, Rahko PS, Blauwet LA, Canaday B, Finstuen JA, Foster MC, et al. Guidelines for Performing a Comprehensive Transthoracic Echocardiographic Examination in Adults: Recommendations from the American Society of Echocardiography. *J Am Soc Echocardiogr* 2019;32:1-64.
  114. Panza JA, Petrone RK, Fananapazir L, Maron BJ. Utility of continuous wave Doppler echocardiography in the noninvasive assessment of left ventricular outflow tract pressure gradient in patients with hypertrophic cardiomyopathy. *J Am Coll Cardiol* 1992;19:91-9.
  115. Vainrib A, Massera D, Sherrid MV, Swistel DG, Bamira D, Ibrahim H, et al. Three-dimensional imaging and dynamic modeling of systolic anterior motion of the mitral valve. *J Am Soc Echocardiogr* 2021;34:89-96.
  116. Sabbah HN, Stein PD. Mechanism of early systolic closure of the aortic valve in discrete membranous subaortic stenosis. *Circulation* 1982;65:399-402.
  117. Opatowsky AR, Pickard SS, Geva T. Imaging adult patients with discrete subvalvar aortic stenosis. *Curr Opin Cardiol* 2017;32:513-20.
  118. Bruce CJ, Nishimura RA, Tajik AJ, Schaff HV, Danielson GK. Fixed left ventricular outflow tract obstruction in presumed hypertrophic obstructive cardiomyopathy: implications for therapy. *Ann Thorac Surg* 1999;68:100-4.
  119. Jaber WA, Nishimura RA, Ommen SR. Not all systolic velocities indicate obstruction in hypertrophic cardiomyopathy: a simultaneous Doppler catheterization study. *J Am Soc Echocardiogr* 2007;20:1009 e5-7.
  120. Baumgartner H, Hung J, Bermejo J, Chambers JB, Edvardsen T, Goldstein S, et al. Recommendations on the echocardiographic assessment of aortic valve stenosis: A focused update from the European Association of Cardiovascular Imaging and the American Society of Echocardiography. *J Am Soc Echocardiogr* 2017;30:372-92.
  121. Scantlebury DC, Geske JB, Nishimura RA. Limitations of Doppler echocardiography in the evaluation of serial stenoses. *Circ Cardiovasc Imaging* 2013;6:850-2.
  122. Kumar S, Van Ness G, Bender A, Yadava M, Minnier J, Ravi S, et al. Standardized goal-directed Valsalva maneuver for assessment of inducible left ventricular outflow tract obstruction in hypertrophic cardiomyopathy. *J Am Soc Echocardiogr* 2018;31:791-8.
  123. El Assaad I, Gauvreau K, Rizwan R, Margossian R, Colan S, Chen MH. Value of exercise stress echocardiography in children with hypertrophic cardiomyopathy. *J Am Soc Echocardiogr* 2020;33:888-894 e2.
  124. Schwammenthal E, Nakatani S, He S, Hopmeyer J, Sagie A, Weyman AE, et al. Mechanism of mitral regurgitation in hypertrophic cardiomyopathy: mismatch of posterior to anterior leaflet length and mobility. *Circulation* 1998;98:856-65.
  125. Yu EH, Omran AS, Wigle ED, Williams WG, Siu SC, Rakowski H. Mitral regurgitation in hypertrophic obstructive cardiomyopathy: relationship to obstruction and relief with myectomy. *J Am Coll Cardiol* 2000;36:2219-25.
  126. Hang D, Schaff HV, Nishimura RA, Lahr BD, Abel MD, Dearani JA, et al. Accuracy of jet direction on Doppler echocardiography in identifying the etiology of mitral regurgitation in obstructive hypertrophic cardiomyopathy. *J Am Soc Echocardiogr* 2019;32:333-40.
  127. Minami Y, Kajimoto K, Terajima Y, Yashiro B, Okayama D, Haruki S, et al. Clinical implications of midventricular obstruction in patients with hypertrophic cardiomyopathy. *J Am Coll Cardiol* 2011;57:2346-55.
  128. Cooley DA, Leachman RD, Wukasch DC. Diffuse muscular subaortic stenosis: surgical treatment. *Am J Cardiol* 1973;31:1-6.
  129. Malcolmson JW, Hamshire SM, Joshi A, O'Mahony C, Dhinoja M, Petersen SE, et al. Doppler echocardiography underestimates the prevalence and magnitude of mid-cavity obstruction in patients with symptomatic hypertrophic cardiomyopathy. *Catheter Cardiovasc Interv* 2018;91:783-9.
  130. Neubauer S, Kolm P, Ho CY, Kwong RY, Desai MY, Dolman SF, et al. Distinct Subgroups in Hypertrophic Cardiomyopathy in the NHLBI HCM Registry. *J Am Coll Cardiol* 2019;74:2333-45.
  131. Shah A, Duncan K, Winson G, Chaudhry FA, Sherrid MV. Severe symptoms in mid and apical hypertrophic cardiomyopathy. *Echocardiography* 2009;26:922-33.
  132. Zoghbi WA, Haichin RN, Quinones MA. Mid-cavity obstruction in apical hypertrophy: Doppler evidence of diastolic intraventricular gradient with higher apical pressure. *Am Heart J* 1988;116:1469-74.
  133. Maron MS, Finley JJ, Bos JM, Hauser TH, Manning WJ, Haas TS, et al. Prevalence, clinical significance, and natural history of left ventricular apical aneurysms in hypertrophic cardiomyopathy. *Circulation* 2008;118:1541-9.
  134. Rowin EJ, Maron BJ, Haas TS, Garberich RF, Wang W, Link MS, et al. Hypertrophic cardiomyopathy with left ventricular apical aneurysm: implications for risk stratification and management. *J Am Coll Cardiol* 2017;69:761-73.
  135. Kunkala MR, Schaff HV, Nishimura RA, Abel MD, Sorajja P, Dearani JA, et al. A translational approach to myectomy for midventricular obstruction in hypertrophic cardiomyopathy. *Ann Thorac Surg* 2013;96:564-70.
  136. Newton N, Liu CY, Croisille P, Bluemke D, Lima JA. Assessment of myocardial fibrosis with cardiovascular magnetic resonance. *J Am Coll Cardiol* 2011;57:891-903.
  137. Dass S, Suttie JJ, Piechnik SK, Ferreira VM, Holloway CJ, Banerjee R, et al. Myocardial tissue characterization using magnetic resonance noncontrast T1 mapping in hypertrophic and dilated cardiomyopathy. *Circ Cardiovasc Imaging* 2012;5:726-33.
  138. Sado DM, White SK, Piechnik SK, Banyersad SM, Treibel T, Captur G, et al. Identification and assessment of Anderson-Fabry disease by cardiovascular magnetic resonance noncontrast myocardial T1 mapping. *Circ Cardiovasc Imaging* 2013;6:392-8.
  139. Avanesov M, Munch J, Weinrich J, Well L, Saring D, Stehning C, et al. Prediction of the estimated 5-year risk of sudden cardiac death and syncope or non-sustained ventricular tachycardia in patients with hypertrophic cardiomyopathy using late gadolinium enhancement and extracellular volume CMR. *Eur Radiol* 2017;27:5136-45.
  140. Gommans DHF, Cramer GE, Bakker J, Dieker HJ, Michels M, Fouraux MA, et al. High T2-weighted signal intensity for risk prediction of sudden cardiac death in hypertrophic cardiomyopathy. *Int J Cardiovasc Imaging* 2018;34:113-20.
  141. Compton G, Nield L, Dragulescu A, Benson L, Grosse-Wortmann L. Echocardiography as a Screening Test for Myocardial Scarring in Children with Hypertrophic Cardiomyopathy. *Int J Pediatr* 2016;2016:1980636.
  142. Yajima R, Kataoka A, Takahashi A, Uehara M, Saito M, Yamaguchi C, et al. Distinguishing focal fibrotic lesions and non-fibrotic lesions in hypertrophic cardiomyopathy by assessment of regional myocardial strain using two-dimensional speckle tracking echocardiography: comparison with multislice CT. *Int J Cardiol* 2012;158:423-32.

143. Spartera M, Damascelli A, Mozes F, De Cobelli F, La Canna G. Three-dimensional speckle tracking longitudinal strain is related to myocardial fibrosis determined by late-gadolinium enhancement. *Int J Cardiovasc Imaging* 2017;33:1351-60.
144. Authors/Task Force members, Elliott PM, Anastasakis A, Borger MA, Borggrefe M, Cecchi F, et al. 2014 ESC Guidelines on diagnosis and management of hypertrophic cardiomyopathy: the Task Force for the Diagnosis and Management of Hypertrophic Cardiomyopathy of the European Society of Cardiology (ESC). *Eur Heart J* 2014;35:2733-79.
145. O'Mahony C, Jichi F, Pavlou M, Monserrat L, Anastasakis A, Rapezzi C, et al. A novel clinical risk prediction model for sudden cardiac death in hypertrophic cardiomyopathy (HCM risk-SCD). *Eur Heart J* 2014;35:2010-20.
146. Miron A, Lafreniere-Roula M, Steve Fan CP, Armstrong KR, Dragulescu A, Papaz T, et al. A validated model for sudden cardiac death risk prediction in pediatric hypertrophic cardiomyopathy. *Circulation* 2020;142:217-29.
147. Spirito P, Bellone P, Harris KM, Bernabo P, Bruzzi P, Maron BJ. Magnitude of left ventricular hypertrophy and risk of sudden death in hypertrophic cardiomyopathy. *N Engl J Med* 2000;342:1778-85.
148. Spirito P, Autore C, Rapezzi C, Bernabo P, Badagliacca R, Maron MS, et al. Syncope and risk of sudden death in hypertrophic cardiomyopathy. *Circulation* 2009;119:1703-10.
149. Yang H, Woo A, Monakier D, Jamorski M, Fedwick K, Wigle ED, et al. Enlarged left atrial volume in hypertrophic cardiomyopathy: a marker for disease severity. *J Am Soc Echocardiogr* 2005;18:1074-82.
150. Rowin EJ, Hausvater A, Link MS, Abt P, Gionfriddo W, Wang W, et al. Clinical profile and consequences of atrial fibrillation in hypertrophic cardiomyopathy. *Circulation* 2017;136:2420-36.
151. Yang WJ, Shim CY, Kim YJ, Kim SA, Rhee SJ, Choi EY, et al. Left atrial volume index: a predictor of adverse outcome in patients with hypertrophic cardiomyopathy. *J Am Soc Echocardiogr* 2009;22:1338-43.
152. Elliott PM, Gimeno JR, Tome MT, Shah J, Ward D, Thaman R, et al. Left ventricular outflow tract obstruction and sudden death risk in patients with hypertrophic cardiomyopathy. *Eur Heart J* 2006;27:1933-41.
153. Gimeno JR, Tome-Esteban M, Lofego C, Hurtado J, Pantazis A, Mist B, et al. Exercise-induced ventricular arrhythmias and risk of sudden cardiac death in patients with hypertrophic cardiomyopathy. *Eur Heart J* 2009;30:2599-605.
154. Lu DY, Hailesealassie B, Ventoulis I, Liu H, Liang HY, Nowbar A, et al. Impact of peak provoked left ventricular outflow tract gradients on clinical outcomes in hypertrophic cardiomyopathy. *Int J Cardiol* 2017;243:290-5.
155. Desai MY, Smedira NG, Bhonsale A, Thamilarasan M, Lytle BW, Lever HM. Symptom assessment and exercise impairment in surgical decision making in hypertrophic obstructive cardiomyopathy: Relationship to outcomes. *J Thorac Cardiovasc Surg* 2015;150:928-935 e1.
156. Ichida M, Nishimura Y, Kario K. Clinical significance of left ventricular apical aneurysms in hypertrophic cardiomyopathy patients: the role of diagnostic electrocardiography. *J Cardiol* 2014;64:265-72.
157. Hanneman K, Crean AM, Williams L, Moshonov H, James S, Jimenez-Juan L, et al. Cardiac magnetic resonance imaging findings predict major adverse events in apical hypertrophic cardiomyopathy. *J Thorac Imaging* 2014;29:331-9.
158. Chan RH, Maron BJ, Olivetto I, Pencina MJ, Assenza GE, Haas T, et al. Prognostic value of quantitative contrast-enhanced cardiovascular magnetic resonance for the evaluation of sudden death risk in patients with hypertrophic cardiomyopathy. *Circulation* 2014;130:484-95.
159. Bruder O, Wagner A, Jensen CJ, Schneider S, Ong P, Kispert EM, et al. Myocardial scar visualized by cardiovascular magnetic resonance imaging predicts major adverse events in patients with hypertrophic cardiomyopathy. *J Am Coll Cardiol* 2010;56:875-87.
160. Mentias A, Raeisi-Giglou P, Smedira NG, Feng K, Sato K, Wazni O, et al. Late gadolinium enhancement in patients with hypertrophic cardiomyopathy and preserved systolic function. *J Am Coll Cardiol* 2018;72:857-70.
161. O'Hanlon R, Grasso A, Roughton M, Moon JC, Clark S, Wage R, et al. Prognostic significance of myocardial fibrosis in hypertrophic cardiomyopathy. *J Am Coll Cardiol* 2010;56:867-74.
162. Olivetto I, Maron BJ, Appelbaum E, Harrigan CJ, Salton C, Gibson CM, et al. Spectrum and clinical significance of systolic function and myocardial fibrosis assessed by cardiovascular magnetic resonance in hypertrophic cardiomyopathy. *Am J Cardiol* 2010;106:261-7.
163. Gersh BJ, Maron BJ, Bonow RO, Dearani JA, Fifer MA, Link MS, et al. 2011 ACCF/AHA Guideline for the Diagnosis and Treatment of Hypertrophic Cardiomyopathy: a report of the American College of Cardiology Foundation/American Heart Association Task Force on Practice Guidelines. Developed in collaboration with the American Association for Thoracic Surgery, American Society of Echocardiography, American Society of Nuclear Cardiology, Heart Failure Society of America, Heart Rhythm Society, Society for Cardiovascular Angiography and Interventions, and Society of Thoracic Surgeons. *J Am Coll Cardiol* 2011;58:e212-60.
164. Maron MS, Rowin EJ, Maron BJ. How to image hypertrophic cardiomyopathy. *Circ Cardiovasc Imaging* 2017;10:e005372.
165. Schulz-Menger J, Bluemke DA, Bremerich J, Flamm SD, Fogel MA, Friedrich MG, et al. Standardized image interpretation and post processing in cardiovascular magnetic resonance: Society for Cardiovascular Magnetic Resonance (SCMR) board of trustees task force on standardized post processing. *J Cardiovasc Magn Reson* 2013;15:35.
166. Flett AS, Hasleton J, Cook C, Hausenloy D, Quarta G, Ariti C, et al. Evaluation of techniques for the quantification of myocardial scar of differing etiology using cardiac magnetic resonance. *JACC Cardiovasc Imaging* 2011;4:150-6.
167. Harrigan CJ, Peters DC, Gibson CM, Maron BJ, Manning WJ, Maron MS, et al. Hypertrophic cardiomyopathy: quantification of late gadolinium enhancement with contrast-enhanced cardiovascular MR imaging. *Radiology* 2011;258:128-33.
168. Lu DY, Yalcin H, Yalcin F, Zhao M, Sivalokanathan S, Valenta I, et al. Stress myocardial blood flow heterogeneity is a positron emission tomography biomarker of ventricular arrhythmias in patients with hypertrophic cardiomyopathy. *Am J Cardiol* 2018;121:1081-9.
169. Cannon RO 3rd, Rosing DR, Maron BJ, Leon MB, Bonow RO, Watson RM, et al. Myocardial ischemia in patients with hypertrophic cardiomyopathy: contribution of inadequate vasodilator reserve and elevated left ventricular filling pressures. *Circulation* 1985;71:234-43.
170. Krams R, Kofflard MJ, Duncker DJ, Von Birgelen C, Carlier S, Kliffen M, et al. Decreased coronary flow reserve in hypertrophic cardiomyopathy is related to remodeling of the coronary microcirculation. *Circulation* 1998;97:230-3.
171. Maron BJ, Wolfson JK, Epstein SE, Roberts WC. Intramural ("small vessel") coronary artery disease in hypertrophic cardiomyopathy. *J Am Coll Cardiol* 1986;8:545-57.
172. Basso C, Thiene G, Mackey-Bojack S, Frigo AC, Corrado D, Maron BJ. Myocardial bridging, a frequent component of the hypertrophic cardiomyopathy phenotype, lacks systematic association with sudden cardiac death. *Eur Heart J* 2009;30:1627-34.
173. Shariat M, Thavendiranathan P, Nguyen E, Wintersperger B, Paul N, Rakowski H, et al. Utility of coronary CT angiography in outpatients with hypertrophic cardiomyopathy presenting with angina symptoms. *J Cardiovasc Comput Tomogr* 2014;8:429-37.
174. van der Velde N, Huurman R, Yamasaki Y, Kardys J, Galema TW, Budde RP, et al. Frequency and significance of coronary artery disease and myocardial bridging in patients with hypertrophic cardiomyopathy. *Am J Cardiol* 2020;125:1404-12.
175. Elliott PM, Kaski JC, Prasad K, Seo H, Slade AK, Goldman JH, et al. Chest pain during daily life in patients with hypertrophic cardiomyopathy: an ambulatory electrocardiographic study. *Eur Heart J* 1996;17:1056-64.
176. Sorajja P, Ommen SR, Nishimura RA, Gersh BJ, Berger PB, Tajik AJ. Adverse prognosis of patients with hypertrophic cardiomyopathy who have epicardial coronary artery disease. *Circulation* 2003;108:2342-8.
177. Schwartzkopff B, Mundhenke M, Strauer BE. Alterations of the architecture of subendocardial arterioles in patients with hypertrophic

- cardiomyopathy and impaired coronary vasodilator reserve: a possible cause for myocardial ischemia. *J Am Coll Cardiol* 1998;31:1089-96.
178. Ciampi Q, Olivotto I, Gardini C, Mori F, Peteiro J, Monserrat L, et al. Prognostic role of stress echocardiography in hypertrophic cardiomyopathy: The International Stress Echo Registry. *Int J Cardiol* 2016;219:331-8.
  179. Cortigiani L, Rigo F, Gherardi S, Galderisi M, Sicari R, Picano E. Prognostic implications of coronary flow reserve on left anterior descending coronary artery in hypertrophic cardiomyopathy. *Am J Cardiol* 2008;102:1718-23.
  180. Tower-Rader A, Betancor J, Lever HM, Desai MY. A comprehensive review of stress testing in hypertrophic cardiomyopathy: assessment of functional capacity, identification of prognostic indicators, and detection of coronary artery disease. *J Am Soc Echocardiogr* 2017;30:829-44.
  181. Peteiro J, Bouzas-Mosquera A, Fernandez X, Monserrat L, Pazos P, Estevez-Loureiro R, et al. Prognostic value of exercise echocardiography in patients with hypertrophic cardiomyopathy. *J Am Soc Echocardiogr* 2012;25:182-9.
  182. O'Gara PT, Bonow RO, Maron BJ, Damske BA, Van Lingen A, Bacharach SL, et al. Myocardial perfusion abnormalities in patients with hypertrophic cardiomyopathy: assessment with thallium-201 emission computed tomography. *Circulation* 1987;76:1214-23.
  183. Cannon RO 3rd, Dilsizian V, O'Gara PT, Udelson JE, Schenke WH, Quyyumi A, et al. Myocardial metabolic, hemodynamic, and electrocardiographic significance of reversible thallium-201 abnormalities in hypertrophic cardiomyopathy. *Circulation* 1991;83:1660-7.
  184. Dilsizian V, Bonow RO, Epstein SE, Fananapazir L. Myocardial ischemia detected by thallium scintigraphy is frequently related to cardiac arrest and syncope in young patients with hypertrophic cardiomyopathy. *J Am Coll Cardiol* 1993;22:796-804.
  185. Udelson JE, Bonow RO, O'Gara PT, Maron BJ, Van Lingen A, Bacharach SL, et al. Verapamil prevents silent myocardial perfusion abnormalities during exercise in asymptomatic patients with hypertrophic cardiomyopathy. *Circulation* 1989;79:1052-60.
  186. Cannon RO 3rd, Dilsizian V, O'Gara PT, Udelson JE, Tucker E, Panza JA, et al. Impact of surgical relief of outflow obstruction on thallium perfusion abnormalities in hypertrophic cardiomyopathy. *Circulation* 1992;85:1039-45.
  187. Timmer SA, Knaapen P. Coronary microvascular function, myocardial metabolism, and energetics in hypertrophic cardiomyopathy: insights from positron emission tomography. *Eur Heart J Cardiovasc Imaging* 2013;14:95-101.
  188. Sciagra R, Calabretta R, Cipollini F, Passeri A, Castello A, Cecchi F, et al. Myocardial blood flow and left ventricular functional reserve in hypertrophic cardiomyopathy: a (13)NH3 gated PET study. *Eur J Nucl Med Mol Imaging* 2017;44:866-75.
  189. Bravo PE, Tahari A, Pozios I, Luo HC, Bengel FM, Wahl RL, et al. Apparent left ventricular cavity dilatation during PET/CT in hypertrophic cardiomyopathy: Clinical predictors and potential mechanisms. *J Nucl Cardiol* 2016;23:1304-14.
  190. Knaapen P, van Dockum WG, Gotte MJ, Broeze KA, Kuijper JP, Zwanenburg JJ, et al. Regional heterogeneity of resting perfusion in hypertrophic cardiomyopathy is related to delayed contrast enhancement but not to systolic function: a PET and MRI study. *J Nucl Cardiol* 2006;13:660-7.
  191. Bravo PE, Pinheiro A, Higuchi T, Rischpler C, Merrill J, Santaularia-Tomas M, et al. PET/CT assessment of symptomatic individuals with obstructive and nonobstructive hypertrophic cardiomyopathy. *J Nucl Med* 2012;53:407-14.
  192. Camici P, Chiriatti G, Lorenzoni R, Bellina RC, Gistri R, Italiani G, et al. Coronary vasodilation is impaired in both hypertrophied and nonhypertrophied myocardium of patients with hypertrophic cardiomyopathy: a study with nitrogen-13 ammonia and positron emission tomography. *J Am Coll Cardiol* 1991;17:879-86.
  193. Cecchi F, Olivotto I, Gistri R, Lorenzoni R, Chiriatti G, Camici PG. Coronary microvascular dysfunction and prognosis in hypertrophic cardiomyopathy. *N Engl J Med* 2003;349:1027-35.
  194. Camaioni C, Knott KD, Augusto JB, Seraphim A, Rosmini S, Ricci F, et al. Inline perfusion mapping provides insights into the disease mechanism in hypertrophic cardiomyopathy. *Heart* 2020;106:824-9.
  195. Kim EK, Lee SC, Chang SA, Jang SY, Kim SM, Park SJ, et al. Prevalence and clinical significance of cardiovascular magnetic resonance adenosine stress-induced myocardial perfusion defect in hypertrophic cardiomyopathy. *J Cardiovasc Magn Reson* 2020;22:30.
  196. Peteiro J, Fernandez X, Bouzas-Mosquera A, Monserrat L, Mendez C, Rodriguez-Garcia E, et al. Exercise echocardiography and cardiac magnetic resonance imaging to predict outcome in patients with hypertrophic cardiomyopathy. *Eur Heart J Cardiovasc Imaging* 2015;16:423-32.
  197. Brown LAE, Onclil SC, Broadbent DA, Johnson K, Fent GJ, Foley JRJ, et al. Fully automated, inline quantification of myocardial blood flow with cardiovascular magnetic resonance: repeatability of measurements in healthy subjects. *J Cardiovasc Magn Reson* 2018;20:48.
  198. Engblom H, Xue H, Akil S, Carlsson M, Hindorf C, Oddstig J, et al. Fully quantitative cardiovascular magnetic resonance myocardial perfusion ready for clinical use: a comparison between cardiovascular magnetic resonance imaging and positron emission tomography. *J Cardiovasc Magn Reson* 2017;19:78.
  199. Petersen SE, Jerosch-Herold M, Hudsmith LE, Robson MD, Francis JM, Doll HA, et al. Evidence for microvascular dysfunction in hypertrophic cardiomyopathy: new insights from multiparametric magnetic resonance imaging. *Circulation* 2007;115:2418-25.
  200. Shin YJ, Lee JH, Yoo JY, Kim JA, Jeon Y, Yoon YE, et al. Clinical significance of evaluating coronary atherosclerosis in adult patients with hypertrophic cardiomyopathy who have chest pain. *Eur Radiol* 2019;29:4593-602.
  201. Zhao L, Ma X, Ge H, Zhang C, Wang Z, Teraoka K, et al. Diagnostic performance of computed tomography for detection of concomitant coronary disease in hypertrophic cardiomyopathy. *Eur Radiol* 2015;25:767-75.
  202. Sellers SL, Fonte TA, Grover R, Mooney J, Weir-McCall J, Lau KP, et al. Hypertrophic Cardiomyopathy (HCM): New insights into Coronary artery remodeling and ischemia from FFRCT. *J Cardiovasc Comput Tomogr* 2018;12:467-71.
  203. Coenen A, Lubbers MM, Kurata A, Kono A, Dedic A, Chelu RG, et al. Coronary CT angiography derived fractional flow reserve: Methodology and evaluation of a point of care algorithm. *J Cardiovasc Comput Tomogr* 2016;10:105-13.
  204. Cheng VY, Berman DS, Rozanski A, Dunning AM, Achenbach S, Al-Mallah M, et al. Performance of the traditional age, sex, and angina typically-based approach for estimating pretest probability of angiographically significant coronary artery disease in patients undergoing coronary computed tomographic angiography: results from the multinational coronary CT angiography evaluation for clinical outcomes: an international multicenter registry (CONFIRM). *Circulation* 2011;124:2423-32. 1-8.
  205. Foldyna B, Udelson JE, Karady J, Banerji D, Lu MT, Mayrhofer T, et al. Pretest probability for patients with suspected obstructive coronary artery disease: re-evaluating Diamond-Forrester for the contemporary era and clinical implications: insights from the PROMISE trial. *Eur Heart J Cardiovasc Imaging* 2019;20:574-81.
  206. Genders TS, Steyerberg EW, Alkadhi H, Leschka S, Desbiolles L, Nieman K, et al. A clinical prediction rule for the diagnosis of coronary artery disease: validation, updating, and extension. *Eur Heart J* 2011;32:1316-30.
  207. Nieman K, Galema TW, Neeffes LA, Weustink AC, Musters P, Moelker AD, et al. Comparison of the value of coronary calcium detection to computed tomographic angiography and exercise testing in patients with chest pain. *Am J Cardiol* 2009;104:1499-504.
  208. Mouden M, Timmer JR, Reiffers S, Oostdijk AH, Knollemans S, Ottervanger JP, et al. Coronary artery calcium scoring to exclude flow-limiting coronary artery disease in symptomatic stable patients at low or intermediate risk. *Radiology* 2013;269:77-83.
  209. Shaw LJ, Hausleiter J, Achenbach S, Al-Mallah M, Berman DS, Budoff MJ, et al. Coronary computed tomographic angiography as a

- gatekeeper to invasive diagnostic and surgical procedures: results from the multicenter CONFIRM (Coronary CT Angiography Evaluation for Clinical Outcomes: an International Multicenter) registry. *J Am Coll Cardiol* 2012;60:2103-14.
210. de Carvalho MS, de Araujo Goncalves P, Garcia-Garcia HM, de Sousa PJ, Dore H, Ferreira A, et al. Prevalence and predictors of coronary artery disease in patients with a calcium score of zero. *Int J Cardiovasc Imaging* 2013;29:1839-46.
  211. Ho CY, Day SM, Colan SD, Russell MW, Towbin JA, Sherrid MV, et al. The burden of early phenotypes and the influence of wall thickness in hypertrophic cardiomyopathy mutation carriers: findings from the HCMNet Study. *JAMA Cardiol* 2017;2:419-28.
  212. Crilly JC, Boehm EA, Blair E, Rajagopalan B, Blamire AM, Styles P, et al. Hypertrophic cardiomyopathy due to sarcomeric gene mutations is characterized by impaired energy metabolism irrespective of the degree of hypertrophy. *J Am Coll Cardiol* 2003;41:1776-82.
  213. Maron MS, Olivetto I, Harrigan C, Appelbaum E, Gibson CM, Lesser JR, et al. Mitral valve abnormalities identified by cardiovascular magnetic resonance represent a primary phenotypic expression of hypertrophic cardiomyopathy. *Circulation* 2011;124:40-7.
  214. Captur G, Lopes LR, Mohun TJ, Patel V, Li C, Bassett P, et al. Prediction of sarcomere mutations in subclinical hypertrophic cardiomyopathy. *Circ Cardiovasc Imaging* 2014;7:863-71.
  215. Nagueh SF, McFalls J, Meyer D, Hill R, Zoghbi WA, Tam JW, et al. Tissue Doppler imaging predicts the development of hypertrophic cardiomyopathy in subjects with subclinical disease. *Circulation* 2003;108:395-8.
  216. Maron BJ, Nishimura RA, McKenna WJ, Rakowski H, Josephson ME, Kieval RS. Assessment of permanent dual-chamber pacing as a treatment for drug-refractory symptomatic patients with obstructive hypertrophic cardiomyopathy. A randomized, double-blind, crossover study (M-PATHY). *Circulation* 1999;99:2927-33.
  217. Gadler F, Linde C, Juhlin-Dannfeldt A, Ribeiro A, Ryden L. Influence of right ventricular pacing site on left ventricular outflow tract obstruction in patients with hypertrophic obstructive cardiomyopathy. *J Am Coll Cardiol* 1996;27:1219-24.
  218. Barold SS, Ilercil A, Herweg B. Echocardiographic optimization of the atrioventricular and interventricular intervals during cardiac resynchronization. *Europace* 2008;10(Suppl 3):iii88-95.
  219. Nampiarampil RG, Swistel DG, Schlame M, Saric M, Sherrid MV. Intraoperative two- and three-dimensional transesophageal echocardiography in combined myectomy-mitral operations for hypertrophic cardiomyopathy. *J Am Soc Echocardiogr* 2018;31:275-88.
  220. Messmer BJ. Extended myectomy for hypertrophic obstructive cardiomyopathy. *Ann Thorac Surg* 1994;58:575-7.
  221. Nicoara A, Skubas N, Ad N, Finley A, Hahn RT, Mahmood F, et al. Guidelines for the use of transesophageal echocardiography to assist with surgical decision-making in the operating room: a surgery-based approach: from the American Society of Echocardiography in collaboration with the Society of Cardiovascular Anesthesiologists and the Society of Thoracic Surgeons. *J Am Soc Echocardiogr* 2020;33:692-734.
  222. Sherrid MV, Chaudhry FA, Swistel DG. Obstructive hypertrophic cardiomyopathy: echocardiography, pathophysiology, and the continuing evolution of surgery for obstruction. *Ann Thorac Surg* 2003;75:620-32.
  223. Nagueh SF, Lakkis NM, He ZX, Middleton KJ, Killip D, Zoghbi WA, et al. Role of myocardial contrast echocardiography during nonsurgical septal reduction therapy for hypertrophic obstructive cardiomyopathy. *J Am Coll Cardiol* 1998;32:225-9.
  224. Faber L, Seggewiss H, Gleichmann U. Percutaneous transluminal septal myocardial ablation in hypertrophic obstructive cardiomyopathy: results with respect to intraprocedural myocardial contrast echocardiography. *Circulation* 1998;98:2415-21.
  225. Faber L, Ziemssen P, Seggewiss H. Targeting percutaneous transluminal septal ablation for hypertrophic obstructive cardiomyopathy by intraprocedural echocardiographic monitoring. *J Am Soc Echocardiogr* 2000;13:1074-9.
  226. Kuhn H, Gietzen FH, Schafers M, Freick M, Gockel B, Strunk-Muller C, et al. Changes in the left ventricular outflow tract after transcatheter ablation of septal hypertrophy (TASH) for hypertrophic obstructive cardiomyopathy as assessed by transoesophageal echocardiography and by measuring myocardial glucose utilization and perfusion. *Eur Heart J* 1999;20:1808-17.
  227. Flores-Ramirez R, Lakkis NM, Middleton KJ, Killip D, Spencer WH 3rd, Nagueh SF. Echocardiographic insights into the mechanisms of relief of left ventricular outflow tract obstruction after nonsurgical septal reduction therapy in patients with hypertrophic obstructive cardiomyopathy. *J Am Coll Cardiol* 2001;37:208-14.